Doctorate Program in Molecular Oncology and Endocrinology
Doctorate School in Molecular Medicine

XXIV cycle - 2008–2011
Coordinator: Prof. Massimo Santoro

“The role of Methylglyoxal in the pathogenesis of endothelial insulin resistance and vascular damage in type 2 diabetes”

Cecilia Nigro

University of Naples Federico II
Dipartimento di Biologia e Patologia Cellulare e Molecolare
“L. Califano”

Administrative Location

Dipartimento di Biologia e Patologia Cellulare e Molecolare “L. Califano”
Università degli Studi di Napoli Federico II

Partner Institutions

Italian Institutions
Università degli Studi di Napoli “Federico II”, Naples, Italy
Istituto di Endocrinologia ed Oncologia Sperimentale “G. Salvatore”, CNR, Naples, Italy
Seconda Università di Napoli, Naples, Italy
Università degli Studi di Napoli “Parthenope”, Naples, Italy
Università degli Studi del Sannio, Benevento, Italy
Università degli Studi di Genova, Genova, Italy
Università degli Studi di Padova, Padova, Italy
Università degli Studi “Magna Graecia”, Catanzaro, Italy
Università degli Studi di Udine, Udine, Italy

Foreign Institutions
Université Libre de Bruxelles, Bruxelles, Belgium
Universidade Federal de Sao Paulo, Brazil
University of Turku, Turku, Finland
Université Paris Sud XI, Paris, France
University of Madras, Chennai, India
University Pavol Jozef Šafàrik, Kosice, Slovakia
Universidad Autonoma de Madrid, Centro de Investigaciones Oncologicas (CNIO), Spain
Johns Hopkins School of Medicine, Baltimore, MD, USA
Johns Hopkins Krieger School of Arts and Sciences, Baltimore, MD, USA
National Institutes of Health, Bethesda, MD, USA
Ohio State University, Columbus, OH, USA
Albert Einstein College of Medicine of Yeshiwa University, N.Y., USA

Supporting Institutions
Dipartimento di Biologia e Patologia Cellulare e Molecolare “L. Califano”, Università degli Studi di Napoli “Federico II”, Naples, Italy
Istituto di Endocrinologia ed Oncologia Sperimentale “G. Salvatore”, CNR, Naples, Italy
Istituto Superiore di Oncologia, Italy

Italian Faculty

Salvatore Maria Aloj
Francesco Saverio Ambesi Impiombato
Francesco Beguinot
Maria Teresa Berlingieri
Bernadette Biondi
Francesca Carlomagno
Gabriella Castoria
Maria Domenica Castellone
Angela Celetti
Lorenzo Chiariotti
Vincenzo Ciminale
Annamaria Cirafici
Annamaria Colao
Sabino De Placido
Gabriella De Vita
Monica Fedele
Pietro Formisano
Alfredo Fusco
Domenico Grieco
Michele Grieco
Maddalena Illario
Massimo Imbriaco
Paolo Laccetti
Antonio Leonardi
Paolo Emidio Macchia
Barbara Majello
Rosa Marina Melillo
Claudia Miele
Nunzia Montuori
Roberto Pacelli
Giuseppe Palumbo
Silvio Parodi
Nicola Perrotti
Maria Giovanna Pierantoni
Rosario Pivonello
Giuseppe Portella
Giorgio Punzo
Maria Fiammetta Romano
Antonio Rosato
Giuliana Salvatore
Massimo Santoro
Giampaolo Tortora
Donatella Tramontano
Giancarlo Troncone
Giancarlo Vecchio,
Giuseppe Viglietto
Mario Vitale

“The role of Methylglyoxal in the pathogenesis of endothelial insulin resistance and vascular damage in type 2 diabetes”

TABLE OF CONTENTS

Page

LIST OF PUBLICATIONS.....3

ABSTRACT.....**4**

BACKGROUND.....**6**
1.1 Insulin Resistance: a common feature of different metabolic disorders and their complications.....6
1.1.1 Insulin action.....8
1.2 Endothelium……..…12
1.2.1 Insulin action on endothelium.....13
1.3 Endothelial dysfunction……....14
1.4 Reciprocal relationships between endothelial dysfunction and insulin resistance……16
1.4.1 Potential mechanisms……..…18
1.5 Mechanisms of Glucotoxicity……...……20
1.6 Methylglyoxal……..…….28
1.6.1 Damaging effects of Methylglyoxal……29
1.6.2 Detoxification of methyglyoxal: the Glyoxalase system……...……31

AIMS OF THE STUDY……...…….……**33**

MATERIALS AND METHODS……**34**

RESULTS.....**36**
2.1 Effect of MGO on insulin signaling in endothelial cells in vitro.....36
2.2 Effect of MGO on insulin sensitivity in vivo.2.2 . ……..…..44

DISCUSSION **46**

CONCLUSIONS……..…..**51**

ACKNOWLEDGEMENTS……..**52**

REFERENCES……..**53**

LIST OF PUBLICATIONS

This dissertation is based upon the following publications:

1. Lombardi A, Ulianich L, Treglia AS, Nigro C, Parrillo L, Lofrumento DD, Nicolardi G, Garbi C, Beguinot F, Miele C, Di Jeso B. Increased hexosamine biosynthetic pathway flux dedifferentiates INS-1E cells and murine islets by an extracellular signal-regulated kinase (ERK)1/2-mediated signal transmission pathway. Diabetologia 2011 Oct 18 [Epub ahead of print].

2. Beguinot F and Nigro C. Measurement of Glucose Homeostasis in vivo: Glucose and Insulin Tolerance Tests. Chapter IV-2a, Methods Mol Biol 2011 [in press].

3. Ungaro P, Teperino R, Mirra P, Longo M, Ciccarelli M, Raciti GA, Nigro C, Miele C, Formisano P, Beguinot F. Hepatocyte nuclear factor (HNF)-4α-driven epigenetic silencing of the human PED gene. Diabetologia 2010; 53:1482–1492.

ABSTRACT

It has now become evident that insulin exerts a direct action on vascular cells, thereby conditioning the outcome and progression of vascular complication associated with diabetes. However, the mechanisms through which insulin signaling is impaired in the vascular endothelium remain still unclear. Chronic hyperglycaemia per se promotes insulin resistance and plays a pivotal role in the outcome and progression of diabetes-associated vascular complications. Hyperglycaemia may act through different mechanisms, including generation of advanced glycation end products (AGEs). In this work we evaluated the role of the AGEs precursor methylglyoxal (MGO) in the generation of endothelial insulin-resistance in cellular and animal models.

Time-courses experiments were performed on bovine aortic endothelial cells (BAEC) incubated with different concentrations of MGO. The glyoxalase 1 inhibitor "SpBrBzGSHCp2" was used to increase the endogenous levels of MGO. For the *in vivo* study, C57bl6 mice were intraperitoneally injected with a MGO solution at steadily increasing concentrations (50 to 75mg/kg) for 7 weeks.

MGO incubation induces a 50% reduction of IRS1 phosphorylation, the loss of IRS1-p85 interaction and of the downstream Akt activation in response to insulin, whilst MAPK is more active in BAEC treated with MGO. The insulin-induced Akt activation is reverted by the inhibition of ERK through the use of MEK inhibitor U0126 in BAEC treated with MGO. Furthermore, downstream Akt, MGO is able to inhibit eNOS activation in response to insulin, and this was paralleled by a 60% decrease of insulin-induced NO production in BAEC. Similar results were obtained in BAEC treated with SpBrBzGSHCp2 compared to controls. Intraperitoneally administration of MGO to mice caused insulin resistance (ITT AUC: C57MGO 10163±1979 vs C57 7787±1174 mg/dl/120', p=0.01) and reduced serum NO by 2.5-fold compared to untreated mice. Western blots of lysates of aortae from MG-treated mice revealed a reduction of insulin-induced Akt activation.

In conclusion, this work shows that MGO impairs insulin signaling in endothelial cells and insulin effect on endothelial NO production both *in vitro* and *in vivo*. A possible role in these effects may be played by ERK. Further investigations of the molecular mechanisms by which hyperglycaemia compromises insulin action in vascular cells may allow to develop new strategies to preserve endothelial function in diabetic subjects.

Abbreviations:

AGE	Advanced Glycation End products
AKT/PKB	protein kinase B
CEL	Nε-carboxyethyl-lysine
CML	Nε-carboxymethyl-lysine
CVD	cardiovascular disease
DAG	diacylglycerol
ECE-1	Endothelin Converting Enzyme-1
ECM	Extra Cellular Matrix
eNOS	endothelial Nitric Oxide Synthase
ERK	Extracellular signal Regulated Kinase
ET1	Endothelin-1
GLOI	Glyoxalase I
GLUT4	Glucose Transporter type 4
GSH	Glutathione
HGA	Human Glycated Albumin
IR	Insulin Receptor
IRS	Insulin-Receptor Substrate
JNK	Jun N-terminal Kinase
MAP	Mitogen Activated Protein
MGO	Methylglyoxale
N-GlcNAc	N-Acetyl Glucosamine
NO	Nitric Oxide
PI3K	Phosphatidyl Inositol 3-Kinase
PKC	Protein Kinase C
RAGE	Receptor for Advanced Glycation End products
ROS	Radical Oxygen Species
SpBrBzGSH	Bromobenzylglutathione cyclopentyl diester
T1D	Type 1 Diabetes
T2D	Type 2 Diabetes
vSMC	vascular Smooth Muscle Cells

BACKGROUND

1.1 Insulin Resistance: a common feature of different metabolic disorders and their complications.

Insulin resistance plays a major patho-physiological role in type 2 diabetes and is tightly associated with major public health problems including obesity, hypertension, coronary artery disease, dyslipidemias, and a cluster of metabolic and cardiovascular abnormalities that define the metabolic syndrome (De Fronzo and Ferrannini 1991; Petersen et al. 2007). Insulin resistance is defined clinically as the inability of a known quantity of exogenous or endogenous insulin to produce its biological effects, as the increase of glucose uptake and utilization. Several mechanisms have been proposed as possible causes underlying the development of insulin resistance and the insulin resistance syndrome. These include: genetic abnormalities of one or more proteins of the insulin action cascade, fetal malnutrition and increases in visceral adiposity (Lebovitz et al. 2001).

As reported above, insulin-resistance is a hallmark of type 2 diabetes, a complex heterogeneous group of metabolic conditions characterized by elevated levels of serum glucose and resulting from defects in both insulin secretion and insulin sensitivity. It is associated with an increased and premature risk of cardiovascular disease as well as specific microvascular complications, including retinopathy, nephropathy, and neuropathy (Srinivasan et al. 2008). Type 2 diabetes pathogenesis results from interactions of a number of genes with environmental factors such as obesity, age, and nutrition. Multiple prospective studies have documented an association between insulin resistance and accelerated cardiovascular disease (CVD) in patients with type 2 diabetes. The molecular causes of insulin resistance are responsible for the impairment in insulin-stimulated glucose metabolism and contribute to the accelerated rate of CVD in type 2 diabetes patients. The current epidemic of diabetes is being driven by the obesity epidemic, which represents a state of tissue fat overload. Accumulation of toxic lipid metabolites (fatty acyl CoA, diacylglycerol, ceramides) in muscle, liver, adipocytes, beta cells and arterial tissues contributes to insulin resistance, beta cell dysfunction and accelerated atherosclerosis in type 2 diabetes (DeFronzo et al. 2010). These complex metabolic disorders are complicated by vascular disease (De Fronzo et al. 2009). Hyperglycaemia is the major risk factor for microvascular complications (Stratton et al. 2000). Hyperglycaemia toxic effects regard above all those tissues in which cellular glucose uptake is insulin-independent and that are unable to block glucose entrance, like retina, kidney, blood vessels and nerves

(Schleicher and Nerlich 1996). Thus, the metabolic alterations caused by hyperglycaemia affect different cell types, leading to both macrovascular and microvascular dysfunctions (Tooke 1995), and involving all the vascular tissue components together with circulating cells that infiltrate the vascular wall itself. Diabetic microangiopaty involves all body districts, although it leads to typical morphological features, regarding the specific organ structures and functions such as retina, nerves and renal glomeruli. Diabetic macroangiopaty consists on macrovascular damage of heart, brain and lower extremities arteries.

Although microvascular complications are a major cause of morbidity, macrovascular complications represent the primary cause of mortality with heart attacks and stroke accounting for around 80% of all deaths (Morrish et al. 2001).

Diabetes mellitus is commonly associated with systolic/diastolic hypertension. Much evidence indicates that the link between diabetes and essential hypertension is hyperinsulinemia. The reasons for the association of insulin resistance and essential hypertension can be sought in at least four general types of mechanisms: Na^+ retention, sympathetic nervous system overactivity, disturbed membrane ion transport, and proliferation of vascular smooth muscle cells. Calorie restriction (in the overweight patients) and regular physical exercise, can improve tissue sensitivity to insulin and lower blood pressure in both normotensive and hypertensive individuals. Insulin resistance and hyperinsulinemia are also associated with an atherogenic plasma lipid profile. Elevated plasma insulin concentrations enhance very-low-density lipoprotein (VLDL) synthesis, leading to hypertriglyceridemia. Progressive elimination of lipid and apolipoproteins from the VLDL particle leads to an increased formation of intermediate-density and low-density lipoproteins, both of which are atherogenic. Last, insulin, independent of its effects on blood pressure and plasma lipids, is known to be atherogenic. The hormone enhances cholesterol transport into arteriolar smooth muscle cells and increases endogenous lipid synthesis by these cells. Insulin also stimulates the proliferation of arteriolar smooth muscle cells, augments collagen synthesis in the vascular wall, increases the formation of and decreases the regression of lipid plaques, and stimulates the production of various growth factors (DeFronzo et al. 1991).

Together with type 2 diabetes, obesity rapresents an important risk factor for the development of cardiovascular diseases (Kearney et al. 2007). Nowadays, the adipose tissue is considered as an endocrine organ able to produce substances called adipo(cyto)kines that have different effects on lipid metabolism, closely involved in metabolic syndrome, and cardiovascular risk. The increased cardiovascular risk can be related also to peculiar dysfunction in the endocrine activity of adipose tissue observed in obesity responsible of vascular impairment (including endothelial dysfunction), prothrombotic tendency, and low-grade chronic inflammation (Maresca et al. 2011). In the setting of obesity, the over-

production of proinflammatory and pro-thrombotic adipokines is associated with insulin resistance. This mechanism represents the pathophysiological basis for the development of metabolic syndrome (Espinola-Klein et al. 2011). Excess fat, also deposited in visceral organs, generates chronic low-grade inflammation that eventually triggers insulin resistance and the associated comorbidities of metabolic syndrome (hypertension, atherosclerosis, dyslipidaemia and diabetes mellitus). The perivascular adipose tissue has a paracrine function, including the release of adipose-derived relaxant and contractile factors, akin to the role of the vascular endothelium, and contributing to the cardiovascular pathophysiology of the metabolic syndrome (Achike et al. 2011).

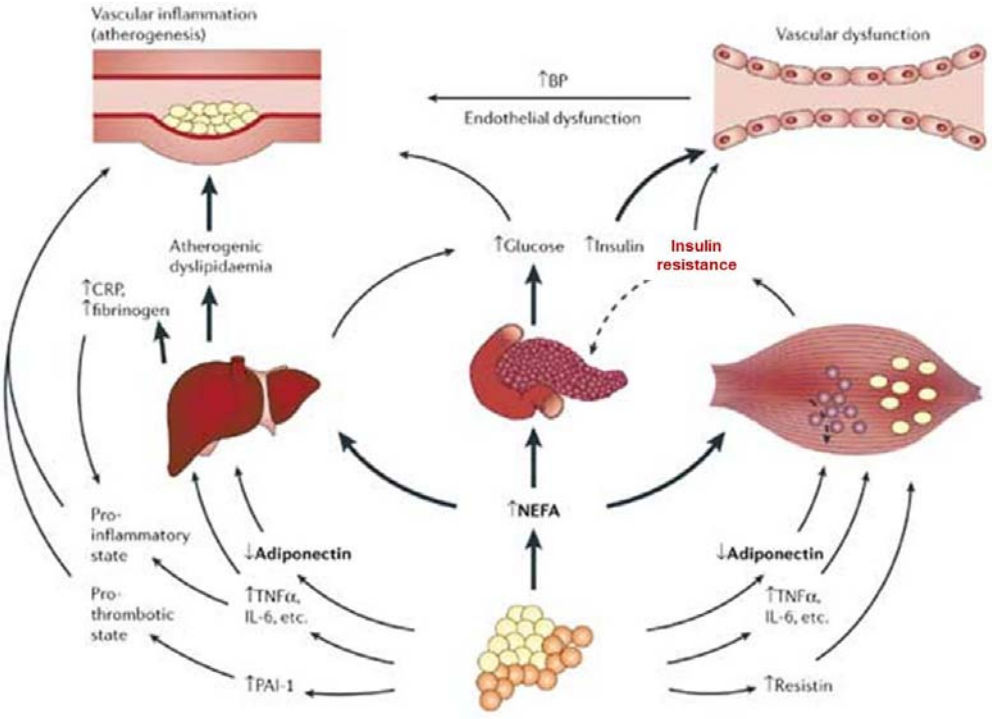

Figure 1: Metabolic and cardiovascular complications related to metabolic syndrome.

1.1.1 Insulin action.

Insulin is the most potent anabolic hormone known. Secreted by pancreatic beta cells in response to the increase in plasmatic glucose and amino acids levels after feeding, insulin promotes the synthesis and storage of carbohydrates, lipids and proteins, while inhibiting their degradation and release into the circulation. Insulin

stimulates the uptake of glucose, amino acids and fatty acids into cells, and increases the expression and the activity of enzymes that catalyse glycogen, lipid and protein synthesis, while inhibiting the activity or the expression of those that catalyse degradation. Insulin increases glucose uptake in muscle and fat, and it inhibits hepatic glucose production (glycogenolyisis and gluconeogenesis) in liver, thus serving as the primary regulator of blood glucose concentration. Insulin also stimulates cell growth and differentiation, and promotes the storage of substrates in fat, liver and muscle by stimulating lipogenesis, glycogen and protein synthesis, and inhibiting lipolysis, glycogenolysis and protein breakdown (Figure 1) (Saltiel and Kahn 2001).

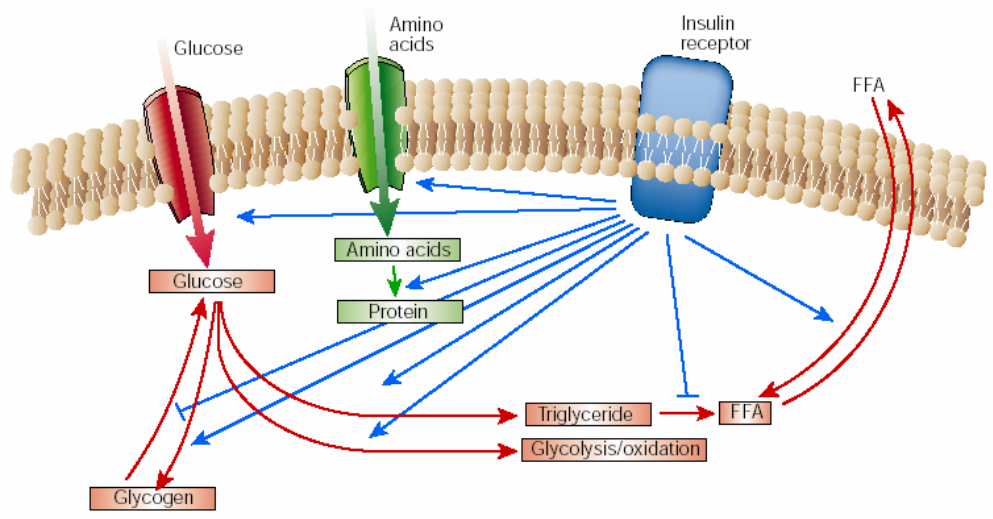

Figure 2: The regulation of metabolism by insulin. Insulin promotes the synthesis and the storage of carbohydrates, lipids and proteins. Indeed, insulin stimulates the uptake of glucose, amino acids and fatty acids into cells, and increases the expression or the activity of enzymes that catalyse glycogen, lipid and protein synthesis, while inhibiting the activity or the expression of those that catalyse degradation.

Insulin action is mediated through the insulin receptor (IR), a transmembrane glycoprotein with intrinsic protein tyrosine kinase activity. The insulin receptor belongs to a subfamily of receptor tyrosine kinases that includes the insulin-like growth factor (IGF)-I receptor and the insulin receptor-related receptor (IRR). These receptors are tetrameric proteins consisting of two α- and two β-subunits that function as allosteric enzymes where the α-subunit inhibits the tyrosine kinase activity of the β-subunit. Insulin binding to the α-subunit leads to derepression of the kinase activity of the β-subunit followed by transphosphorylation of the β-

subunits and conformational change of the α subunits that further increases kinase activity. Several intracellular substrates of the insulin receptor kinases have been identified (Figure 2). Four of these belong to the family of insulin-receptor substrate (IRS) proteins (White et al. 1998). Other substrates include Gab-1 and isoforms of Shc10 (Pessin and Saltiel 2000). The phosphorylated tyrosines in these substrates act as 'docking sites' for proteins that contain SH2 (Src homology-2) domains. Many of these SH2 proteins are adaptor molecules, such as the p85 regulatory subunit of PI(3)K and Grb2, or CrkII, which activate small G proteins by binding to nucleotide exchange factors. Others are themselves enzymes, including the phosphotyrosine phosphatase SHP2 and the cytoplasmic tyrosine kinase Fyn. PI(3)K has a pivotal role in the metabolic and mitogenic actions of insulin (Shepherd et al. 1995). It consists of a p110 catalytic subunit and a p85 regulatory subunit that possesses two SH2 domains that interact with tyrosinephosphorylated motifs in IRS proteins (Myers MG Jr 1992). PI(3)K catalyses the phosphorylation of phosphoinositides on the 3-position to produce phosphatidylinositol-3-phosphates, especially PtdIns(3,4,5)P3, which bind to the pleckstrin homology (PH) domains of a variety of signalling molecules thereby altering their activity, and subcellular localization (Lietzke et al. 2000). Phosphotidylinositol-3-phosphates regulate three main classes of signalling molecules: the AGC family of serine/threonine protein kinases, the Rho family of GTPases, and the TEC family of tyrosine kinases. PI(3)K also might be involved in regulation of phospholipase D, leading to hydrolysis of phosphatidylcholine and increases in phosphatidic acid and diacylglycerol. The best characterized of the AGC kinases is phosphoinositide-dependent kinase 1 (PDK1), one of the serine kinases that phosphorylates and activates the serine/threonine kinase Akt/PKB (Alessi et al. 1997). Akt/PKB has a PH domain that also interacts directly with PtdIns(3,4,5)P3, promoting membrane targeting of the protein and catalytic activation. Akt/PKB has a pivotal role in the transmission of the insulin signal, by phosphorylating the enzyme GSK-3, the forkhead transcription factors and cAMP response element-binding protein. Other AGC kinases that are downstream of PI(3)K signaling include the atypical PKCs, such as PKC-ζ. Akt/PKB and/or the atypical PKCs are required for insulin stimulated glucose transport (Standaert et al. 1997).

As is the case for other growth factors, insulin stimulates the mitogen activated protein (MAP) kinase extracellular signal regulated kinase (ERK) (Figure 2). This pathway involves the tyrosine phosphorylation of IRS proteins and/or Shc, which in turn interact with the adapter protein Grb2, recruiting the Son-of-sevenless (SOS) exchange protein to the plasma membrane for activation of Ras. The activation of Ras also requires stimulation of the tyrosine phosphatase SHP2, through its interaction with receptor substrates such as Gab-1 or IRS1/2. Once activated, Ras operates as a molecular switch, stimulating a serine kinase cascade

through the stepwise activation of Raf, MEK and ERK. Activated ERK can translocate into the nucleus, where it catalyses the phosphorylation of transcription factors such as p62TCF, initiating a transcriptional programme that leads to cellular proliferation or differentiation (Boulton et al. 1991).

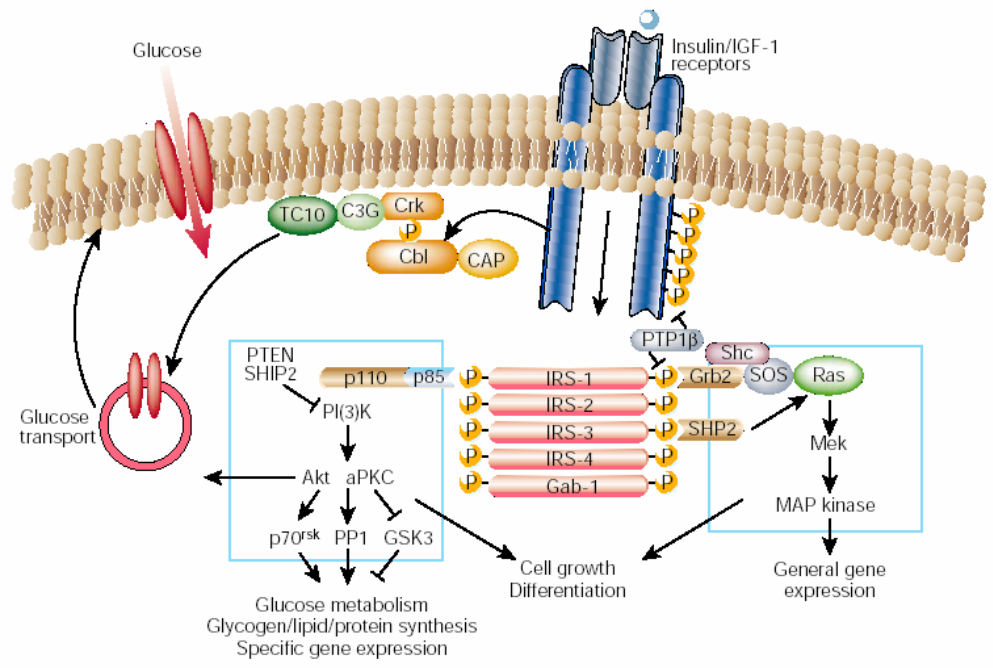

Figure 3: Signal transduction in insulin action. The insulin receptor is a tyrosine kinase that undergoes autophosphorylation, and catalyses the phosphorylation of cellular proteins such as members of the IRS family, Shc and Cbl. Upon tyrosine phosphorylation, these proteins interact with signaling molecules through their SH2 domains, resulting in a diverse series of signaling pathways, including activation of PI(3)K and downstream PtdIns(3,4,5)P3 dependent protein kinases, Ras and the MAP kinase cascade. These pathways act in a concerted fashion to coordinate the regulation of vesicle trafficking, protein synthesis, enzyme activation and inactivation, and gene expression, which results in the regulation of glucose, lipid and protein metabolism.

In addition to the above mentioned metabolic insulin action exerted on its canonical target tissues (muscle, fat and liver), it has recently become evident that insulin also acts on endothelium where, through the activation of its own receptor, it regulates the vascular tone (Sherrer et al. 1994).

1.2 Endothelium.

By the nature of its location, the endothelium acts as a blood container, but in addition, it actively regulates the passage of nutrients, hormones, and macromolecules into the surrounding tissue (Cersosimo and DeFronzo 2006). It is covered by a glycocalyx that contributes to the selectivity of its barrier function (van Haaren et al. 2003). Furthermore, the endothelium ensures the fluidity of blood by its contribution to hemostasis. Indeed, living endothelial cells are needed to prevent and limit blood coagulation and the formation of a platelet thrombus and to produce fibrinolysis regulators (van Hinsbergh 2001). The interaction between flowing blood and endothelium not only involves the interaction of blood constituents and cells with the endothelium, but also includes the sensing of mechanical forces, in particular shear forces that are exerted by the flowing blood on the endothelium. This sensing enables the endothelial cell to respond by acute vasoregulation and by inducing chronic adaptation of the blood vessel. Acute vasoregulation is achieved by the production of vasodilator factors, such as nitric oxide (NO), endothelium derived hyperpolarization factor (EDHF), and prostaglandins (PGI2/PGE2), of which the relative contribution varies between the different types of vessels (Shimokawa et al. 1996). Furthermore, in specific conditions, the endothelium is also able to induce the potent vasoconstrictor endothelin-1 (ET-1). Insulin also acts as a regulator of vasoregulation, as it is able to induce NO and ET-1 release (Schroeder et al. 1999; Cardillo et al. 1999; Ferri et al. 1995). Through the production of these chemical mediators, the "endothelial system" exerts actions on the surrounding vascular smooth muscle cells (vSMC) and cells in the blood leading to: vasodilation (bradykinin, NO) or vasoconstriction (ET-1, angiotensin II, radical oxygen species-ROS) of vSMC, stimulation of growth and changes in phenotypic characteristics of vSMC (angiotensin II, ROS) or inhibition of vSMC proliferation (NO), and manteinance of blood fluidity and normal coagulation (plasminogen activator inhibitor I) (Pandolfi and De Filippis 2007). Another important function of the endothelium lies in the regulation of a proper recruitment of leukocytes at sites of inflammation or an immune reaction. Again, both acute responses and chronic adaptation can cause induction of leukocyte adhesion molecules and other gene products. Inflammatory activation of the endothelium can occur, for example, after exposure to bacterial lipopolysaccaride and inflammatory cytokines, of which the potent inducers interleukin-1 (IL-1) and tumor necrosis factor-alpha (TNFα) have drawn the most attention. Inflammatory activation can also be induced by reactive oxygen intermediates (ROIs), which can be generated by the inflammation process itself and by disturbed metabolic conditions (Gimbrone 1999). Finally, the endothelium is the major vector in angiogenesis, the formation of new microvessels. This is not only important in development, growth, and tissue repair,

but also in capillary perfusion of muscle. Furthermore, in a number of diseases, an improper angiogenesis response causes unwanted growth, risk for local haemorrhage by immature vessels, or insufficient blood supply (Carmeliet 2005).

1.2.1 Insulin action on endothelium.

As reported above, endothelium is a new target tissue of insulin action. Insulin acts on endothelium as a mediator of vasoregulation, inducing the release of the vasodilator NO and the vasoconstrictor ET-1 (Schroeder et al. 1999). Insulin binding to its receptor on the endothelial cells activates the insulin receptor substrates: IRS-1 and IRS-2, thereby activating two different branches of insulin signaling. On one side, phosphatidyl inositol 3-kinase(PI3K) complexes with the phosphorylated IRS-1, activates by phosphorylation PKB/Akt, that in turns phosphorylates endothelial nitric oxide synthase (eNOS) at Ser1177 inducing its dimerization, NO release, and thus, vasodilatation (Zeng et al. 2000). The eNOS dimer generates NO by means of the conversion of arginine in(to) NO and L-cytrulline by a ratio of 1 to 1. This is an oxygen and NADPH-dependent reaction. Once produced, NO acts on vSMCs inducing their relaxation through the inhibition of the contractile apparatus and the activation of the cytosolic guanilate cyclase (cGC), leading to the increase of cyclic guanosine monophosphate (cGMP) intracellular levels (Andreozzi et al. 2007).

On the other side, through the activation of IRS-2, insulin activates the pro-atherogenic Ras-Raf-MAPK pathway which is associated with gene expression, mitogenesis, cell growth and, in the vascular endothelial cells, the activation of endothelin converting enzyme-1 (ECE-1) that produces the vasoconstrictor ET-1. Most of ET-1 is released at the abluminal side, where acts on vSMC inducing their contraction and proliferation, in addition to its chemotactic action to circulating monocyte (Cardillo et al. 1999; Kubota et al. 2003; Montagnani et al. 2002).

Defective insulin signalling causes reduced eNOS expression, inadequate production of NO and ET-1 and endothelial dysfunction both in vitro and in vivo (Bakker et al. 2009; Vincent et al. 2003; Federici et al. 2004). A selective impairment of the insulin-activated Akt signaling pathway with an intact MAPK pathway have been shown to underlie the profound insulin resistance in type 2 diabetic and obese non-diabetic individuals (Cusi et al. 2000). Furthermore, vasodilatation in response to insulin is blunted in skeletal muscle arterioles from insulin resistant animals, due to altered NO release through the PI3K/eNOS pathway (Eringa et al. 2007). In arteries from type 2 diabetic patients, the Akt signaling pathway is also downregulated leading to a decreased NO availability and therefore compromising arterial function (Okon et al. 2005).

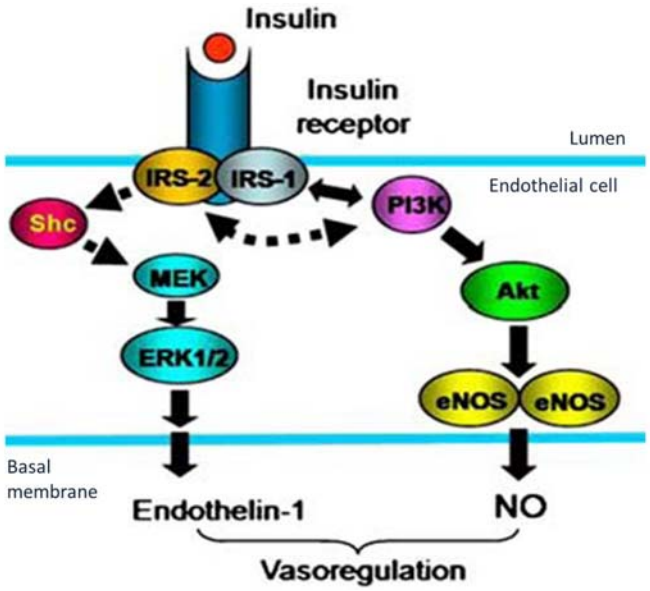

Figure 4: Insulin signal transduction in endothelial cells.

1.3 Endothelial dysfunction.

The functioning of the endothelium is flexible and adapts to various types of metabolic, mechanical, and inflammatory stress (Cines et al. 1998; Pober and Sessa 2007). However, when this functioning becomes inadequate, e.g., loss of NO generation, or exaggerated, e.g., improper inflammatory activation, one speaks of endothelial dysfunction. From a mechanistic point of view, as many endothelial dysfunctions exist as endothelial functions. They include changes in barrier function and hemostasis, reduced vasodilator responses, improper inflammatory activation, and angiogenesis (Table 1). In the clinical context, endothelial dysfunction is regarded as an important and early factor in the pathogenesis of atherothrombosis (Gimbrone 1999; Ross 1999) and vascular complications of diabetes (Stehouwer et al. 1997) and is associated with a number of traditional risk factors including hypercholesterolemia, smoking, hypertension, diabetes mellitus, insulin resistance and, more recently, obesity (Brook et al. 2001).

Type of endothelial dysfunction
Structural changes in endothelial barrier and matrix
Increased basal membrane thickness
Reduced glycocalyx
Formation of advanced glycation end products and improper matrix crosslinking
Microalbuminuria
Reduced vasodilator response (hypertension)
Reduced nitric oxide production
Increased endothelin-1 synthesis
Increased inflammatory activation
Increased expression of cell adhesion molecules and leukocyte adhesion
Increased production of and response to circulating mediators, including C-reactive protein
Altered hemostasis
Elevated plasma levels of von Willebrand factor
Reduced TM, increased plasminogen activator inhibitor-1

Table 1: Endothelial dysfunctions associated with the occurrence and severity of vascular complications in diabetes.

In diabetes, the basement membrane is thickened and altered in composition, because of the enhanced synthesis of matrix proteins by transforming growth factor beta (TGF-β) activity (Chen et al. 2001). At the same time, the thickness of the glycocalyx, which contains large amounts of heparan sulfate proteoglycans, is markedly reduced (Nieuwdorp et al. 2006a, 2006b). Loss of the glycocalyx leads to the adhesion of mononuclear cells and platelets to the endothelial surface, attenuated NO availability, and to an increased leakage of macromolecules through the endothelium of many vessels in hyperglycemia and diabetes (Berg et al. 2006). Hyperglycemia is an etiological factor of endothelial barrier injury, as it can stimulate crosslinking and modification of matrix proteins by glyco-oxidation (Naka Y et al. 2004).

A key feature of endothelial dysfunction is the reduced vasodilator response, that limits the delivery of nutrients and hormones to the distal tissues. Two mechanisms play an important role: the decreased bioavailability of the vasodilator NO, and the increased synthesis of ET-1 by activated endothelial cells inducing vasoconstriction. The bioavailability of NO is determined by a balance of NO production by eNOS and reduction of active NO by quenching of NO by ROIs. ROIs, and superoxide anion in particular, react with NO and form peroxynitrite that contributes to eNOS uncoupling, thus aggravating reduced NO production. Moreover, ROIs reduce the availability of tetrahydrobiopterin (BH4), a cofactor required for NO synthesis from eNOS, and inhibits the enzyme dimethylarginine dimethylaminohydrolase (DDAH) that converts the endogenous eNOS inhibitor

asymmetric dimethylarginine (ADMA), thus suppressing NO production (Lin et al. 2002). Insulin resistance and oxidative stress, such as that induced by hyperglycemia, can both contribute to an increased production of the potent vasoconstrictor ET-1. The balance between NO- and ET-1-dependent pathways plays a major role in vasoregulation by insulin and the dysfunction of vasoregulation in diabetes and obesity. Other vasodilating factors such as endothelium-derived hyperpolarization factor (EDHF) may also be altered in diabetic animals (De Vriese et al. 2000).

The generation of ROIs and AGEs also activates the nuclear factor kappa-B (NF-κB) pathway with, subsequently, the activation of numerous genes involved in inflammation, including C reactive protein (CRP), PECAM-1, VCAM-1 and ICAM-1 (Pober and Sessa 2007). As they represent major receptors controlling the influx of monocytes and other inflammatory cells into the arterial wall, their expression is considered as a hallmark in the etiology of atherosclerosis (Gimbrone et al. 1999).

Several proteins involved in hemostasis have been evaluated as potential risk indicators of cardiovascular disease in diabetes (Alessi and Juhan-Vague 2008). Among these: increased soluble thrombomodulin and Von Willembrant Factor (vWF) levels may point to a procoagulant state; decreased plasminogen activator and increased PAI-1 levels may point to reduced fibrinolysis.

Finally, the regeneration function of endothelial cells as represented by angiogenesis is dysfunctional in hyperglycemia and diabetes. Diabetes patients have poor wound healing, impaired collateral formation after vascular occlusion or myocardial infarction, and an increased risk of rejection of transplanted organs (Martin et al. 2003). Reduced vascularization probably also contributes to diabetic neuropathy. In contrast, an excessive neovascularization is observed in the eyes of patients with diabetic retinopathy, where hyperinsulinemia and overactivation of insulin and insulin-like growth factor-1 receptors contribute to VEGF expression (Aiello 2005).

1.4 Reciprocal relationships between endothelial dysfunction and insulin resistance.

Many risk factors for CVD, including dyslipidemia, hypertension, diabetes, obesity, and physical inactivity enhance the risk of developing both endothelial dysfunction and insulin resistance. Thus, endothelial dysfunction and insulin resistance frequently co-exist (Muniyappa 2008).

Recent studies report that higher levels of circulating plasma markers of endothelial dysfunction (PAI-1, vWF, E-selectin, ICAM-1) increase the risk of developing diabetes, supporting a potential causal role for endothelial dysfunction

in insulin resistance (Meigs et al. 2006). The central role of endothelium in regulating metabolic actions of insulin is also evident by the presence of insulin resistance and hypertension in eNOS knockout mice. In addition to microvascular changes including reduced capillary density, these animals show reduced glucose disposal, energy expenditure, increased triglyceride and FFA levels, and impaired mitochondrial function (Duplain et al. 2001). These studies prove that in animal models like in humans, partial defects in endothelial function characterized by reduced NO bioavailability are sufficient to cause cardio-metabolic abnormalities (insulin resistance and dyslipidemia) under pathogenic conditions (e.g., caloric excess, physical inactivity, inflammation).

On the other hand, in humans with metabolic insulin resistance (obese and type 2 diabetic subjects) there is parallel impairment in insulin's ability to induce vasodilation. At the cellular level, a key feature of insulin resistance is the pathway-selective impairment in PI3K-dependent signaling pathways while other insulin signaling branches including Ras/MAPK-dependent pathways are relatively unaffected. This has important pathophysiological implications because metabolic insulin resistance is typically accompanied by compensatory hyperinsulinemia to maintain euglycemia. In the vasculature and elsewhere, hyperinsulinemia will overdrive unaffected MAPK-dependent pathways leading to an imbalance between PI3K- and MAPK-dependent of insulin functions. The imbalance between PI3K/Akt/eNOS/NO and MAPK/ET-1 vascular actions of insulin provoked by dyslipidemia, hyperglycemia, and inflammatory cytokines may contribute to both impaired vascular and metabolic insulin actions. Indeed, compensatory hyperinsulinemia that typically accompanies pathway selective

insulin resistance (in PI3K pathways) activates unopposed MAPK pathways leading to enhanced pro-hypertensive and atherogenic actions of insulin (Kim et al. 2006).

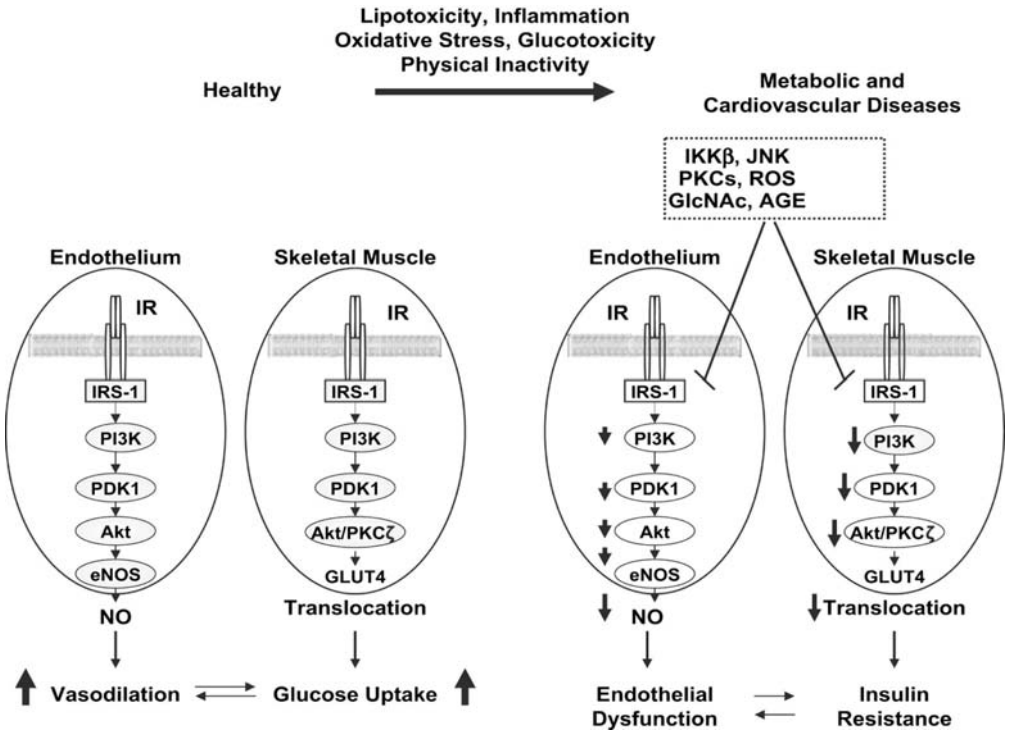

Figure 5: Relationship between insulin resistance and endothelial dysfunction. Parallel PI3k–dependent insulin-signaling pathways in metabolic and vascular tissues synergistically couple metabolic and vascular physiology under healthy conditions (on the left). Parallel impairment in insulin-signaling pathways under pathological conditions contributes to synergistic coupling of insulin resistance and endothelial dysfunction (on the right).

1.4.1 Potential mechanisms.

Shared causal factors such as glucotoxicity, lipotoxicity, inflammation, and oxidative stress interact at multiple levels to create reciprocal relationships between insulin resistance and endothelial dysfunction that may help to explain the frequent clustering of metabolic and cardiovascular disorders.

Proinflammatory Cytokines

Insulin resistance and endothelial dysfunction are characterized by elevated circulating markers of inflammation (Kim et al. 2006). Visceral fat accumulation may play a key role in the development of the systemic pro-inflammatory state associated with insulin resistance (Hotamisligil 2006). Among these cytokines, TNF-α activates a variety of serine kinases including JNK and IKKβ that directly or indirectly increase serine phosphorylation of IRS-1/2, leading to decreased

insulin-stimulated activation of PI3K/Akt/eNOS in endothelial cells (Gustafson et al. 2007; Anderson et al. 2004; Eringa 2004; Zhang et al. 2003). In addition, TNF-α increases ET-1 secretion in a MAPK-dependent fashion (Sury 2006). Similarly, C-reactive protein (CRP) has important biological actions to inhibit insulin-evoked NO production in endothelial cells through specific inactivation of the PI3K/Akt/eNOS pathway, and increases endothelial ET-1 production. IL-6 also inhibits insulin-stimulated increases in eNOS activity and NO production in the endothelium (Andreozzi et al. 2007). Systemic infusion of high doses of TNF-α results in the loss of insulin-induced increases in glucose uptake, limb blood flow, and capillary recruitment in rat hind limb (Zhang et al. 2003). Thus, proinflammatory cytokines may contribute to coupling metabolic and vascular insulin resistance manifested by impaired insulin signaling and endothelial dysfunction.

Adipokines

Adipocyte-derived hormones such as leptin and adiponectin have both metabolic and vascular actions. Adiponectin is an anti-inflammatory peptide whose circulating levels are positively correlated with insulin sensitivity and that may serve to link obesity with insulin resistance (Koh et al. 2005). Similar to insulin, adiponectin has vasodilator actions as it stimulates NO production, enhances NO bioavailability by upregulating eNOS expression and reducing ROS production in endothelial cells (Motoshima et al. 2004). Decreased plasma adiponectin levels are observed in patients with obesity, type 2 diabetes, hypertension, metabolic syndrome, and CVD (Lau et al. 2005). Leptin is a key regulator of appetite, body weight and energy balance in the CNS and acts directly on the vasculature, where it induces endothelium-dependent vasodilation through a PI3K/Akt/eNOS pathway (Vecchione et al. 2002). Leptin evoked vasodilation is opposed by sympathetically-induced vasoconstriction. In contrast to its vasodilator effects, leptin also increases sympathetic nerve activity. Paradoxically, circulating leptin levels are elevated in obesity, apparently contradicting the beneficial effects of leptin. To explain this, recent studies have demonstrated the impairment of leptin's metabolic effects and leptin-induced NO production, i.e. "leptin resistance", in obesity and human hypertension. Therefore, resistance to the vasodilator effects of leptin may contribute to vascular dysfunction in obesity (Bakker et al. 2008).

Lipotoxicity

Patients with type 2 diabetes mellitus or metabolic syndrome have a distinctive dyslipidemia characterized by hypertriglyceridemia, elevated blood levels of apolipoprotein B, small, dense LDL cholesterol, and low levels of HDL cholesterol. This contributes to endothelial dysfunction, atherosclerosis, and insulin resistance. Treatment of vascular endothelial cells with FFA impairs

insulin-stimulated activation of PI3K, PDK1, Akt and eNOS. Elevated cellular levels of lipid metabolites such as diacylglycerols, ceramide, and long-chain fatty acyl CoAs activate serine kinases such as PKC and IKKβ that cause insulin resistance by increasing serine phosphorylation of IRS-1 (Du et al. 2006; Kim et al. 2005; Wang et al. 2006). In support of these findings, raising circulating FFA levels significantly impairs insulin induced increases in skeletal muscle capillary recruitment with a concomitant decrease in glucose disposal (Clerk 2002). Moreover, FFA infusion in humans accentuates insulin-mediated ET-1 release. These studies suggest that in the context of pathway selective impairment of PI3K signaling induced by elevated FFA levels, insulin stimulates increased ET-1 secretion through an unopposed MAPK signaling that leads to relative vasoconstriction and insulin resistance.

Glucotoxicity

Hyperglycemia associated with impaired glucose tolerance and diabetes causes insulin resistance and endothelial dysfunction by increasing oxidative stress, formation of advanced glycation end products (AGEs), and flux through the hexosamine biosynthetic pathway. Hyperglycaemia impairs insulin action in skeletal and cardiac muscle as well as in vascular endothelium. Activity of Akt and eNOS in vasculature and muscle is significantly attenuated in patients with diabetes when compared with non-diabetics (Kashyap et al. 2005. By contrast with deleterious effects on the PI3K/Akt/eNOS pathway, hyperglycemia enhances endothelial ET-1 secretion and thereby alters the balance between NO and ET-1 to favor vasoconstriction and endothelial dysfunction. An oral glucose load significantly increases plasma ET-1, in insulin-resistant, but not in healthy individuals (Desideri et al. 1997). Thus, a parallel increase in ET-1 activity and diminished NO bioactivity associated with hyperglycemia and insulin resistance may contribute to abnormal vascular function. This illustrates the altered balance between the vasodilator and vasoconstrictor actions of insulin in insulin resistant states that contributes to reciprocal relationships between insulin resistance and endothelial dysfunction (Muniyappa et al. 2008).

1.5 Mechanisms of Glucotoxicity.

Four main molecular mechanisms have been implicated in glucose-mediated vascular damage. These include: increased polyol pathway flux; activation of protein kinase C (PKC) isoforms; increased hexosamine pathway flux; and increased advanced glycation end-product (AGE) formation. All seem to reflect a single hyperglycaemia-induced process of overproduction of superoxide by the mitochondrial electron-transport chain (Brownlee 2001).

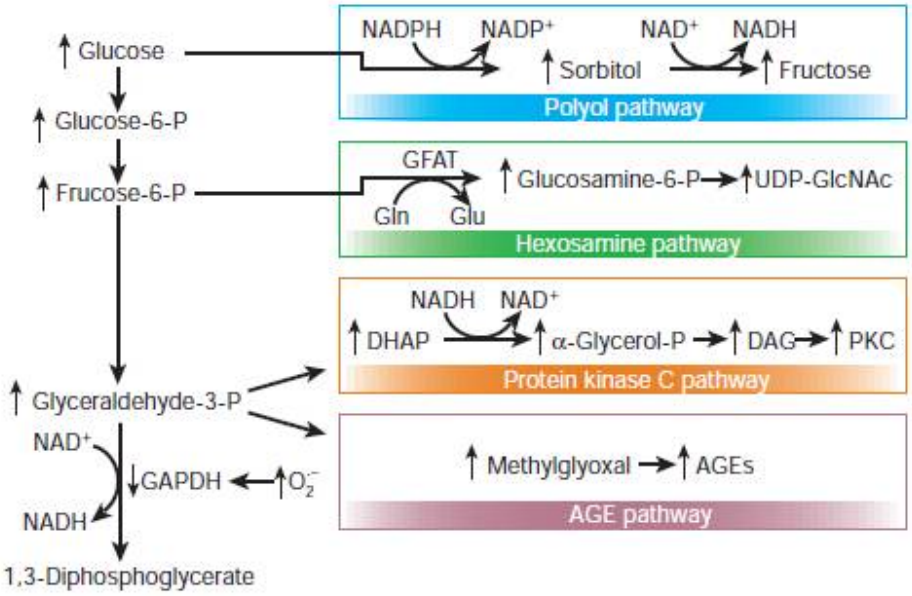

Figure 6: Potential mechanism by which hyperglycaemia -induced mitochondrial superoxide overproduction activates four pathways of hyperglycaemic damage.

The first mechanism includes the aldose reductase activity. It's the first enzyme in the polyol pathway, that catalyses the NADPH-dependent reduction of a wide variety of carbonyl compounds, including glucose. Aldose reductase has a low affinity for glucose, and at the normal glucose concentrations, metabolism of glucose by this pathway is a very small percentage of total glucose use. But in a hyperglycaemic environment, increased intracellular glucose results in its increased enzymatic conversion to the polyalcohol sorbitol, with concomitant decreases in NADPH. In the polyol pathway, sorbitol is oxidized to fructose by the enzyme sorbitol dehydrogenase, with NAD^+ reduced to NADH. The mechanisms proposed to explain the potential detrimental effects of hyperglycaemia-induced increases in polyol pathway flux, include sorbitol-induced osmotic stress, decreased $(Na^+ + K^+)$ATPase activity, an increase in cytosolic NADH/NAD^+ and a decrease in cytosolic NADPH. Sorbitol does not diffuse easily across cell membranes, and it was originally suggested that this resulted in osmotic damage to microvascular cells. It has also been proposed that reduction of glucose to sorbitol

by NADPH consumes NADPH. As NADPH is required for regenerating reduced glutathione (GSH), this could induce or exacerbate intracellular oxidative stress.

The PKC family comprises at least eleven isoforms, nine of which are activated by the lipid second messenger diacylglycerol (DAG), that is increased by intracellular hyperglycaemia in cultured microvascular cells and in the retina and renal glomeruli of diabetic animals. Hyperglycaemia seems to achieve this primarily by increasing *de novo* DAG synthesis from the glycolytic intermediate dihydroxyacetone phosphate, through reduction of the latter to glycerol-3-phosphate and stepwise acylation (Koya and King 1998). Besides, it may also activate PKC isoforms indirectly through both ligation of AGE receptors (Portilla et al. 2000) and increased activity of the polyol pathway (Keogh et al. 1997), presumably by increasing reactive oxygen species. The activation of PKC-β and PKC-δ has been shown to mediate blood flow abnormalities by depressing nitric oxide production and/or increasing endothelin-1 activity (Fig. 3), inhibiting the insulin-stimulated expression of eNOS mRNA (Kuboki et al. 2000), increasing ET1-stimulated MAPK activity, and inducing the expression of the permeability enhancing factor VEGF in smooth muscle cells (Williams et al. 1997). Moreover, activation of PKC contributes to increased microvascular matrix protein accumulation by inducing expression of TGF-β1, fibronectin and type IV collagen both in cultured mesangial cells and in glomeruli of diabetic rats (Koya et al. 1997). Hyperglycaemia-induced activation of PKC has also been implicated in the overexpression of the fibrinolytic inhibitor PAI-1, the activation of NF-kB and of various NAD(P)H-dependent oxidases, leading to a pro-inflammatory state (Yerneni et al. 1999) and the increase of ROS formation.

Shunting of excess of intracellular glucose into the hexosamine pathway might also cause several manifestations of diabetic complications (Kolm-Litty et al. 1998). (Fig. 4). In the physiological state, about 1-3% of intracellular glucose is diverted from glycolysis to this pathway, through which fructose-6-phosphate is converted to N-acetylglucosamine by fructose-6-phosphate amidotransferase (GFAT). Next, N-acetylglucosamine is transformed to N-acetylglucosamine 1-6 bisphosphate, and then, to UDP-N-acetylglucosamine, the allosteric inhibitor of GFAT and substrate of O-GlcNAc transferase (OGT), which catalyzes the binding of N-acetylglucosamine to serine and threonine residues through the O-glycosylation of various proteins. Among these, it has been demonstrated that the covalent modification of the transcription factor Sp1 by N-GlcNAc makes this factor more transcriptionally active, explaining the hyperglycaemia-induced increase of PAI-1 activation. In addition to transcription factors, another example of O-linked GlcNAc protein modification relevant to diabetic complications is the inhibition of eNOS activity by hyperglycaemia-induced O-acetylglucosaminylation at the Akt site of the eNOS protein (Du et al. 2001). Studies performed in our laboratory have demonstrated that high levels of GlcN,

similar to those found in diabetic patients, cause insulin-resistance in both human and rat myotubes through the induction of ER Stress. Moreover, GlcN-induced ER stress impairs GLUT4 production and insulin-induced glucose uptake via an ATF6-dependent decrease of the GLUT4 regulators MEF2A and PGC1α (Iadicicco et al. 2010). Furthermore, we have also found that GlcN-induced ER Stress causes de-differentiation of β-cells both in INS-1E cells and in primary mouse islets. This is shown by the down-regulation of beta cell markers and of the transcription factor, pancreatic and duodenal homeobox 1 (figure 7a-d). The de-differentiation of β-cells is associated to the loss of their physiological function as demonstrated by the inhibition of glucose-stimulated insulin-secretion in figure 7.e (Lombardi et al. 2011).

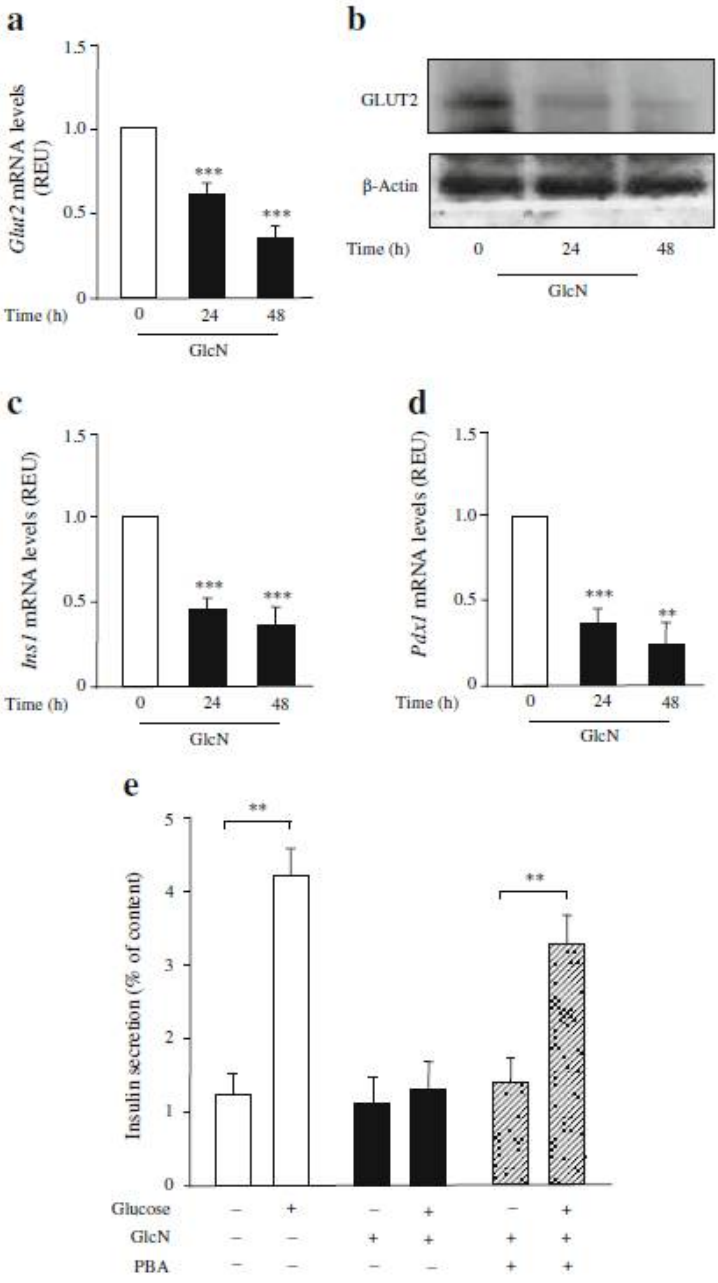

Figure 7: Effects of GlcN on beta cell-associated gene expression and glucose-induced insulin secretion in INS-1E cells.

Thus, activation of the hexosamine pathway by hyperglycaemia may result in many changes in both gene expression and protein function, which together contribute to the pathogenesis of diabetic complications.

AGEs are a heterogeneous family of irreversible non-enzymatically glycated molecules. AGEs form by the Maillard process, a non-enzymatic reaction between ketones or aldehydes and the amino groups of proteins, nucleic acids and lipids, contributing to the aging of these molecules and to the pathological complications of diabetes. In high glucose conditions, glucose reacts non-enzymatically with the amino groups of proteins to form a Shiff base, by means of a reversible protein glycosilation. If hyperglycemia persists, a Shiff base can rearrange to form a ketoamine adduct, so-called Amadori product, as a more stable glycated product. Finally, these early products eventually undergo further "irreversible" chemical modifications generating different classes of advanced glycation end products. Recent studies have suggested that AGEs can arise not only directly from sugars, but also from carbonyl compounds derived from the autoxidation of sugar (i.e.:glyoxal) and the fragmentation of the intermediate products or de-phosphorylation of triose phosphates, like MGO. These are highly reactive dicarbonyls, which can react with lysine and arginine functional groups on proteins, leading to the formation of stable AGE compounds, such as N-(carboxymethyl)lysine (CML) and N-(carboxyethyl)lysine (CEL) (Yamagishi and Takeuchi 2004).

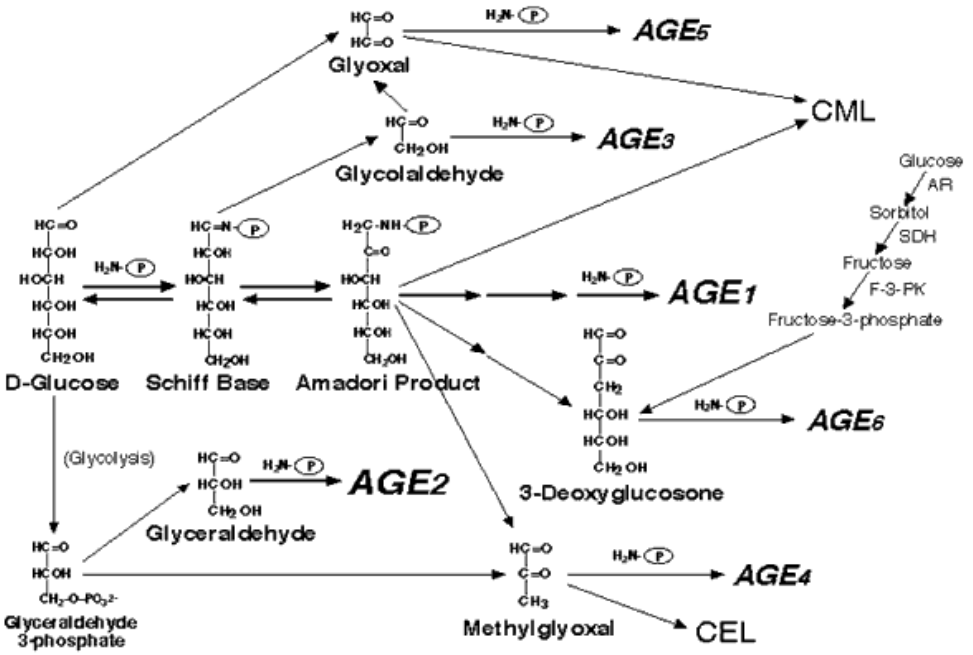

Figure 8: Alternative routes for the formation of AGEs.

AGEs are prevalent in the diabetic vasculature and contribute to the development of atherosclerosis. The presence and accumulation of AGEs in many different cell types affect extracellular and intracellular structure and function. AGEs contribute to a variety of microvascular and macrovascular diabetic complications through the formation of cross-links between molecules in the basement membrane of the extracellular matrix and by engaging the receptor for advanced glycation end products (RAGE). Activation of RAGE by AGEs causes upregulation of the transcription factor nuclear factor-kβ and its target genes. AGE-bound RAGE increases endothelial permeability to macromolecules. AGEs block nitric oxide activity in the endothelium and cause the production of reactive oxygen species. In the ECM, AGEs form on a variety of different molecules, including lipids, collagen, laminin, elastin, and vitronectin. The formation of AGEs on ECM molecules alters the constitution of the matrix and increases stiffness. AGEs also activate the transforming growth factor (TGF)-receptor to stimulate cell growth, leading to increased ECM production. AGEs that bind to RAGE on the endothelial cell surface lead to a signaling cascade, stimulating NAD(P)H oxidase and increasing ROS, p21 RAS, and MAPKs. In addition, the ligand-RAGE interaction also may stimulate signaling via p38 MAPK and Rac/Cdc. A key target of RAGE signaling is NF-kB. NF-kB is translocated to the nucleus, where it increases transcription of a number of different proteins, including endothelin-1, ICAM-1, E-selectin, and tissue factor. AGE and ligands for RAGE, such as HMGB1 and S100 calgranulins, trigger inflammatory pathways. Moreover, AGE may decrease NO availability by the decreased activity of NOS and by quenching NO. Then, AGEs activate monocytes, causing increased expression of macrophage scavenger receptor (MSR) class A receptors and CD36 receptors, leading to increased OxLDL uptake and foam cell formation, as represented in figure 9 (Goldin et al. 2006).

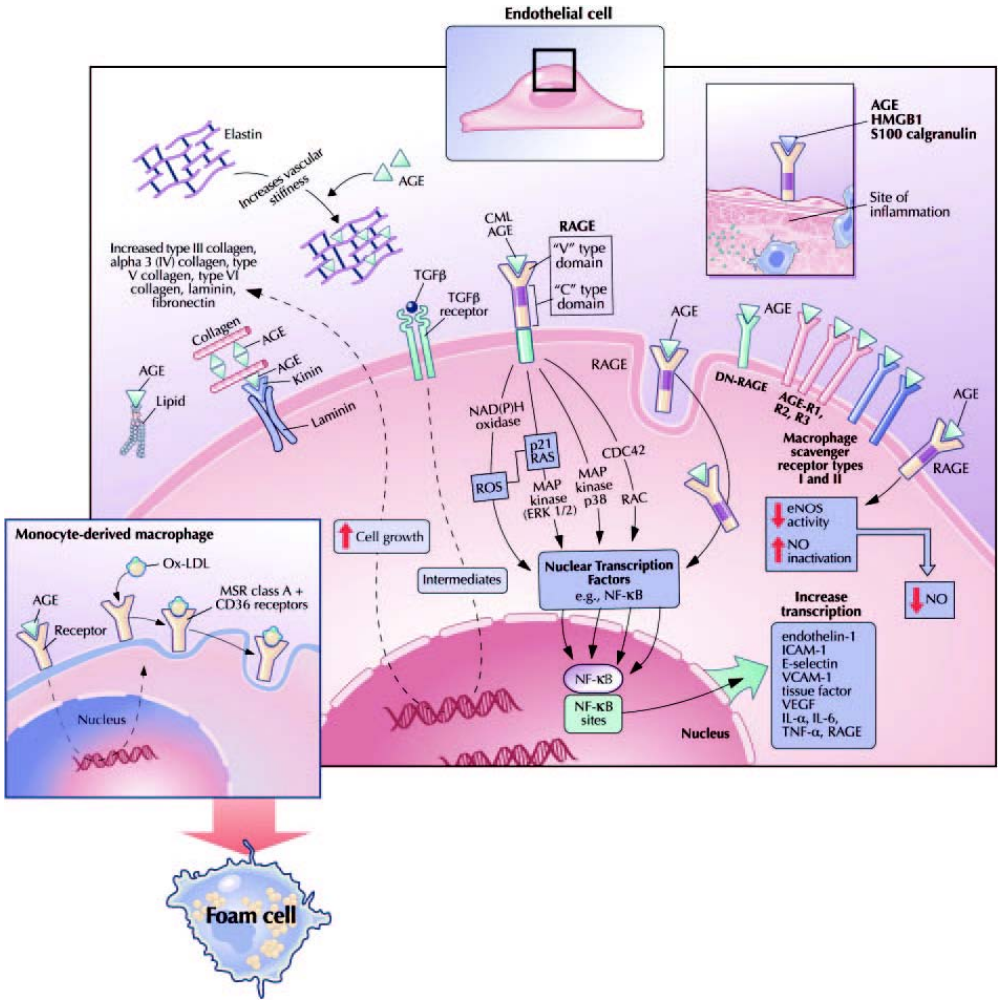

Figure 9: The extracellular and intracellular effects of AGEs.

Besides the vasculature, the accumulation of AGEs that occurs in a hyperglycaemic environment also affects the insulin sensitivity of skeletal muscle. Indeed, as we have recently shown, in both L6 myotubes and in mice fed a high AGEs diet human glycated albumin (HGA) induces insulin resistance by activating protein kinase C α(PKCα), through the formation of a multimolecular complex including RAGE/IRS-1/Src and PKCα (Miele et al. 2003; Cassese et al. 2008).

Finally, it has recently become clear that AGEs also influence physiological aging and neurodegenerative diseases (Schlotter et al. 2009; Bierhaus and Nawroth 2009).

1.6 Methylglyoxal.

One of the main precursors of AGEs is Methylglyoxal (MGO). It belongs to a class of reactive carbonyl species known as the α-oxoaldehydes. These molecules contain 2 adjacent carbonyl groups and are therefore referred to as dicarbonyls . This chemical moiety makes the dicarbonyls a highly reactive class of carbonyl species, generated from carbohydrate metabolism and autoxidation, collectively referred to as 'glycation'(Fleming et al. 2010). MGO is formed mainly by the fragmentation of Amadori products or the spontaneous degradation of triosephosphates (glyceraldehyde-3-phosphate and dihydroxyacetone phosphate) and also by the metabolism of ketone bodies, threonine degradation and the fragmentation of glycated proteins. Recent estimates for the concentration of MGO in human blood plasma are in the range of 100–120 nM, while cellular concentrations for MGO are in the range of 1–5 μM (Thornalley 2008). MGO serum concentration increases by 5-6 fold in patients affected by T1D, and by 2-3 fold in T2D patients (McLellan et al. 2002). As the formation of dicarbonyls is closely linked to the rate of glycolysis within the cell and the presence of glycolytic intermediates, it would be expected that under conditions where there is either an increase in glycolytic flux or an increased dependence on glycolysis for energy, the rate of dicarbonyls formation will be increased. This has been shown to be the case in patients with diabetes mellitus, where complications such as nephropathy, neuropathy and retinopathy can be linked to increases in cellular levels of AGEs (Beisswenger et al. 2003).

MGO is a potent glycating agents. As described above, glycation of proteins is a complex series of parallel and sequential reactions, that occur in all tissues and body fluids. Historically, the reactions of lysyl side chain and N-terminal amino groups with glucose to form fructosyl-lysine and fructosamines, respectively, have been the major glycation processes studied. The formation of these adducts under physiological conditions is now generally classified as an early glycation process. Later-stage reactions form stable end-stage adducts, the AGEs. Important AGEs quantitatively are hydroimidazolones derived from arginine residues modified by MGO. There is also concurrent formation of minor lysine derived adducts Nε-carboxymethyl-lysine (CML) and Nε-carboxyethyl-lysine (CEL) residues, and bis(lysyl) crosslinks (GOLD and MOLD). DNA is susceptible to glycation by MGO too. The nucleotide most reactive under physiological conditions is deoxyguanosine (dG). The presence of nucleotide dG-MGO in DNA is associated with increased mutation frequency, DNA strand breaks and cytotoxicity (Thornalley 2008).

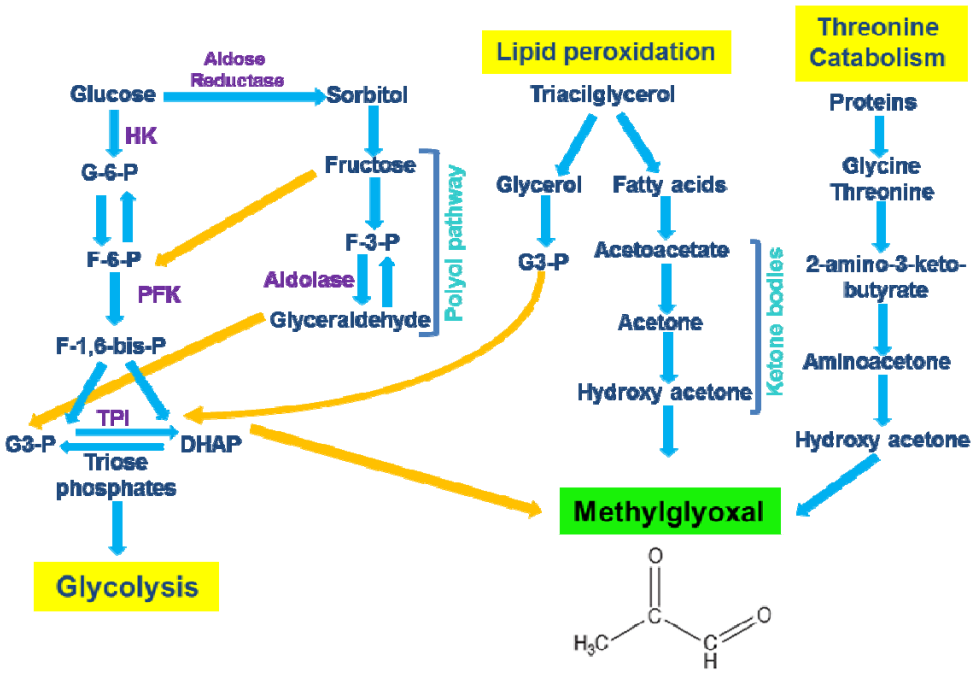

Figure 10: Non-enzymatic reactions leading to MGO formation. MGO derives from triose-phosphates dephosphorylation, from lipid peroxidation and from threonine catabolism.

1.6.1 Damaging effects of Methylglyoxal.

The physiological importance of protein glycation is under intensive investigation. Particularly damaging effects are produced by covalent crosslinking of proteins which confers resistance to proteolysis. Protein modification is also damaging when amino acid residues are located in sites of protein-protein interaction, enzyme-substrate interaction and protein-DNA interaction (for transcription factors) (Fleming et al. 2010). The interaction of MGO with amino acids can induce oxidative stress and free radical production, involved in the pathogenesis of chronic diabetic complications, included retinopathy, nephropathy, and neuropathy. Moreover, MGO can increase oxidative stress trough the glycosylation and inactivation of antioxidant enzymes (i.e., glutathione reductase and glutathione peroxidase) (Kim et al. 2008). A bioinformatics analysis of receptor binding domains indicated that arginine residues have the highest probability of being located in such sites (19.6%) (Gallet et al. 2000). The major modification of proteins by MGO is on arginine residues. Formation of hydroimidazolones causes structural distortion, loss of side chain charge and functional impairment. Studies looking at the modification of human serum

albumin and vascular basement membrane type IV collagen by MGO have shown that formation of the hydroimidazolone causes loss of albumin electrostatic interaction due to the disruption of arginine-directed hydrogen bonding (Ahmed et al. 2005), and endothelial cell detachment, anoikis and inhibition of angiogenesis because of the formation of hydroimidazolone residues at hotspot modification sites in integrin-binding sites of collagen (Dobler D et al. 2006).

The oxidative damage induced by MGO-amino acids interaction leads to cytotoxicity and apoptosis as well. Indeed, it has been demonstrated that high levels of MGO can cause the apoptosis of bovine retina's pericytes through the activation of the transcriptional factor NF-kβ; and treatment of pericytes with anti-inflammatory agents inhibits the cytotoxicity induced by NF-kβ in response to MGO (Kim et al 2004). How MGO triggers apoptosis is not clear yet. Probably, Jun N-terminal Kinase (JNK) is activated by MGO and induces the cytochrome C release from mitochondria leading to mitochondrial dysfunction, oxidative stress, and then, cell death (Takagi et al. 2004).

Furthermore, direct effects of MGO on lifespan have been demonstrated in the model organism C. elegans, in which increased detoxification of MGO by overexpression of its detoxifying enzyme Glyoxalase I (GLOI) increased lifespan by 40%, while RNAi-mediated silencing of GLO-I decreased lifespan by 40%. Overexpression of GLO-I also decreased dicarbonyl-derived AGEs as well as the concentration of markers of oxidative and nitrosative damage (Morcos et al. 2008; Schlotter et al. 2009).

The association between high levels of MGO and insulin-resistance have been documented by several studies. Fructose-fed rats show serum accumulation of MGO together with increased triglycerides and insulin levels, hypertension and decreased insulin-stimulated glucose uptake in adipose tissue (Jia and Wu 2007). Also 3T3L-1 adipocytes treated with MGO show a reduced insulin signal transduction: the decreased phosphorylation of IRS-1, the reduced PI3K activity and glucose uptake in response to insulin stimulation. Moreover, MGO treatment of L6 skeletal muscle cells reduces the insulin dependent activation of IRS1/PI3K/Akt signaling activation and glucose uptake, independently of the formation of intracellular reactive oxygen species (Riboulet-Chavey et al. 2006). As demonstrated by our recent studies, also β-cell function is impaired by MGO, which inhibits insulin-induced IRS/PI3K/PKB pathway activation, abolishes glucose-indiced insulin secretion and the insulin- and glucose-induced expression of Ins1, Gck and Pdx1 mRNA in INS-1E cells (F. Fiory et al. 2011).

1.6.2 Detoxification of methyglyoxal: the Glyoxalase system.

Present in the cytosol of all cells, the glyoxalase system catalyses the conversion of reactive, acyclic α-oxoaldehydes into the corresponding α-hydroxyacids. It is composed of two enzymes, glyoxalase I and glyoxalase II, and a catalytic amount of GSH. Glyoxalase I catalyses the isomerization of the hemithioacetal, formed spontaneously from α-oxoaldehyde (RCOCHO) and GSH, into S-2-hydroxyacylglutathione derivatives [RCH(OH)CO-SG]:

$$RCOCHO + GSH \leftrightarrow RCOCH(OH)\text{-}SG \rightarrow RCH(OH)CO\text{-}SG$$

Glyoxalase II catalyses the conversion of S-2-hydroxyacylglutathione derivatives into α-hydroxyacids and re-forms GSH consumed in the glyoxalase I-catalysed reaction step. The major physiological substrate for glyoxalase I is MGO, and this accumulates markedly when glyoxalase I is inhibited in situ by cell-permeable glyoxalase I inhibitors and by depletion of GSH. Other substrates are glyoxal (formed by lipid peroxidation and the fragmentation of glycated proteins), hydroypyruvaldehyde (HOCH2COCHO) and 4,5-doxovalerate (H-COCOCH2CH2CO2H). Glyoxalase I activity prevents the accumulation of these reactive α-oxoaldehydes and thereby suppresses α-oxoaldehyde-mediated glycation reactions. It is, therefore, a key enzyme of the antiglycation defence.

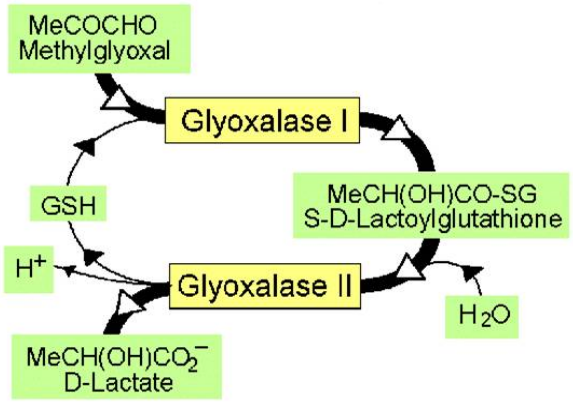

Figure 11: The glyoxalase system.

Glyoxalase I activity is present in all human tissues. Specific activities of fetal tissues are approximatively 3 times higher than those of corresponding adult tissues. Human glyoxalase I is a dimer, expressed at a diallelic genetic locus, GLO, which encodes two similar subunits in heterozygotes; the three alloenzymes are designated GLO 1-1, GLO 1-2 and GLO 2-2. All alloenzymes have molecular mass of 46 kDa (Thornalley 2003).

The active site is situated in the dimer interface, with the inhibitor and essential Zn^{2+} ion interacting with side chains from both subunits. The zinc binding site (human isoform) comprises two structurally equivalent residues from each domain – Gln-33A, Glu-99A, His-126B, Glu-172B and two water molecules in octahedral co-ordination. S-Glycolylglutathione, S-D-lactoylglutathione and S-L-glyceroylglutathione are formed from glyoxal, MGO and hydroypyruvaldehyde respectively by glyoxalase I, and hydrolysed to glycolate, D-lactate and L-glycerate respectively by glyoxalase II (Clelland and Thornalley 1991).

The suppression of α-oxoaldehyde-mediated glycation by glyoxalase I is particularly important in diabetes and uraemia, where α-oxoaldehyde concentrations are increased. Convincing experimental evidence that glyoxalase I suppresses the formation of AGEs came from studies of endothelial cells in normoglycaemic and hyperglycaemic culture. Hyperglycaemia induced increases in the concentrations of MGO, D-lactate and AGEs. Overexpression of glyoxalase I prevented totally the increase in MGO and cellular protein AGEs, and increased the concentration of D-lactate (Shinohara et al. 1998). Furthermore, Glo-I overexpression in diabetic rats reduced hyperglycaemia-induced levels of carbonyl stress, AGEs, and oxidative stress (Brouwers et al. 2011). This indicated that glyoxalase I has a critical role in suppressing the formation of protein AGEs. The activity of glyoxalase I is proportional to the cellular concentration of GSH. Indeed, experimental depletion of GSH, by oxidative or non-oxidative mechanisms, induced marked accumulation of MGO and much smaller increase in glyoxal, and induced cytotoxicity (Abordo et al. 1999). The cytotoxicity associated with the accumulation of MGO and other glyoxalase I substrates should be avoided under normal physiological states. Hence the function of glyoxalase I is the detoxification of α-oxoaldehydes as part of the enzymatic defence against glycation. In certain disease states, such as cancer and microbial infections, one may wish to induce cytotoxicity of tumour cells and microbial organisms pharmacologically. A cell-permeable glyoxalase I inhibitor achieves this. SpBrBzGSH (S-p-bromobenzylglutathione) is a potent inhibitor of human glyoxalase I. Diesterification of SpBrBzGSH stabilizes this GSH conjugate to extracellular degradation by γ-glutamyl transpeptidase and makes it cell permeable. Inside cells, SpBrBzGSH diesters are de-esterified and glyoxalase I is inhibited. SpBrBzGSHCp2 (SpBrBzGSH cyclopentyl diester) is a potent antitumour agent in vitro and has antitumour activity in vivo (Thornalley et al. 1996). Surprisingly, more recent studies have shown overexpression of glyoxalase I associated with multidrug resistance in cancer chemotherapy, where potent antitumuoral activity was achieved with SpBrBzGSHCp2, suggesting a role of MGO-induced apoptosis in the mechanism of action of some antitumour drugs (Thornalley 2003).

AIMS OF THE STUDY

Diabetes Mellitus is an important risk factor for the development of micro- and macro-vascular disease. As a result, diabetic subjects have a much higher risk than healthy subjects of developing atherosclerosis, nephropathy and heart attack. Endothelial dysfunction plays a pivotal role in the onset and progression of diabetic vascular complication. Several metabolic disorders cause endothelial damage, by modifying the balance between NO production and its inactivation. In particular, insulin-resistance, characteristic of type 2 diabetes, plays a key role in the development of endothelial dysfunction. Indeed, in addition to its classical hypoglycaemic function, insulin also acts as a vaso-regulatory hormone. Although the mechanism by which insulin action is altered in the endothelium of diabetic subjects is still unclear, it's known that chronic hyperglycaemia is involved in the onset of insulin-resistance and in the progression of diabetic vascular complications. The aim of this study is to investigate the effects of methylglyoxal, one of the main products of chronic hyperglycaemia, on the insulin sensitivity of endothelium and on endothelial function both *in vitro* and *in vivo*, in order to identify the molecular mechanism/s by which this reactive metabolite may alter the vascular functions.

MATERIALS AND METHODS

Reagents. Media, sera and antibiotics for cell culture were from Lonza (Walkersville, MD, USA). Protein electrophoresis and western blot reagents were from Bio-Rad (Richmond, VA, USA) and ECL reagents from Pierce (Rockford, USA). Protein-A sepharose and MGO (40% in water solution) were from Sigma (St Louis, MO, USA). Insulin was from Eli Lilly (FI, Italy). The antibodies used were anti-phospho-TyrIRS-1 (Millipore, Billerica, MA, USA), anti-IRS-1, anti-p85, anti-GSK-3β, (Upstate biotechnology, Lake Placid, NY), anti-Akt, anti-phospho-Ser473Akt, anti-phospho-Ser21GSK3β, anti-eNOS, anti-phospho-Ser1177eNOS, anti-phospho-Thr497eNOS (Cell Signaling Technology, Inc. Beverly, MA), anti-ERK1/2, anti-phospho-ERK1/2 (Santa Cruz, CA, USA). U0126 were from ENZO Lifescience (FI, Italy). The inhibitor of glyoxalase 1 (SpBrBzGSHCp2) was kindly provided by A. Bierhaus (University of Heidelberg, Heidelberg, Germany). All other chemicals were from Sigma (St Louis, MO, USA).

Cell culture procedure. Bovine aortic endothelial cells were plated in T75 flask and grown in Dulbecco's modified Eagle's medium (DMEM) containing 1 g/liter glucose supplemented with 10% (v/v) fetal bovine serum and 2mM glutamine. Cultures were maintained at 37 °C in a humidified atmosphere containing 5% (v/v) CO2. Cells were starved in serum-free medium containing 0.2% (wt/vol.) BSA, pretreated or not with MGO 500 μM for the appropriated times, and then exposed or not to 100 nmol/l insulin. Where indicated, cells were pretreated for 30 minutes with U0126 15 μM, or 48 hours with 10 μM SpBrBzGSHCp2.

Western Blot analysis. For Western blot analysis, cells were solubilized in lysis buffer (50 mM HEPES, pH 7.5, 150 mM NaCl, 10 mM EDTA, 10 mM Na2P2O7, 2 mM Na3VO4, 100 mM NaF, 10% glycerol, 1% Triton X-100, 1 mM phenylmethylsulfonylfluoride, 10 μg/ml aprotinin) for 2 h at 4°C. Cell lysates were clarified by centrifugation at 13000 rpm for 20 min. To analyze the phosphorylation of IRS-1 and its interaction with p85, 250 μg of protein lysates were incubated with IRS-1 antibodies and then precipitated with protein A-Sepharose. Cell lysates or immunoprecipitated proteins were then separated by SDS-PAGE and transferred into 0.45-μm Immobilon-P membranes (Millipore, Bedford, MA). Upon incubation with primary and secondary antibodies, immmunoreactive bands were detected by ECL according to the manufacturer's instructions.

Measurement of NO. NO measurement was performed on cell culture medium or on mice serum. For the *in vitro* experiments, after treatments, culture medium was collected, centrifuged at 1000xg for 15 minutes, and the supernatant used as a sample solution for the detection. Serum was collected from the animals after cervical dislocation, treated with Centricon 10 (Amicon, Beverly, MA) at 7500 rpm for 1 hour at 4 °C to remove haemoglobin and proteins. NO concentration was detected by the use of Nitrate/nitrite Assay Kit Colorimetric (Sigma-Aldrich Chemie GmbH, Switzerland). This assay uses the Griess reaction that forms a chomophoric azo-derivatives which absorbs light at 540-570 nm.

Animals and MG administration. 4-Week-old C57/BL6 female mice (n. 30) were purchased from the Charles River Laboratories (Milan, Italy). Animals were kept under a 12-h light/12-h dark cycle, and all experimental procedures and euthanasia described below were approved by Institutional Animal Care and Utilization Committee. MG was administered intraperitoneally over 5 consecutive days each week for 7 consecutive weeks. The initial dose administered was 50 mg/kg of body weight for the first 2 weeks, followed by a dose of 60 mg/kg of body weight for weeks 3 and 4, and finally a dose of 75 mg/kg of body weight for the last 3 weeks. Body weight was recorded weekly throughout the study. The animals were divided into 3 groups and injected with a 40% MGO solution (10 mice), physiologic solution (10 mice), or not treated (10 mice). After 7 weeks of treatment, animals from each group were sacrificed by cervical dislocation, the sera were collected, and the aortae isolated and homogenized as previously reported (Cassese et al. 2008).

Insulin tolerance test. Mice were fasted for 4 hours followed by intraperitoneal (IP) insulin injection (0.75 IU/kg body weight). Whole venous blood was obtained from the tail vein at 0, 15, 30, 60, 90 and 120 min after the injection. Blood glucose was measured using an automatic gluco-meter (One Touch, Lifescan, Daly).

Statistical procedures. Data were analysed with Statview software (Abacus-concepts) by one-factor analysis of variance. p values of less than 0.05 were considered statistically significant.

RESULTS

2.1 Effect of MGO on insulin signaling in endothelial cells *in vitro*.

It has recently been demonstrated that MGO alters tyrosine phosphorylation of IRS-1 in response to insulin in L6 rat skeletal muscle cells (Riboulet-Chavey et al. 2006). Aiming at analyze if this α-ketoaldehyde had the same effects in bovine aortic endothelial cells (BAEC), these cells were treated with or without 500 μM of MGO over 16 hours, and then, stimulated with 100 nM insulin for 10 minutes. Cells were lysated and 500 μg of proteins per sample were immunoprecipitated with anti-IRS-1 antibodies. The immunoprecipitates were processed by SDS-PAGE and analyzed trough immunoblot by anti-phospho-tyrosine antibodies, in order to test the tyrosine-phosphorylation levels of the immunoprecipitated proteins. As shown in figure 12.a, 10 minutes of 100 nM insulin incubation induces a two-fold increase of IRS-1 tyrosine-phosphoylation in control cells. On the contrary, insulin is not able to induce any significant increase of IRS-1 tyrosine-phosphorylation in BAEC treated with 500 μM MGO for 16 hours. This result suggests that MGO impairs insulin-dependent activation of IRS-1 in endothelial cells.

It has previously been demonstrated that MGO exerts an inhibitory effect on PI3-K activation and on the interaction of its regulatory subunit p85 with phosphorylated IRS-1 (Riboulet-Chavey et al. 2006). Hence, we tested whether MGO produced this effect also in endothelial cells. As shown in figure 12.b, insulin increases by 2.5-fold the interaction between PI3-K regulatory subunit p85 and IRS-1 in control cells, whilst no interaction was observed after insulin stimulation in MGO-treated cells.

To verify whether the inhibitory effect of MGO on IRS-1 tyrosine-phosphorylation in response to insulin may lead to alterations in the signal transduction pathway downstream PI3-K, we checked the phosphorylation levels of Akt/PKB, a serine-kinase activated by PI3-K. As shown in figure 12.c, insulin induces a ~30% increase of Akt phosphorylation on serine 473 in control cells. By contrast, on serine 473 phosphorylation is not increased in response to insulin in cells treated with MGO for 16 hours. To confirm the MGO dependent inhibition of Akt activity in response to insulin, we tested the serine phosphorylation levels of the Akt substrate GSK3β. In figure 12.d is shown that 16 hours of MGO treatment inhibits the insulin-dependent serine phosphorylation of GSK3β, confirming that MGO is able to impair insulin-induced Akt activity.

Since in endothelial cells the activation of the IRS-1/PI3K/Akt pathway by insulin results in the production of the vasodilator nitric oxide mediated by eNOS, we analyzed the activation levels of this enzyme in BAEC treated with MGO.

eNOS can be phosphorylated by Akt on different residues producing opposite effects: the phosphorylation on serine 1177 induces a 15-20 fold increase of the enzymatic activity; the phosphorylation on threonine 497 induces the inhibition of the enzymatic activity (Andreozzi et al. 2007). Insulin stimulation causes a 2-fold reduction of threonine 497 phosphorylation levels in BAEC (figure 12.f) whilst, as expected, the phosphorylation on serine 1177 follows the opposite trend in these cells (figure 12.e). On the contrary, insulin is not able to reduce eNOS threonine 497 phosphorylation in cells pretreated with MGO for 16 hours (figure 12.f), whereas the phosphorylation levels on serine 1177 are strongly reduced both in the presence and in the absence of insulin stimulation (figure 12.e).

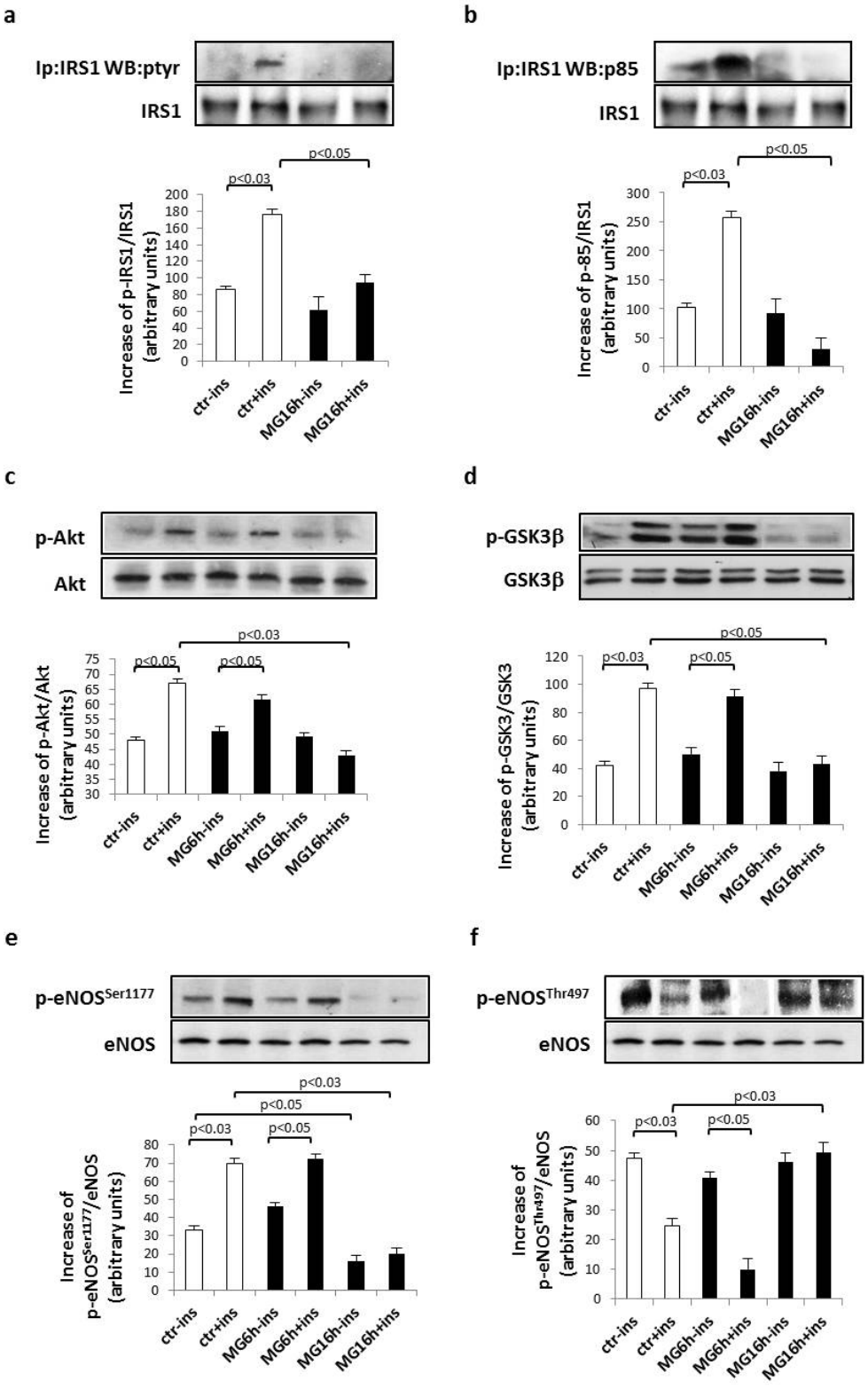
a
Ip:IRS1 WB:ptyr
IRS1
Increase of p-IRS1/IRS1 (arbitrary units)
p<0.03
p<0.05
ctr-ins
ctr+ins
MG16h-ins
MG16h+ins
b
Ip:IRS1 WB:p85
IRS1
Increase of p-85/IRS1 (arbitrary units)
p<0.03
p<0.05
c
p-Akt
Akt
Increase of p-Akt/Akt (arbitrary units)
p<0.05
p<0.05
p<0.03
MG6h-ins
MG6h+ins
d
p-GSK3β
GSK3β
Increase of p-GSK3/GSK3 (arbitrary units)
p<0.03
p<0.05
p<0.05
e
p-eNOSSer1177
eNOS
Increase of p-eNOSSer1177/eNOS (arbitrary units)
p<0.03
p<0.05
p<0.03
f
p-eNOSThr497
eNOS
Increase of p-eNOSThr497/eNOS (arbitrary units)
p<0.03
p<0.05
p<0.03

Figure 12: MGO impairs the insulin-stimulated activation of IRS1/PI3K/Akt pathway in endothelial cells. Bovine aortic endothelial cells (BAEC) were treated with 500 µM MGO for 6 or 16 hours and stimulated or not with 100 nM insulin for 10 minutes. Protein lysates obtained from these cells, by TAT1% treatment, were immunoprecipitated with anti-IRS-1 antibody and then analyzed by Western Blot with anti-p-tyrosine, anti-p85 and anti-IRS-1 antibodies as normalization of the protein content (**a**, **b**); or directly tested by Western Blot assay with anti-p-Akt, anti-Akt (**c**), anti-p-GSK3β, anti-GSK3β (**d**), anti-pSer1177-eNOS, anti-pThr495-eNOS, anti-eNOS (**e**, **f**), as indicated. To ensure accurate normalization, the same blots were probed with anti-14-3-3 antibody. The bars in the graphs represent the mean ± standard deviation of the values obtained by the densitometric analysis of at least three independent experiments. Statistical significance was evaluated using the Student's t test. A value of $p<0.05$ was considered statistically significant.

In order to verify whether the inhibitory effect of MGO on eNOS activity would be followed by an impaired production of nitric oxide by endothelial cells, we measured nitric oxide content in the culture medium by means of a colorimetric assay. As shown in figure 13, the levels of nitric oxide into the culture medium of BAEC pretreated with MGO are reduced by 50% after insulin stimulation, compared to the control cells.

Taken together, these results indicate that MGO is able to alter the insulin signal transduction and nitric oxide production in endothelial cells.

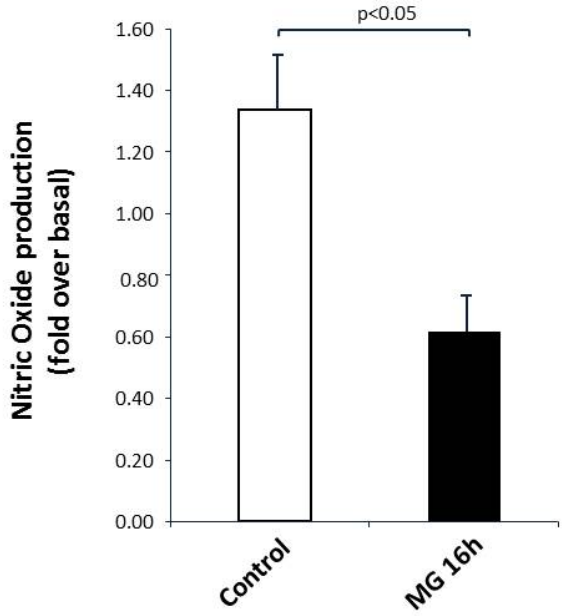

Figure 13: MGO reduces the nitric oxide produced by endothelial cells in response to insulin. BAECs were incubated with 500 μM MGO for 16 hours, and stimulated or not with 100 nM insulin for 10 minutes. After treatment, culture medium was collected and tested for nitric oxide concentration by a colorimetric assay. The bars in the graph represent the increase of nitric oxide medium content after insulin stimulation, over basal condition. Values are expressed as means ± standard deviation of triplicate determinations. Statistical analysis was performed as reported in figure 12.

Besides inducing the activation of the signal transduction that leads to the production of the vasodilator nitric oxide, insulin is also able to induce the release of the vasoconstrictor endothelin-1 by endothelial cells, through the activation of the MAPK cascade, and then, the endothelin converting enzyme-1 (ECE-1) (Kubota et al. 2003). Thus, in order to investigate whether the MAPK pathway as well may be altered by MGO, we analyzed the phosphorylation levels of ERK1/2. In figure 14 is shown that insulin stimulation induces a 1.7-fold increase of ERK phosphorylation in endothelial cells. We found that 16 hours of MGO treatment causes a significant increase of ERK phosphorylation in endothelial cells in basal conditions, with no further increase after insulin stimulation. This is an interesting finding considering that, in addition to the induction of endothelin-1 release, is reported that ERK is also able to phosphorylate IRS-1 on serine and threonine residues, thereby inhibiting its function (Gual et al. 2005).

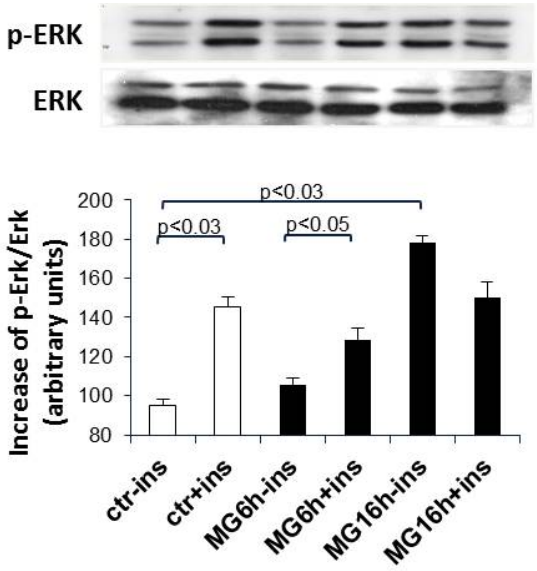

Figure 14: ERK activation is increased by MGO incubation. BAECs were treated as reported in figure 12. The Western Blot analysis was performed with anti-p-ERK and anti-ERK antibodies. Statistical analysis was performed as reported in figure 12.

The data described so far show that the incubation of endothelial cells with high extracellular concentrations of MGO leads to altered insulin signaling and reduced insulin-dependent nitric oxide production, showing that MGO impairs endothelial insulin sensitivity. We then decided to investigate the effects of endogenous MGO concentration increased by inhibiting the MGO detoxifying enzyme "glyoxalase 1" (Thornalley 2008). To this aim we performed time course tests treating endothelial cells with different concentrations of the glyoxalase inhibitor "SpBrBzGSHCp2" (Thornalley et al. 2006). We found that after 48 hours of 10μM SpBrBzGSHCp2 treatment, insulin signaling is impaired in endothelial cells. As shown in figure 15, treatment of BAEC with 10μM SpBrBzGSHCp2 up to 48 hours causes a complete loss of insulin-induced phosphorylation of Akt on serine 473 (figure 15.a) and of eNOS on serine 1177 (figure 15.b), compared to control cells. On the contrary, ERK activation is increased in basal condition compared to control cells, and these phosphorylation levels remain unchanged after insulin stimulation in cells treated with glyoxalase 1 inhibitor (figure 15.c).

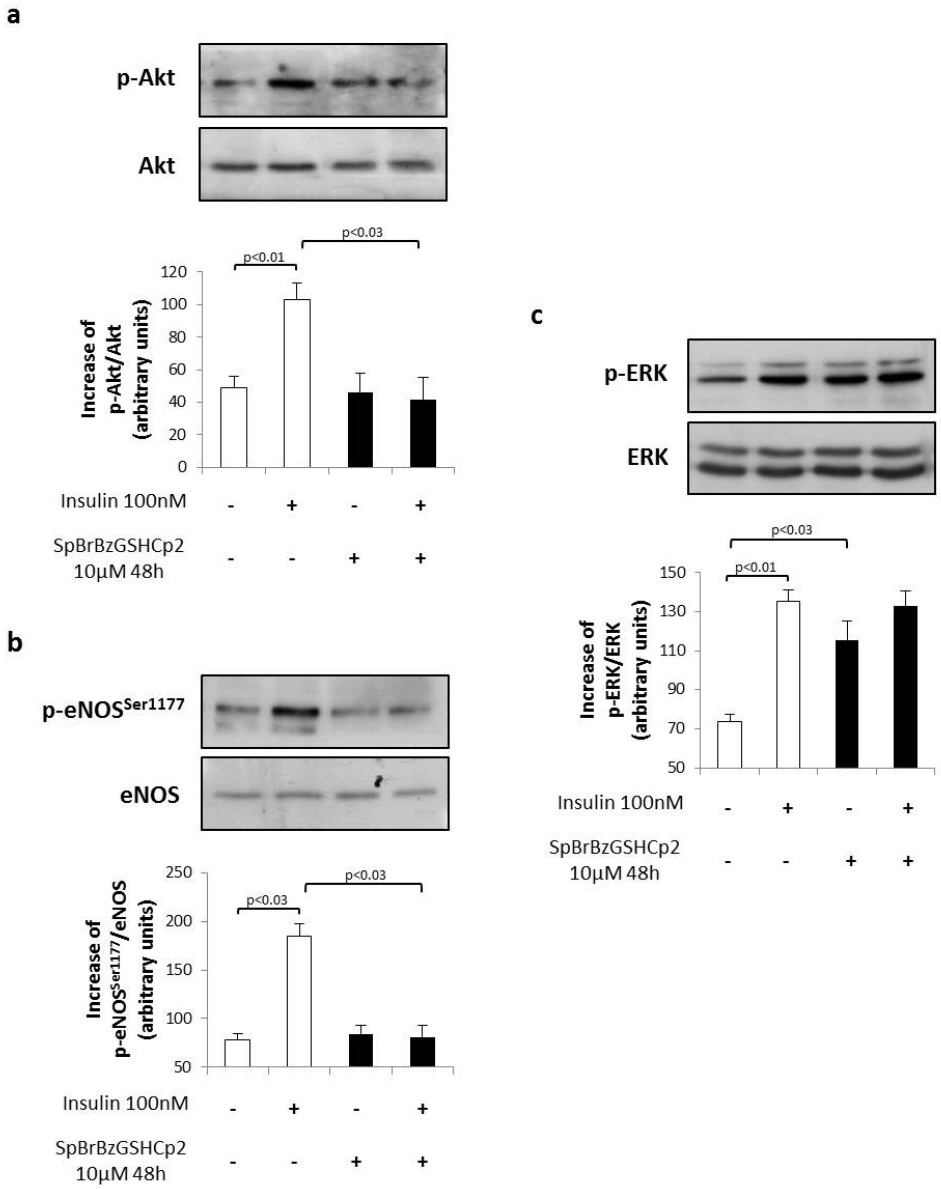

Figure 15: The inhibition of glyoxalase 1 by SpBrBzGSHCp2 alters insulin signaling in BAECs similarly to the exogenous MGO incubation. BAECs were treated with 10 µM of the glyoxalase I inhibitor «SpBrBzGSHCp2» for 48 hours and stimulated or not with 100 nM insulin for 10 minutes. Protein lysates obtained from these cells were analyzed by Western Blot assay with anti-p-Akt, anti-Akt (**a**), anti-p-Ser1177-eNOS, anti-eNOS (**b**), anti-p-ERK and anti-ERK antibodies (**c**), as indicated. To ensure accurate normalization, the same blots were probed with anti-tubulin antibody. Statistical analysis was performed as reported in figure 12.

Both in the endothelial cells incubated with MGO and in those treated with glyoxalase 1 inhibitor, we noticed the activation of ERK at basal state. This let us to hypothesize that ERK could have a role in the harmful effect exerted by MGO on the insulin-depedent IRS-1/PI3K/Akt/eNOS pathway activation. In order to verify this hypothesis, we inhibited ERK activation pretreating the cells with the MEK inhibitor U0126, and then, incubated them with MGO. As demonstrated in figure 16, whilst the only incubation of endothelial cells with MGO leads to the basal activation of ERK and to the loss of insulin-dependent Akt activation (16.a), the total inhibition of ERK is paralleled to a rescue of Akt serine-phosphorylation in response to insulin in the cells pretreated with U0126 (16.b).

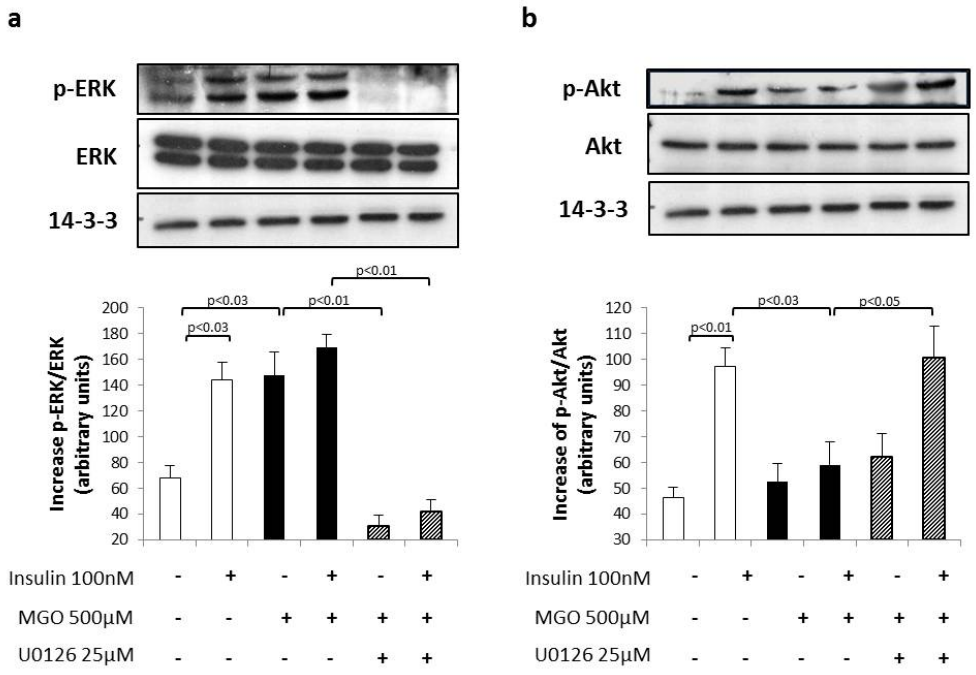

Figure 16: The inhibition of ERK restores the insulin-dependent Akt phosphorylation. BAECs were pre-incubated with 25 µM of the MEK inhibitor "U0126" for 30 minutes, and then, 500 µM MGO were added to the culture medium for 16 hours. Next, the cells were stimulated or not with 100 nM insulin for 10 minutes. Protein lysates obtained from these cells were analyzed by Western Blot assay with anti-p-Akt, anti-Akt (**a**), anti-p-ERK and anti-ERK antibodies (**b**), as indicated. To ensure accurate normalization, the same blots were probed with anti-14-3-3 antibody. Statistical analysis was performed as reported in figure 12.

2.2 Effect of MGO on insulin sensitivity *in vivo*.

In addition to the above reported experiments carried out *in vitro* in endothelial cells, we also investigated the effect of MGO on insulin sensitivity *in vivo*. To this aim, we performed a well established protocol of intraperitoneal administration of MGO to C57bl6 mice over 7 weeks (Berlanga et al. 2005). The animals were divided into 3 groups, each one including 10 animals: Group 1 included control untreated mice; Group 2 mice injected with physiologic solution, and Group 3 mice injected with MGO solution (see under Materials and Methods). At the end of the treatments, insulin tolerance in the three groups of animals was assessed. Group 1 and group 2 didn't show any significant differences of both insulin sensitivity and nitric oxide concentration. As shown in figure 17, blood glucose levels of Group 3 mice over the 120 min following insulin injection are significantly higher than control groups, thus indicating that MGO administration induces a systemic insulin resistant state.

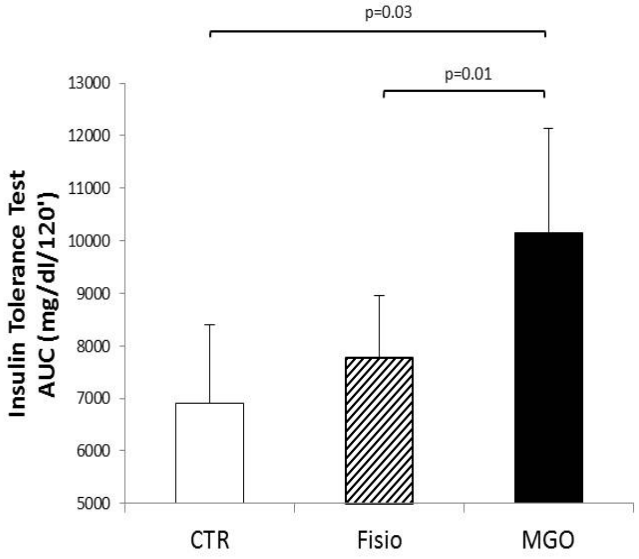

Figure 17: MGO administration impairs insulin sensitivity *in vivo*. C57BL6 mice were peritoneally injected with 50 to 75 mg/kg MGO, or with physiologic solution (CTR), over 5 days each week for 7 consecutive weeks. After treatment, ITT were performed. The bars in the graph correspond to the area under the curves representing the blood glucose levels of the animals over the 2 hours following the insulin injection (0.75 U/kg). Values are expressed as means ± standard deviation for 10 mice in each group.

Afterward, we analyzed whether MGO may induce endothelium-specific insulin resistance, by analyzing insulin-dependent Akt activation in aortae isolated from the 3 groups of mice and measuring nitric oxide serum levels. Western blots of lysates of aortae from Group 3 revealed a reduction of insulin-induced Akt activation (figure 18.a). Moreover, as shown in figure 18.b, in Group 3 insulin stimulation of nitric oxide release is reduced by ~2.5 fold compared to control groups of mice, suggesting that MGO is able to induce an endothelium-specific insulin resistant state also *in vivo*.

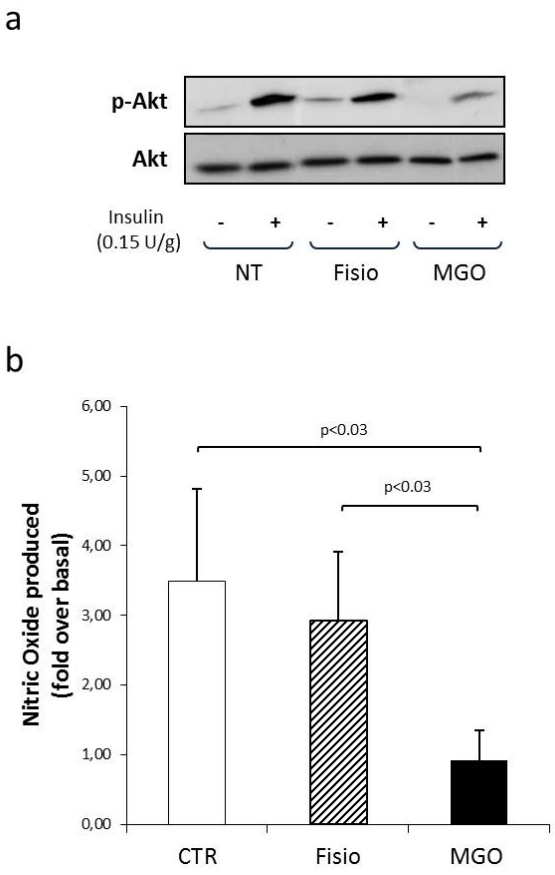

Figure 18: MGO administration reduces Akt activation in mice isolated aortae and serum nitric oxide in C57bl6 mice. C57BL6 mice were treated as described in figure 17. **(a)** Aortae were isolated from the 3 groups of mice, omogenized in JS buffer and the protein extracts analyzed by Western Blot with anti-p-Akt and anti-Akt antibodies. **(b)** 5 animals for each group were peritoneally injected with insulin (0.15 U/g), and then, blood was collected. NO serum concentration was measured by a colorimetric assay. The bars in the graph represent the increase of NO concentration in insulin stimulated mice sera, over not insulin stimulated ones. Values are expressed as means ± standard deviation for 10 mice in each group.

DISCUSSION

Type 2 diabetes is an important risk factor for the development of cardiovascular disease (Schalkwijk and Stehouwer 2005). This metabolic disorder is mainly characterized by peripheral insulin resistance and altered pancreatic β-cell function. Both these dysfunctions cause hyperglycaemia that, together with insulin resistance, plays an important role in the onset and progression of vascular dysfunction (Bakker et al. 2009). Several studies have recently highlighted how insulin, besides its function as regulator of glucose homeostasis, has important nonmetabolic hemodynamic actions (Cersosimo and De Fronzo 2006). As demonstrated by Federici et al. (2004), alterations of endothelial insulin pathway induce an abnormal production of the vasoregulators ET-1 and NO, and consequently, endothelial dysfunction. A widely accepted hypothesis on the mechanisms implicated in glucose-mediated vascular damage includes the increased production of AGEs (Brownlee 2001; Schalkwijk and Stehouwer 2005). These products result by the formation of covalent bonds between sugars (or derivatives) and protein, lipids and nucleic acids, making their function modified. Although it has been demonstrated that high AGEs levels are associated to altered vasodilation in type 2 diabetes, and that they can inhibit endothelium-dependent vasodilation, which specific AGEs are responsible for these effects and which molecular pathways are involved remain still unclear.

In the present study, we sought to investigate the role of MGO, one of the main AGEs precursor, in the induction of endothelial insulin resistance. Recent studies suggest that MGO may have a role in this sense. Indeed, it has been found that higher serum and adipose tissue MGO concentrations are closely related to insulin resistance. It has been observed a reduced activation of insulin signaling, in particular of IRS-1 phosphorylation, PI3-K activity and glucose uptake in 3T3-L1 adipocytes treated with MGO (Xuming and Lingyun 2007). Moreover, Riboulet-Chavey et al. (2006) demonstrated that the exposure of L6 skeletal muscle cells to MGO impairs the insulin signaling pathways. However, the effect of MGO on insulin signaling in endothelial cell, whose altered function is crucial not only in the progression of diabetic vascular complication but also in the worsening of peripheral insulin sensitivity, remains to be investigated. In order to explore this aspect, we performed a detailed analysis of insulin signal transduction in bovine aortic endothelial cells (BAEC) treated with concentrations of MGO that we found to be not toxic for the cells, through vitality and apoptosis assays (data not shown). Our results show that insulin is not able to induce IRS-1 tyrosine phosphorylation in endothelial cells treated with MGO, despite the unchanged levels of the total protein content. These data suggest that changes in IRS synthesis/degradation are not involved in the impairment of its tyrosine-phosphorylation, since IRS protein

levels are unaltered after MGO treatment. MGO is a reactive dicarbonyl molecule that can modify lysine and arginine residues in proteins. Recently, we have shown that this also occurs in INS-1E cells, as incubation with MGO induces the formation of CEL– and argpyrimidine–IRS adducts. Interestingly, on rat IRS-1, proximal to YMXM motifs, which have been implicated in p85 binding, Lys602 near Y608MPM and Arg622 near Y628MPM are found (White 1998; Van Obberghen et al. 2001). It is likely that adduct binding to Lys602 and/or Arg622 could lead to reduced tyrosine phosphorylation of IRS-1/2 resulting in decreased p85 anchoring by IRS. An alternative or additional scenario could be a similar modification of the Lys and/or Arg residues located within the IRS PH or PTB domains, which are essential for optimal IRS tyrosine phosphorylation by IR (Fiory et al. 2011). Our future plan is to detect the possible formation of these adducts also in endothelial cells, by using antibodies against AGE-adducts.

One of the main function of phosphorylated tyrosines of IRS proteins is to allow the interaction and, consequently, the activation of other proteins, among which PI3-K. Indeed, PI3-K is activated by the binding of its regulatory subunit p85 to the phosphorylated tyrosine of IRS-1. Thus, we sought to verify whether MGO could influence IRS-1/p85 interaction. Consistent with the reduction of IRS-1 tyrosine phosphorylation, the levels of p85 associated with IRS-1 are not increased by insulin-stimulation in endothelial cells treated with MGO. Furthermore, the activation of the downstream PI3K effector Akt is reduced as well. Additionally, the reduced activation of Akt was followed by the decrease of serine-phosphorylation of its substrate GSK3β, confirming that Akt kinase activity is impaired by MGO.

As described by Bakker et al. (2009), in addition to the signal cascade leading to the production of the vasodilator nitric oxide, insulin binding to its receptor also triggers the activation of another branch of insulin signaling, that involves activation of MEK, ERK1/2, and endothelin converting enzyme leading to the rapid release of ET-1. Interestingly, despite the impaired activation of IRS1/Akt in presence of MGO, ERK1/2 appears to be activated already in basal condition by MGO incubation, whilst insulin stimulation is not able to induce a further significant increase of ERK1/2 phosphorylation. Further investigations are in progress to analyze the whole MAPK cascade activation and ET-1 release by endothelial cells, in order to clarify whether MGO acts directly on ERK activation, or if the latter is activated by the increased activity of the upstream kinases MEK, RAF or IRS-2, and if this leads to an increased ET-1 production as well. Given the documented ability of ERK1/2 to phosphorylate IRS-1 on specific serine sites, thereby inhibiting its function (Gual et al. 2005; Bard-Chapeau et al. 2005), we hypothesized that, through the hyperactivation of ERK1/2, MGO may exert its noxious effect on insulin-dependent IRS-1/PI3K/Akt signal transduction. In order to validate this hypothesis, we inhibited ERK1/2 phosphorylation by pretreating

BAEC with the MEK inhibitor U0126. We found that the inhibition of ERK1/2 results in a rescue of insulin-dependent Akt phosphorylation, suggesting that ERK1/2 iperactivation may play a role in the detrimental effect of MGO on PI3K/Akt pathway. Future experiments aiming at analyzing the IRS-1 phosphorylation on specific serines will allow to confirm whether the hypothesized mechanism involving ERK1/2 is pivotal in this MGO-mediated effect. However, how MGO may induce ERK1/2 activation in endothelial cells remains to be clarified. Several studies report that hyperglycaemia can induce glucotoxicity by oxidative stress (Brownlee 2001; Nishikawa et al. 2000), known to be causative of ERK activation (Glotin et al. 2006). Guo et al. (2009) demonstrated that methylglyoxal induces insulin resistance and salt sensitivity by increasing oxidative stress in Sprague-Dawley rats. Whilst recent studies demonstrate that MGO leads to oxidative stress in a time and dose dependent manner, it has been also shown that MGO causes insulin-resistance in L6 cells at time and doses of incubations lower than those necessary to induce oxidative stress (Riboulet-Chavey et al. 2006). Thus, we will test whether MGO concentrations that induce insulin-resistance in BAEC could also cause ROS increase and if oxidative stress is responsible for ERK activation in endothelial cells.

Once demonstrated that MGO impairs insulin signaling, we sought to verify whether this alteration leads to modification of NO levels produced by endothelial cells. NO is a key molecule secreted by endothelium acting and acts as the major mediator of insulin action on vascular homeostasis. Evidences suggest that NO plays an important role in regulating both blood pressure and glucose levels, thus impaired NO availability is pivotal in the development and progression of diabetes vascular complications. Indeed, recent studies showed inverse correlation between NO level and the diabetic state. Reduced NO availability may not only be of relevance to the development of atherosclerotic complications in diabetes, but also interferes with insulin-mediated postprandial glucose disposal and possibly contributes to the development of insulin resistance (Shiekh et al. 2011). Thus, to test the ability of high MGO levels of inducing an altered NO production also *in vitro* in BAEC, we first investigated the activity of eNOS, the enzyme that catalyzes the conversion of arginine to citrulline and NO. eNOS activity is regulated by phosphorylation at multiple sites, but two of the better-characterized sites are serine 1177 (Ser1177) and threonine 495 (Thr495). Ser1177 is rapidly phosphorylated by Akt in response to insulin, resulting in increased eNOS activity and NO production. By contrast, Thr495 is constitutively phosphorylated in endothelial cells, and it is thought to be a negative regulatory site causing a decrease in enzyme activity (Fleming and Busse 2003; Andreozzi et al. 2007). We found that MGO inhibits insulin induced phosphorylation on eNOS Ser1177 and, on the other side, prevents insulin effect on the inhibitory phosphorylation on Thr497. Furthermore, the reduced activation of eNOS was paralleled by a 60%

reduction of insulin-dependent NO production by BAEC. Taken together, these results demonstrate that MGO impairs insulin signaling thereby inhibiting insulin-mediated NO production by endothelial cells.

Although in the described experiments we used MGO concentration found to be not toxic for BAEC, is reported that the use of millimolar concentrations to demonstrate impairment of insulin signalling could be of unlikely physiological relevance. For this reason, to investigate the effects of increased MGO concentrations, it could be more appropriate to increase endogenous MGO concentrations by inhibiting its detoxifying enzyme glyoxalase 1 with specific cell permeable inhibitors, or decrease glyoxalase 1 by siRNA techniques (Thornalley 2008). Thus, we treated BAEC with the glyoxalase 1 inhibitor "$SpBrGSHCp_2$", and we found the complete loss of insulin-stimulated Akt activation and Ser1177-eNOS phosphorylation, together with a significant increase of ERK1/2 activation in basal condition compared to control cells. Interestingly, these results confirmed those obtained in BAEC incubated with exogenous MGO. The intracellular MGO content in BAEC treated with the glyoxalase 1 inhibitor, together with the activity of the enzyme shoul be determinid to confirm reduced activity of the enzyme by $SpBrGSHCp_2$ treatment. However, it has been already published that the incubation with the same concentrations of the inhibitor (10 μM) over the same period of time (48 h) that we used in BAEC, induces a two-fold increase of MGO intracellular concentration in HL60 cells (Thornalley et al. 1996). Moreover, current studies by Bierhaus et al. report a ~30% reduction of glyoxalase 1 activity, corresponding to a two-fold increase of MGO plasma levels, in diabetics compared to healthy subjects. These evidence make us confident that our experimental conditions have been appropriately chosen. Further investigations are in progress to test whether also the balance of NO/ET-1 production by endothelial cells is compromised by glyoxalase 1 inhibition.

In this work we also provide evidence that MGO administration is able to affect insulin sensitivity and insulin-dependent serum NO content *in vivo*. Previous studies demonstrated that increased serum and adipose tissue MGO levels in fructose-fed rats correlate with the development of insulin-resistance (Xuming and Lingyun 2007). Also administration of 1% MGO in drinking water or acute i.v. administration of MGO induce insulin resistance and glucose intolerance in Sprague-Dowley rats (Guo et al. 2009; Dhar et al. 2010). Moreover, Brouwers et al. (2010) provided evidence that hyperglycaemia-induced impairment of endothelium-dependent vasorelaxation is mediated by increased intracellular MGO levels, supporting our interest in investigating the role of MGO on endothelial function *in vivo*.

C57Bl6 mice treated chronically with intraperitoneal injection of MGO become insulin resistant compared to untreated mice. This is paralleled by a reduction of insulin-induced Akt phosphorylation in aortae isolated from MGO treated mice.

As a consequence, MGO-treated mice feature a 3-fold reduction of insulin-induced NO serum concentrations compared to control mice, suggesting that MGO is able to induce vascular insulin resistance and endothelial disfunction also *in vivo*.

CONCLUSIONS

In hyperglycemic conditions, the abnormal accumulation of MGO is related to the development of diabetes complications in various tissues and organs. In particular, vascular dysfunction causes most of the excess morbidity and mortality in diabetes mellitus. This work shows that MGO alters insulin sensitivity in vascular tissue *in vitro* and *in vivo*. Indeed, both the exogenous MGO incubation and the increased intracellular MGO levels, following the glyoxalase 1 inhibition, impairs the insulin-mediated activation of IRS-1/PI3K/Akt/eNOS pathway and the consequent release of NO by endothelial cells *in vitro*. On the contrary, MGO causes the hyperactivation of ERK at basal state. Interestingly, the inhibition of ERK is paralleled to a rescue of Akt activation in response to insulin, suggesting that ERK plays a role in the harmful effect exerted by MGO on endothelial insulin-sensitivity. These results are strongly supported by data obtained *in vivo*. Indeed, MGO administration to C57 mice reduces insulin-induced Akt activation in isolated aortae and NO serum levels. Moreover, insulin tolerance tests show a reduced insulin sensitivity in MGO treated mice, compared to controls.

Further investigations of the molecular mechanisms by which the glucose metabolite MGO compromises insulin action in vascular cells may allow to develop new strategies to preserve endothelial function in diabetic subjects.

Acknowledgements

First of all I would like to thank my tutor, Prof. Francesco Beguinot, for having allowed me to carry out my work in his laboratory and giving me his continual support, for believing in me, and for the numerous opportunities he has given me that stimulated my scientific development.

I would also like to thank Prof. Pietro Formisano for his constant help and unfailing support, for his valuable suggestions and for his ability to inspire us every day with his strength and determination.

I would particularly like to thank Dr Claudia Miele for all she has taught me, for having supported me day after day and, above all, for believing in me and having greater confidence in me than myself had.

I would also like to mention Prof. Angelika Bierhaus who kindly encouraged me in my project and allowed me to spend a week gaining valuable experience in her laboratory.

Further thanks must go to Drs Fiory, Cassese, Mirra, Lombardi and Ilardi and to all my colleagues in the Diablab whose collaboration has proved essential for my work and for my scientific development. I thank you because, in spite of difficult moments, you succeeded in transforming the laboratory into a pleasant workplace in a decidedly constructive and challenging context.

An affectionate thank you to Dr Claudia Iadicicco for having been an excellent study companion, an outstanding work colleague but, more importantly, a friend who has been able to understand and help me greatly.

Thanks to Alessia and Alessandra, two excellent students, whose enthusiasm and keen interest in laboratory work have been of great help to me in this last year of particularly hard work.

A special thanks goes to Michele, the best "colleague" and partner for life that God could have placed at my side.

Any word of gratitude to my family will never be sufficient to express my thanks for all they have done for me. Their presence and support have always been fundamental to the carrying out of even the smallest step, as it was in the achievement of this new goal …Thank you for everything!

REFERENCES

Abordo EA, Minhas HS, Thornalley PJ. Accumulation of alpha-oxoaldehydes during oxidative stress: a role in cytotoxicity. Biochem Pharmacol 1999; 58(4):641-8.

Achike FI, To NH, Wang H, Kwan CY. Obesity, metabolic syndrome, adipocytes and vascular function: A holistic viewpoint. Clin Exp Pharmacol Physiol 2011; 38(1):1-10.

Ahmed N, Dobler D, Dean M, Thornalley PJ. Peptide mapping identifies hotspot site of modification in human serum albumin by methylglyoxal involved in ligand binding and esterase activity. J Biol Chem 2005;280:5724–5732.

Aiello LP. Angiogenic pathways in diabetic retinopathy. N Engl J Med 2005; 353:839–841.

Alessi DR, James SR, Downes CP, Holmes AB, Gaffney PR, Reese CB, Cohen P. Characterization of a 3-phosphoinositide-dependent protein kinase which phosphorylates and activates protein kinase Balpha Curr Biol 1997; 7:261–269.

Alessi MC, Juhan-Vague I. Metabolic syndrome, haemostasis and thrombosis. Thromb Haemost 2008; 99:995–1000.

Anderson HD, Rahmutula D, Gardner DG. Tumor necrosis factor-alpha inhibits endothelial nitric oxide synthase gene promoter activity in bovine aortic endothelial cells. J Biol Chem 2004; 279(2):963–969.

Andreozzi F, Laratta E, Procopio C, Hribal ML, Sciacqua A, Perticone M, Miele C, Perticone F, Sesti G. Interleukin-6 impairs the insulin signaling pathway, promoting production of nitric oxide in human umbilical vein endothelial cells. Mol Cell Biol 2007; 27(6):2372-83.

Bakker W, Eringa EC, Sipkema P, van Hinsbergh VW. Endothelial dysfunction and diabetes: roles of hyperglycemia, impaired insulin signaling and obesity. Cell Tissue Res 2009; 335(1):165-89.

Bard-Chapeau EA, Hevener AL, Long S, Zhang EE, Olefsky JM, Feng GS. Deletion of Gab1 in the liver leads to enhanced glucose tolerance and improved hepatic insulin action. Nat Med. 2005; 11(5):567-71.

Beisswenger PJ, Howell SK, Nelson RG, Mauer M, Szwergold BS. α-Oxoaldehyde metabolism and diabetic complications. Biochem Soc Trans 2003; 31:1358–1363.

Berg BM van den, Nieuwdorp M, Stroes ES, Vink H. Glycocalyx and endothelial (dys) function: from mice to men. Pharmacol Rep 2006; 58(Suppl):75–80.

Bierhaus A, Nawroth PP. The Alzheimer's Disease-Diabetes Angle: Inevitable Fate of Aging or Metabolic Imbalance Limiting Successful Aging. Journal of Alzheimer's Disease 2009; 16:673–675.

Boulton TG, Nye SH, Robbins DJ, Ip NY, Radziejewska E, Morgenbesser SD, DePinho RA, Panayotatos N, Cobb MH, Yancopoulos GD. ERKs: a family of protein serine/threonine kinases that are activated and tyrosine phosphorylated in response to insulin and NGF. Cell 1991; 65:663–675.

Brook RD, Bard RL, Rubenfire M, Ridker PM, Rajagopalan S. Usefulness of visceral obesity (waist/hip ratio) in predicting vascular endothelial function in healthy overweight adults. Am J Cardiol 2001; 88:1264–1269.

Brouwers O, Niessen PM, Ferreira I, Miyata T, Scheffer PG, Teerlink T, Schrauwen P, Brownlee M, Stehouwer CD, Schalkwijk CG. Overexpression of Glyoxalase-I redices hyperglicaemia-induced levels of Advanced Glycation End Products and oxidative stress in diabetic rats. J Biol Chem 2011; 286(2):1374-1380.

Brouwers O, Niessen PM, Haenen G, Miyata T, Brownlee M, Stehouwer CD, De Mey JG, Schalkwijk CG. Hyperglycaemia-induced impairment of endothelium-dependent vasorelaxation in rat mesenteric arteries is mediated by intracellular methylglyoxal levels in a pathway dependent on oxidative stress. Diabetologia 2010; 53:989–1000.

Brownlee M. Biochemistry and molecular cell biology of diabetic complications. Nature 2001; 414:813-820.

Cardillo C, Nambi SS, Kilcoyne CM, Choucair WK, Katz A, Quon MJ, Panza JA Insulin stimulates both endothelin and nitric oxide activity in the human forearm. Circulation 1999; 100:820–825.

Carmeliet P. Angiogenesis in life, disease and medicine. Nature 2005; 438:932–936.

Cassese A, Esposito I, Fiory F, Barbagallo AP, Paturzo F, Mirra P, Ulianich L, Giacco F, Iadicicco C, Lombardi A, Oriente F, Van Obberghen E, Beguinot F, Formisano P, Miele C. In Skeletal Muscle Advanced Glycation End Products (AGEs) Inhibit Insulin Action and Induce the Formation of Multimolecular Complexes Including the Receptor for AGEs. J Biol Chem 2008; 283(52):36088–36099.

Cersosimo E, DeFronzo RA. Insulin resistance and endothelial dysfunction: the road map to cardiovascular diseases. Diabetes Metab Res Rev 2006; 22:423–436.

Chen S, Hong SW, Iglesias-de la Cruz MC, Isono M, Casaretto A, Ziyadeh FN. The key role of the transforming growth factor-beta system in the pathogenesis of diabetic nephropathy. Ren Fail 2001; 23:471–481.

Cines DB, Pollak ES, Buck CA, Loscalzo J, Zimmerman GA, McEver RP, Pober JS, Wick TM, Konkle BA, Schwartz BS, Barnathan ES, McCrae KR, Hug BA, Schmidt AM, Stern DM. Endothelial cells in physiology and in the pathophysiology of vascular disorders. Blood 1998; 91:3527–3561.

Clelland JD and Thornalley JP. S-2-hydroxyacylglutathione-derivatives: enzymatic preparation, purification and characterization. J Chem Soc 1991; Perkin Trans 1:3009-3015.

Clerk LH, Rattigan S, Clark MG. Lipid infusion impairs physiologic insulin-mediated capillary recruitment and muscle glucose uptake in vivo. Diabetes 2002; 51(4):1138–1145.

Cusi K, Maezono K, Osman A, Pendergrass M, Patti ME, Pratipanawatr T, DeFronzo RA, Kahn CR, Mandarino LJ. Insulin resistance differentially affects the PI3-kinase and MAP kinase-mediated signaling in human muscle. J Clin Invest 2000; 105:311–20.

De Vriese AS, Verbeuren TJ, Van de Voorde J, Lameire NH, Vanhoutte PM. Endothelial dysfunction in diabetes. Br J Pharmacol 2000; 130:963–974.

DeFronzo RA, Ferrannini E. Insulin resistance. A multifaceted syndrome responsible for niddm, obesity, hypertension, dyslipidemia, and atherosclerotic cardiovascular disease. Diabetes Care 1991; 14(3):173–194.

DeFronzo RA. From the triumvirate to the ominous octet: a new paradigm for the treatment of type 2 diabetes mellitus. Diabetes 2009; 58:773–795.

DeFronzo RA. Insulin resistance, lipotoxicity, type 2 diabetes and atherosclerosis: the missing links. The Claude Bernard Lecture 2009. Diabetologia 2010; 53:1270–1287.

Desideri G, Ferri C, Bellini C, De Mattia G, Santucci A. Effects of ace inhibition on spontaneous and insulin-stimulated endothelin-1 secretion: In vitro and in vivo studies. Diabetes 1997; 46(1):81–86.

Dobler D, Ahmed N, Song L, Eboigbodin KE, Thornalley PJ. Increased dicarbonyl metabolism in endothelial cells in hyperglycemia induces anoikis and impairs angiogenesis by RGD and GFOGER motif modification. Diabetes 2006; 55: 1961–1969.

Du X, Edelstein D, Obici S, Higham N, Zou MH, Brownlee M. Insulin resistance reduces arterial prostacyclin synthase and enos activities by increasing endothelial fatty acid oxidation. J Clin Invest 2006; 116(4):1071–1080.

Du XL, Edelstein D, Dimmeler S, Ju Q, Sui C, Brownlee M. Hyperglycemia inhibits endothelial nitric oxide synthase activity by posttranslational modification at the AKT site. J Clin Invest 2001; 108(9):1341-8.

Duplain H, Burcelin R, Sartori C, Cook S, Egli M, Lepori M, Vollenweider P, Pedrazzini T, Nicod P, Thorens B, Scherrer U. Insulin resistance, hyperlipidemia, and hypertension in mice lacking endothelial nitric oxide synthase. Circulation 2001; 104(3):342-345.

Eringa EC, Stehouwer CD, Roos MH, Westerhof N, Sipkema P. Selective resistance to vasoactive effects of insulin in muscle resistance arteries of obese Zucker (fa/fa) rats. Am J Physiol Endocrinol Metab 2007; 293:E1134–9.

Eringa EC, Stehouwer CD, van Nieuw Amerongen GP, Ouwehand L, Westerhof N, Sipkema P. Vasoconstrictor effects of insulin in skeletal muscle arterioles are mediated by erk1/2 activation in endothelium. Am J Physiol Heart Circ Physiol 2004; 287(5):H2043–H2048.

Espinola-Klein C, Gori T, Blankenberg S, Munzel T. Inflammatory markers and cardiovascular risk in the metabolic syndrome. Front Biosci 2011; 1(16):1663-74.

Federici M, Pandolfi A, De Filippis EA, Pellegrini G, Menghini R, Lauro D, Cardellini M, Romano M, Sesti G, Lauro R, Consoli A. G972R IRS-1 variant impairs insulin regulation of endothelial nitric oxide synthase in cultured human endothelial cells. Circulation 2004; 109(3):399-405.

Ferri C, Pittoni V, Piccoli A, Laurenti O, Cassone MR, Bellini C, Properzi G, Valesini G, De Mattia G, Santucci A. Insulin stimulates endothelin-1 secretion from human endothelial cells and modulates its circulating levels in vivo. J Clin Endocrinol Metab 1995; 80:829–835.

Fiory F, Lombardi A, Miele C, Giudicelli J, Beguinot F, Van Obberghen E. Methylglyoxal impairs insulin signalling and insulin action on glucose-induced insulin secretion in the pancreatic beta cell line INS-1E. Diabetologia 2011; on line 10.1007/s00125-011-2280-8.

Fleming I, Busse R. Molecular mechanisms involved in the regulation of the endothelial nitric oxide synthase. Am J Physiol Regul Integr Comp Physiol. 2003; 284(1):R1-12.

Fleming TH, Humpert PM, Nawroth PP, Bierhaus A. Reactive metabolites and AGE/RAGE-mediated cellular dysfunction affect the Aging process. Gerontology 2011; 57(5):435-43.

Gallet X, Charloteaux B, Thomas A, Brasseur R. A fast method to predict protein interaction sites from sequences. J Mol Biol 2000; 302:917–926.

Gimbrone MA Jr. Endothelial dysfunction, hemodynamic forces, and atherosclerosis. Thromb Haemost 1999; 82:722–726.

Glotin AL, Calipel A, Brossas JY, Faussat AM, Tréton J, Mascarelli F. Sustained versus transient ERK1/2 signaling underlies the anti- and proapoptotic effects of

oxidative stress in human RPE cells. Invest Ophthalmol Vis Sci 2006; 47(10):4614-23.

Goldin A, Beckman JA, Schmidt AM, Creager MA. Advanced Glycation End Products : Sparking the Development of Diabetic Vascular Injury. Circulation 2006; 114:597-605.

Gual P, Le Marchand-Brustel Y, Tanti JF. Positive and negative regulation of insulin signaling through IRS-1 phosphorylation. Biochimie 2005; 87:99-109.

Guo Q, Mori T, Jiang Y, Hu C, Osaki Y, Yoneki Y, Sun Y, Hosoya T, Kawamata A, Ogawa S, Nakayama M, Miyata T, Ito S. Methylglyoxal contributes to the development of insulin resistance and salt sensitivity in Sprague-Dawley rats. Hypertens 2009; 27(8):1664-71.

Gustafson B, Hammarstedt A, Andersson CX, Smith U. Inflamed adipose tissue: A culprit underlying the metabolic syndrome and atherosclerosis. Arterioscler Thromb Vasc Biol 2007;27(11):2276-2283.

Haaren PM van, VanBavel E, Vink H, Spaan JA. Localization of the permeability barrier to solutes in isolated arteries by confocal microscopy. Am J Physiol Heart Circ Physiol 2003; 285: H2848–H2856.

Hinsbergh VW van. The endothelium: vascular control of haemostasis. Eur J Obstet Gynecol Reprod Biol 2001; 95:198–201.

Hotamisligil GS. Inflammation and metabolic disorders. Nature 2006;444(7121):860–867.

Iadicicco C, Raciti GA, Ulianich L, Vind BF, Gaster M, Andreozzi F, Longo M, Teperino R, Ungaro P, Di Jeso B, Formisano P, Beguinot F, Miele C. Glucosamine-induced endoplasmic reticulum stress affects GLUT4 expression via activating transcription factor 6 in rat and human skeletal muscle cells. Diabetologia 2010; 53:955–965.

Jia X, Wu L. Accumulation of endogenous methylglyoxal impaired insulin signaling in adipose tissue of fructose-fed rats. Mol Cell Biochem 2007; 306:133-139.

Kashyap SR, Roman LJ, Lamont J, Masters BS, Bajaj M, Suraamornkul S, et al. Insulin resistance is associated with impaired nitric oxide synthase activity in skeletal muscle of type 2 diabetic subjects. J Clin Endocrinol Metab 2005; 90(2):1100–1105.

Kearney MT, Duncan ER, Kahn M, Wheatcroft SB. Insulin resistance and endothelial cell dysfunction: studies in mammalian models. Exp Physiol 2007; 93.1:158–163.

Keogh RJ, Dunlop ME, Larkins RG. Effect of inhibition of aldose reductase on glucose flux, diacylglycerol formation, protein kinase C, and phospholipase A2 activation. Metabolism 1997; 46:41–47.

Kim F, Tysseling KA, Rice J, Pham M, Haji L, Gallis BM, et al. Free fatty acid impairment of nitric oxide production in endothelial cells is mediated by ikkbeta. Arterioscler Thromb Vasc Biol 2005; 25(5):989–994.

Kim HY, Oi Y, Kim M, Yokozawa T. Protective Effect of Lipoic Acid against Methylglyoxal-Induced Oxidative Stress in LLC-PK1 Cells. J Nutr Sci Vitaminal 2008; 54:104-112.

Kim J, Son JW, Lee JA, Oh YS, Shinn SH. Methylglyoxal Induces Apoptosis Mediated by Reactive Oxygen Species in Bovine Retinal Pericytes. J Korean Med Sci 2004; 19: 95-100.

Kim JA, Montagnani M, Koh KK, Quon MJ. Reciprocal relationships between insulin resistance and endothelial dysfunction: Molecular and pathophysiological mechanisms. Circulation 2006; 113(15):1888–1904.

Koh KK, Han SH, Quon MJ. Inflammatory markers and the metabolic syndrome: Insights from therapeutic interventions. J Am Coll Cardiol 2005; 46(11):1978–1985.

Kolm-Litty V, Sauer U, Nerlich A, Lehmann R, Schleicher ED. High glucose-induced transforming growth factor beta1 production is mediated by the hexosamine pathway in porcine glomerular mesangial cells. J Clin Invest 1998; 101:160–169.

Koya D, Jirousek MR, Lin YW, Ishii H, Kuboki K, King GL. Characterization of protein kinase C beta isoform activation on the gene expression of transforming growth factor-beta, extracellular matrix components, and prostanoids in the glomeruli of diabetic rats. J Clin Invest 1997; 100:115–126.

Koya D, King GL. Protein kinase C activation and the development of diabetic complications. Diabetes 1998; 47:859–866.

Kuboki K, Jiang ZY, Takahara N, Ha SW, Igarashi M, Yamauchi T, Feener EP, Herbert TP, Rhodes CJ, King GL. Regulation of endothelial constitutive nitric oxide synthase gene expression in endothelial cells and in vivo a specific vascular action of insulin. Circulation 2000; 101:676–681.

Kubota T, Kubota N, Moroi M, Terauchi Y, Kobayashi T, Kamata K, Suzuki R, Tobe K, Namiki A, Aizawa S, Nagai R, Kadowaki T, Yamaguchi T. Lack of insulin receptor substrate-2 causes progressive neointima formation in response to vessel injury. Circulation 2003; 107(24):3073-80.

Lau DC, Dhillon B, Yan H, Szmitko PE, Verma S. Adipokines: Molecular links between obesity and atheroslcerosis. Am J Physiol Heart Circ Physiol 2005; 288(5):H2031–H2041.

Lietzke SE, Bose S, Cronin T, Klarlund J, Chawla A, Czech MP, Lambright DG. Structural basis of 3-phosphoinositide recognition by pleckstrin homology domains. Mol Cell 2000; 6:385–394.

Lin KY, Ito A, Asagami T, Tsao PS, Adimoolam S, Kimoto M, Tsuji H, Reaven GM, Cooke JP. Impaired nitric oxide synthase pathway in diabetes mellitus: role of asymmetric dimethylarginine and dimethylarginine dimethylaminohydrolase. Circulation 2002; 106:987–992.

Lombardi A, Ulianich L, Treglia AS, Nigro C, Parrillo L, Lofrumento DD, Nicolardi G, Garbi C, Beguinot F, Miele C, Di Jeso B. Increased hexosamine biosynthetic pathway flux dedifferentiates INS-1E cells and murine islets by an extracellular signal-regulated kinase (ERK)1/2-mediated signal transmission pathway. Diabetologia 2011; in press.

Maresca F, D'Ascoli GL, Ziviello F, Petrillo G, Di Palma V, Russo A, Grieco A, Cirillo P. Obesity and ischemic heart disease. Is there a link between wellness' diseases?. Monaldi Arch Chest Dis. 2011; 76(1):13-21.

Martin A, Komada MR, Sane DC. Abnormal angiogenesis in diabetes mellitus. Med Res Rev 2003; 23:117–145.

McLellan AC, Thornalley PJ, Benn J, Sonksen PH. Glyoxalase system in clinical diabetes mellitus and correlation with diabetic complications. Clin Sci 1994; 87: 21-29.

Meigs JB, O'Donnell CJ, Tofler GH, Benjamin EJ, Fox CS, Lipinska I, Nathan DM, Sullivan LM, D'Agostino RB, Wilson PW. Hemostatic markers of endothelial dysfunction and risk of incident type 2 diabetes: The framingham offspring study. Diabetes 2006; 55(2):530–537.

Miele C, Riboulet A, Maitan MA, Oriente F, Romano C, Formisano P, Giudicelli J, Beguinot F, Van Obberghen E. Human glycated albumin affects glucose metabolism in L6 skeletal muscle cells by impairing insulin-induced insulin receptor substrate (IRS) signaling through a protein kinase C alpha-mediated mechanism. J Biol Chem 2003; 278:47376–47387.

Montagnani M, Ravichandran LV, Chen H, Esposito DL, Quon MJ. Insulin receptor substrate-1 and phosphoinositide-dependent kinase-1 are required for insulin-stimulated production of nitric oxide in endothelial cells. Mol Endocrinol 2002; 16(8):1931-42.

Morcos M, Du X, Pfisterer F, Hutter H, Sayed AA, Thornalley P, Ahmed N, Baynes J, Thorpe S, Kukudov G, Schlotterer A, Bozorgmehr F, El Baki RA, Stern D, Moehrlen F, Ibrahim Y, Oikonomou D, Hamann A, Becker C, Zeier M, Schwenger V, Miftari N, Humpert P, Hammes HP, Buechler M, Bierhaus A, Brownlee M, Nawroth PP. Glyoxalase I prevents mitchondrial protein modification and enhances lifespan in Caenorhabditis elegans. Aging Cell 2008; 7:260–269.

Morrish NJ, Wang SL, Stevens LK Fuller JH, Keen H. Mortality and causes of death in the WHO multinational study of vascular disease in diabetes. Diabetologia 2001; 44(Suppl 2):S14–S21.

Motoshima H, Wu X, Mahadev K, Goldstein BJ. Adiponectin suppresses proliferation and superoxide generation and enhances enos activity in endothelial cells treated with oxidized ldl. Biochem Biophys Res Commun 2004; 315(2):264–271.

Muniyappa R, Iantorno M, Quon MJ. An integrated view of insulin resistance and endothelial dysfunction. Endocrinol Metab Clin North Am 2008; 37(3): 685–x.

Myers MG Jr, Backer JM, Sun XJ, Shoelson S, Hu P, Schlessinger J, Yoakim M, Schaffhausen B, White MF. IRS-1 activates phosphatidylinositol 38-kinase by associating with src homology 2 domains of p85. Proc Natl Acad Sci USA 1992; 89 :10350–10354.

Naka Y, Bucciarelli LG, Wendt T, Lee LK, Rong LL, Ramasamy R, Yan SF, Schmidt AM. RAGE axis: animal models and novel insights into the vascular complications of diabetes. Arterioscler Thromb Vasc Biol 2004; 24:1342–1349.

Nieuwdorp M, Haeften TW van, Gouverneur MC, Mooij HL, Lieshout MH van, Levi M, Meijers JC, Holleman F, Hoekstra JB, Vink H, Kastelein JJ, Stroes ES. Loss of endothelial glycocalyx during acute hyperglycemia coincides with endothelial dysfunction and coagulation activation in vivo. Diabetes 2006b; 55:480–486

Nieuwdorp M, Mooij HL, Kroon J, Atasever B, Spaan JA, Ince C, Holleman F, Diamant M, Heine RJ, Hoekstra JB, Kastelein JJ, Stroes ES, Vink H. Endothelial glycocalyx damage coincides with microalbuminuria in type 1 diabetes. Diabetes 2006a; 55:1127–1132.

Nishikawa T, Edelstein D, Du XL, Yamagishi S, Matsumura T, Kaneda Y, Yorek MA, Beebe D, Oates PJ, Hammes HP, Giardino I, Brownlee M. Normalizing mitochondrial superoxide production blocks three pathways of hyperglycaemic damage. Nature 2000; 404(6779):787-90.

Okon EB, Chung AW, Rauniyar P, Padilla E, Tejerina T, McManus BM, Luo H, van Breemen C. Compromised arterial function in human type 2 diabetic patients. Diabetes 2005; 54:2415–23.

Pandolfi A and De Filippis EA. Chronic hyperglicaemia and nitric oxide bioavailability play a pivotal role in pro-atherogenic vascular modifications. Genes Nutr 2007; 2(2): 195-208.

Pessin JE, Saltiel AR (2000). Signaling pathways in insulin action: molecular targets of insulin resistance. J Clin Invest. 106(2):165-9.

Petersen KF, Dufour S, Savage DB, Bilz S, Solomon G, Yonemitsu S, et al. The role of skeletal muscle insulin resistance in the pathogenesis of the metabolic syndrome. Proc Natl Acad Sci USA 2007; 104(31):12587–12594.

Pober JS, Sessa WC. Evolving functions of endothelial cells in inflammation. Nat Rev Immunol 2007; 7:803–815.

Portilla D, Dai G, Peters JM, Gonzalez FJ, Crew MD, Proia AD. Etomoxir-induced PPARalpha-modulated enzymes protect during acute renal failure. Am J Physiol Renal Physiol 2000; 278:F667–F675.

Riboulet-Chavey A, Pierron A, Durand I, Murdaca J, Giudicelli J, Van Obberghen E. Methylglyoxal impairs the insulin signaling pathways independently of the formation of intracellular reactive oxygen species. Diabetes 2006; 55:1289-99.

Ross R. Atherosclerosis-an inflammatory disease. N Engl J Med 1999; 340:115–126.

Saltiel AR, Kahn CR. Insulin signalling and the regulation of glucose and lipid metabolism. Nature 2001; 414:799-806.

Schalkwijk CG and Stehouwer CD. Vascular complications in diabetes mellitus: the role of endothelial dysfunction. Clin Sci (Lond) 2005; 109(2):143-59.

Scherrer U, Randin D, Vollenweider P, Vollenweider L, Nicod P. Nitric oxide release accounts for insulin's vascular effects in humans. J Clin Invest 1994; 94: 2511-2515.

Schleicher E, Nerlich A. The role of Hyperglycemia in the Development of Diabetic Complications. Horm Matab Res 1996; 28:367-373.

Schlotterer A, Kukudov G, Bozorgmehr F, Hutter H, Du X, Oikonomou D, Ibrahim Y, Pfisterer F, Rabbani N, Thornalley P, Sayed A, Fleming T, Humpert P, Schwenger V, Zeier M, Hamann A, Stern D, Brownlee M, Bierhaus A, Nawroth P,

Morcos M. C. elegans as model for the study of high glucose-mediated life span reduction. Diabetes 2009; 58:2450–2456.

Schroeder CA Jr, Chen YL, Messina EJ. Inhibition of NO synthesis or endothelium removal reveals a vasoconstrictor effect of insulin on isolated arterioles. Am J Physiol 1999; 276:815–820.

Shepherd PR, Nave BT, Siddle K. Insulin stimulation of glycogen synthesis and glycogen synthase activity is blocked by wortmannin and rapamycin in 3T3-L1 adipocytes: evidence for the involvement of phosphoinositide 3-kinase and p70 ribosomal protein-S6 kinase. Biochem J 1995; 305:25–28.

Shiekh GA, Ayub T, Khan SN, Dar R, and Andrabi KI. Reduced nitrate level in individuals with hypertension and diabetes. J Cardiovasc Dis Res 2011; 2(3): 172–176.

Shimokawa H, Yasutake H, Fujii K, Owada MK, Nakaike R, Fukumoto Y, Takayanagi T, Nagao T, Egashira K, Fujishima M, Takeshita A. The importance of the hyperpolarizing mechanism increases as the vessel size decreases in endotheliumdependent relaxations in rat mesenteric circulation. J Cardiovasc Pharmacol 1996; 28:703–711.

Shinohara M, Thornalley PJ, Giardino I, Beisswenger P, Thorpe SR, Onorato J, Brownlee M. Overexpression of glyoxalase-I in bovine endothelial cells inhibits intracellular advanced glycation endproduct formation and prevents hyperglycemia-induced increases in macromolecular endocytosis. J Clin Invest 1998; 101(5):1142-7.

Srinivasan BT, Jarvis J, Khunti K, Davies MJ. Recent advances in the management of type 2 diabetes mellitus: a review. Postgrad Med J 2008; 84: 524–531.

Standaert ML, Galloway L, Karnam P, Bandyopadhyay G, Moscat J, Farese RV. Protein kinase C-ζ as a downstream effector of phosphatidylinositol 3- kinase during insulin stimulation in rat adipocytes. Potential role in glucose transport. J Biol Chem 1997; 272:30075–30082.

Stehouwer CD, Lambert J, Donker AJ, Hinsbergh VW van. Endothelial dysfunction and pathogenesis of diabetic angiopathy. Cardiovasc Res 1997; 34:55–68.

Stratton LM, Adler AJ, Neil HA, Matthews DR, Manley SE, Cull CA, Hadden D, Turner RC, Holman RR. Association of glycaemia with macrovascular and microvascular complications of type 2 diabetes (UKPDS 35): prospective observational study. BMJ 2000; 321:405–412.

Sury MD, Frese-Schaper M, Muhlemann MK, Schulthess FT, Blasig IE, Tauber MG. Evidence that n-acetylcysteine inhibits tnf-alpha-induced cerebrovascular endothelin-1 upregulation via inhibition of mitogen- and stress-activated protein kinase. Free Radic Biol Med 2006; 41(9):1372-1383.

Takagi Y, Du J, Ma XY, Nakashima I, Nagase F. Phorbol 12-Myristate 13-Acetate Protects Jurkat cells from Methylglyoxal-Induced Apoptosis by Preventing c-Jun N-Terminal Kinase-Mediated Leakage of Cytochrome c in an Extracellular Signal-Regulated Kinase-Dependent Manner. Mol Pharmacol 2004; 65:778-787.

Thornalley PJ, Edwards LG, Kang Y, Wyatt C, Davies N, Ladan MJ, Double J. Antitumor activity of S-p-bromobenzylglutathione Cyclopentyl Diester in Vitro and in vivo. Biochem Pharmacol 1996; 51:1365–1372.

Thornalley PJ. Glyoxalase I: structure, function and a critical role in the enzymatic defence against glycation. Biochemical Society 2003; 31:1343-1348.

Thornalley PJ: Protein and nucleotide damage by glyoxal and methylglyoxal in physiological systems – role in ageing and disease. Drug Metabol Drug Interact 2008; 23: 125–150.

Tooke JE. Microvascular function in human diabetes- A physiological perspective. Diabetes 1995; 44: 721-726.

Van Obberghen E, Baron V, Delahaye L, Emanuelli B, Filippa N, Giorgetti-Peraldi S, Lebrun P, Mothe-Satney I, Peraldi P, Rocchi S, Sawka-Verhelle D, Tartare-Deckert S, Giudicelli J. Surfing the insulin signaling web. Eur J Clin Invest 2001; 3:966–977.

Vecchione C, Maffei A, Colella S, Aretini A, Poulet R, Frati G, et al. Leptin effect on endothelial nitric oxide is mediated through akt-endothelial nitric oxide synthase phosphorylation pathway. Diabetes 2002; 51(1):168–173.

Vincent MA, Barrett EJ, Lindner JR, Clark MG, Rattigan S. Inhibiting NOS blocks microvascular recruitment and blunts muscle glucose uptake in response to insulin. Am J Physiol Endocrinol Metab 2003; 285(1):E123-9.

Wang XL, Zhang L, Youker K, Zhang MX, Wang J, LeMaire SA, et al. Free fatty acids inhibit insulin signaling-stimulated endothelial nitric oxide synthase activation through upregulating pten or inhibiting akt kinase. Diabetes 2006; 55(8):2301–2310.

White MF. The IRS-signaling system: a network of docking proteins that mediate insulin and cytokine action. Recent Prog Horm Res 1998; 53:119–138.

White MF. The IRS-signalling system: a network of docking proteins that mediate insulin action. Mol Cell Biochem 1998; 182: 3–11.

Williams, B., Gallacher, B., Patel, H. & Orme, C. Glucose-induced protein kinase C activation regulates vascular permeability factor mRNA expression and peptide production by human vascular smooth muscle cells in vitro. Diabetes 1997; 46:1497–1503.

Xuming J and Lingyun. Accumulation of endogenous methylglyoxal impaired insulin signaling in adipose tissue of fructose-fed rats. Mol Cell Biochem 2007; 306:133-139.

Yamagishi S, Takeuchi M. Involvement of advanced glycation end-products (AGEs) in Alzheimer's disease. Curr Alzheimer Res 2004; 1(1):39-46.

Yerneni KK, Bai W, Khan BV, Medford RM, Natarajan R. Hyperglycemia-induced activation of nuclear transcription factor kappaB in vascular smooth muscle cells. Diabetes 1999; 48:855–864.

Zeng G, Nystrom FH, Ravichandran LV, Cong LN, Kirby M, Mostowski H, Quon MJ. Roles for insulin receptor, PI3-kinase, and Akt in insulin-signaling pathways related to production of nitric oxide in human vascular endothelial cells. Circulation 2000; 101:1539–45.

Zhang L, Wheatley CM, Richards SM, Barrett EJ, Clark MG, Rattigan S. Tnf-alpha acutely inhibits vascular effects of physiological but not high insulin or contraction. Am J Physiol Endocrinol Metab 2003; 285(3):E654–E660.

Diabetologia
DOI 10.1007/s00125-011-2315-1

ARTICLE

Increased hexosamine biosynthetic pathway flux dedifferentiates INS-1E cells and murine islets by an extracellular signal-regulated kinase (ERK)1/2-mediated signal transmission pathway

A. Lombardi · L. Ulianich · A. S. Treglia · C. Nigro · L. Parrillo · D. D. Lofrumento · G. Nicolardi · C. Garbi · F. Beguinot · C. Miele · B. Di Jeso

Received: 29 April 2011 / Accepted: 25 August 2011
© Springer-Verlag 2011

Abstract
Aims/hypothesis Beta cell failure is caused by loss of cell mass, mostly by apoptosis, but also by simple dysfunction (decline of glucose-stimulated insulin secretion, down-regulation of specific gene expression). Apoptosis and dysfunction are caused, at least in part, by lipoglucotoxicity. The mechanisms implicated are oxidative stress, increase in the hexosamine biosynthetic pathway (HBP) flux and endoplasmic reticulum (ER) stress. Oxidative stress plays a role in glucotoxicity-induced beta cell dedifferentiation, while glucotoxicity-induced ER stress has been mostly linked to beta cell apoptosis. We sought to clarify whether ER stress caused by increased HBP flux participates in a dedifferentiating response of beta cells, in the absence of relevant apoptosis.
Methods We used INS-1E cells and murine islets. We analysed the unfolded protein response and the expression profile of beta cells by real-time RT-PCR and western blot. The signal transmission pathway elicited by ER stress was investigated by real-time RT-PCR and immunofluorescence.
Results Glucosamine and high glucose induced ER stress, but did not decrease cell viability in INS-1E cells. ER stress caused dedifferentiation of beta cells, as shown by down-regulation of beta cell markers and of the transcription factor, pancreatic and duodenal homeobox 1. Glucose-stimulated insulin secretion was inhibited. These effects were prevented by the chemical chaperone, 4-phenyl butyric acid. The extracellular signal-regulated kinase (ERK) signal transmission pathway was implicated, since its inhibition prevented the effects induced by glucosamine and high glucose.
Conclusions/interpretation Glucotoxic ER stress dedifferentiates beta cells, in the absence of apoptosis, through a transcriptional response. These effects are mediated by the activation of ERK1/2.

Keywords Beta cells · Dedifferentiation · ERK1/2 · ER stress

Abbreviations

BETA2	Beta cell E-box transcriptional activator 2
BIP	Binding protein
C/EBP-β	CCAAT/enhancer binding protein β
ER	Endoplasmic reticulum.
ERK	Extracellular signal-regulated kinase
GFAT	Glutamine:fructose-6-phosphate amidotransferase

Electronic supplementary material The online version of this article (doi:10.1007/s00125-011-2315-1) contains peer-reviewed but unedited supplementary material, which is available to authorised users.

A. Lombardi · A. S. Treglia · D. D. Lofrumento · G. Nicolardi · B. Di Jeso (✉)
Dipartimento di Scienze e Tecnologie Biologiche e Ambientali, Università degli Studi del Salento,
73100 Lecce, Italy
e-mail: bruno.dijeso@unisalento.it

L. Ulianich · C. Nigro · L. Parrillo · C. Garbi · F. Beguinot · C. Miele
Dipartimento di Biologia e Patologia Cellulare e Molecolare, Università degli Studi di Napoli Federico II,
Naples, Italy

A. Lombardi · L. Ulianich · C. Nigro · L. Parrillo · F. Beguinot · C. Miele
Istituto di Endocrinologia ed Oncologia Sperimentale del CNR, Università degli Studi di Napoli Federico II,
Naples, Italy

Published online: 18 October 2011

GlcNAc	Glucosamine acylation
GRP78	Glucose-regulated protein 78
GSIS	Glucose-stimulated insulin secretion
HBP	Hexosamine biosynthetic pathway
KRBH	KRB HEPES
KSR2	Kinase suppressor of Ras 2
MAFA	v-Maf musculoaponeurotic fibrosarcoma oncogene family, protein A (avian)
MAPK	Mitogen-activated protein kinase
MEK	MAPK/ERK kinase
MTT	3-(4,5-Dimethylthiazol-2-yl)-2,5-diphenyltetrazolium bromide
NAC	*N*-Acetylcysteine
PBA	4-Phenyl butyric acid
PDX1	Pancreatic and duodenal homeobox 1
PERK	(PKR)-like endoplasmic reticulum kinase
PUGNAc	*O*-(2-Acetamido-2-deoxy-D-glucopyranosylidene) amino-*N*-phenylcarbamate
ROS	Reactive oxygen species
UPR	Unfolded protein response

Introduction

Pancreatic beta cell failure is increasingly recognised as central to progression of type 2 diabetes. Different insults are implicated in beta cell failure. Results obtained in rodent models of the disease, and in cultured rodent and human islet cells show that dyslipidaemia (lipotoxicity) and hyperglycaemia (glucotoxicity) negatively affect beta cell function and mass in human type 2 diabetes [1, 2].

One component of beta cell failure in type 2 diabetes is loss of beta cell mass. Increased apoptosis is, in turn, an important factor contributing to beta cell loss [3]. The other component of beta cell failure is beta cell dysfunction, represented by inhibition of glucose-stimulated insulin secretion (GSIS) and by downregulation of beta cell-specific genes resulting in beta cell dedifferentiation. Several mechanisms have been implicated in glucotoxicity: the generation of reactive oxygen species (ROS) [4, 5], the activation of endoplasmic reticulum (ER) stress [6–8] and an increase in the hexosamine biosynthetic pathway (HBP) flux [9]. However, these mechanisms are greatly interconnected. For example, an increased HBP flux causes hyper-O-glucosamine acylation (GlcNAc) of nuclear and cytoplasmic proteins [10], oxidative stress [11] and ER stress. This last mechanism has been demonstrated in cells other than beta cells [12].

Therefore, it is not clear whether increased HBP flux causes ER stress in beta cells. Moreover, while it is well established that ROS play a role in glucotoxicity-induced beta cell dedifferentiation [11, 13], the notion that glucotoxicity-induced ER stress participates in beta cell dedifferentiation has not been established yet. Rather, ER stress has been mostly associated with beta cell apoptosis [14, 15], linking its effect to loss of beta cell mass, as is the case for lipotoxicity-induced ER stress [16, 17]. Beta cells are particularly susceptible to ER stress, since they synthesise and secrete large quantities of a single protein. Proinsulin synthesis represents 30–50% of the total protein synthesis of the beta cell [18, 19]. In addition, glucose stimulates proinsulin translation [20], as well as increasing the stability of pre-proinsulin and transcription of the insulin gene [21, 22], further increasing the protein load. Therefore, chronic hyperglycaemia causes persistent activation of the unfolded protein response (UPR), beta cell failure and apoptosis. Recently, however, dedifferentiation has been identified as a new response to ER stress. ER stress dedifferentiates chondrocytes, downregulating collagen II and aggrecan [23]. These results were confirmed in vivo in transgenic mice that express mutant collagen X and in which ER stress produces a chondrodysplasia phenotype [24]. We have also shown that following ER stress, thyroid cells dedifferentiate, losing the expression of thyroid-specific genes and of their transcription factors [25].

In this study we sought to clarify whether increased HBP flux causes ER stress in beta cells, and whether this ER stress leads to apoptosis and participates in a dedifferentiating response of beta cells.

Methods

Materials Media, sera and antibiotics were purchased from Invitrogen (Paisley, UK). Chemicals were from Sigma-Aldrich (St Louis, MO, USA). Glucosamine was from Santa Cruz Biotechnology (Santa Cruz, CA, USA). Insulin was measured by radioimmunoassay (Rat Insulin RIA Kit; Linco Research, St Louis, MO, USA). Antibodies were anti-β-actin (monoclonal; Sigma), anti-insulin (Cell Signaling, Danvers, MA, USA), and anti-binding protein (BIP)/glucose-regulated protein 78 (GRP78), anti-phospho extracellular signal-regulated kinase (ERK)1/2, anti-total ERK1/2 and anti-GLUT2 (Santa Cruz). Collagenase P was from Roche Applied Science (Penzberg, Germany).

Cell culture and 3-(4,5-dimethylthiazol-2-yl)-2,5-diphenyltetrazolium bromide assay The clonal beta cell line INS-1E was used between passages 54 and 95. INS-1E cells were cultured in a humidified atmosphere containing 5% (vol./vol.) CO_2 in complete medium composed of RPMI 1640 supplemented with 5% (vol./vol.) heat-inactivated FCS, 1 mmol/l sodium pyruvate, 50 μmol/l 2-mercaptoethanol, 2 mmol/l glutamine, 10 mmol/l HEPES, 100 U/ml penicillin and 100 μg/ml streptomycin. The maintenance culture was

split once a week and cells were seeded at 3×10^6 cells/75 cm^2 in Falcon bottles (BD Biosciences Labware, Franklin Lakes, NJ, USA). The potential presence of mycoplasma was regularly checked using a photometric enzyme immunoassay (Roche, Penzberg, Germany). For most experiments, INS-1E were seeded at 2×10^5 cells/ml in Falcon 24 well plates and used 4 to 5 days thereafter, with one medium change on day 3 or 4. Cell viability was measured by 3-(4,5-dimethylthiazol-2-yl)-2,5-diphenyltetrazolium bromide (MTT) assay as previously reported [26].

Real-time RT-PCR Total RNA was isolated from INS-1E cells and islets using a kit (RNeasy; Qiagen Sciences, Valencia, CA, USA). For real-time RT-PCR analysis, 1 μg RNA was reverse-transcribed using Superscript II Reverse Transcriptase (Invitrogen, Carlsbad, CA, USA). PCRs were analysed using SYBR Green mix (Invitrogen). Reactions were performed using Platinum SYBR Green quantitative PCR Super-UDG (BioRad, Hercules, CA, USA) and a real-time PCR detection system (iCycler IQ multicolour; BioRad). All reactions were performed in triplicate and cyclophilin was used as an internal standard. The primer sequences are shown in the electronic supplementary material (ESM) Table 1.

Insulin secretion GSIS was tested in INS-1E cells between passages 54 and 95. Before the experiments, cells were maintained for 2 h in glucose-free medium. The cells were then washed twice and preincubated for 30 min at 37°C in glucose-free KRB HEPES buffer (KRBH, 135 mmol/l $CaCl_2$, 3.6 mmol/l KCl, 5 mmol/l $NaHCO_3$, 0.5 mmol/l NaH_2PO_4, 0.5 mmol/l $MgCl_2$, 1.5 mmol/l $CaCl_2$ and 10 mmol/l HEPES, pH 7.4). BSA (0.1%, wt/vol.) was added as an insulin carrier. Next, cells were washed once with glucose-free KRBH and then incubated for 30 min in KRBH and stimuli as indicated. Incubation was stopped on ice and the supernatant fractions collected for insulin secretion, which was measured by RIA using rat insulin as standard.

Western blot Western blots were carried out as previously reported [27].

Immunofluorescence Immunofluorescence experiments were performed as previously reported [25].

Islet isolation and ex vivo insulin secretion Islets were isolated from 6-month-old C57Bl/6J mice. Animals were killed by cervical dislocation, the fur was soaked with ethanol and the abdomen was opened. The pancreas was inflated by KRBH injection and excised. The excised pancreas was washed twice with KRBH and digested with collagenase in a water bath (37°C), shaken by hand for 5–8 min. The digested pancreas was treated with Dnase I. The islets were handpicked under a stereo-microscope and cultured for 24 h in complete RPMI 1640 medium. For glucose-induced insulin release, 20 size-matched islets were preincubated at 37°C for 30 min in KRBH and then incubated for 1 h in a shaking water bath at 37°C; incubation was with 500 μl KRBH medium containing 2.8 mmol/l glucose or 2.8 mmol/l glucose plus 16.7 mmol/l glucose. Islets were then pelleted and supernatant fractions collected for measurement of insulin secretion. Insulin concentrations were determined by RIA. Experiments involving animals were conducted in accordance with the Principle of Laboratory Care.

Statistical procedures All data are presented as mean±SE. Statistical differences were determined by one-way or two-way ANOVA as appropriate, and Bonferroni's post hoc testing was performed when applicable. A value of $p<0.05$ was considered to be significant.

Results

Glucosamine and glucose induce ER stress in INS-1E cells The induction of mRNA encoding the diagnostic UPR marker *Bip/Grp78* was examined by real-time RT-PCR after exposure to various concentrations of glucosamine (2.5, 5.0, 7.5 and 10.0 mmol/l; Fig. 1a) and glucose (25 mmol/l; Fig. 2a) for 24 h. Glucosamine dose-dependently induced *Bip* mRNA, with a maximal effect at 7.5 and 10.0 mmol/l (Fig. 1a), and a similar effect at 24 and 48 h (Fig. 1b). As a control for the osmotic effects of these treatments, cells were exposed to 5.0 and 25 mmol/l xylose, which showed no effect (Fig. 1a). As a positive control, INS-1E cells were treated with the widely used inductor of ER stress, tunicamycin. Interestingly, tunicamycin showed a quantitatively similar effect to that of glucosamine (Fig. 1c). Accordingly, BIP protein was induced to a similar degree by glucosamine and tunicamycin (Fig. 1d).

Glucosamine (and tunicamycin) also increased the mRNA levels of other ER stress markers, such as *Chop* (Fig. 1e), spliced (active) *Xbp1* (Fig. 2d) and *Atf6* (Fig. 2e), suggesting that the three major branches of the UPR were activated by glucosamine. However, glucosamine did not decrease viability of INS-1E cells, suggesting that apoptosis was not significantly activated (Fig. 1f). Tunicamycin had an effect similar to that of glucosamine on *Chop*, spliced *Xbp1* and *Atf6* mRNA (Figs 1e and 2d, e).

The ability of azaserine or 6-diazo-5-oxo-norleucine (not shown), which are potent inhibitors of glutamine:fructose-6-phosphate amidotransferase (GFAT), to attenuate glucose- but not glucosamine-induced ER stress (Fig. 2a) suggests that elevated concentrations of glucose caused ER stress

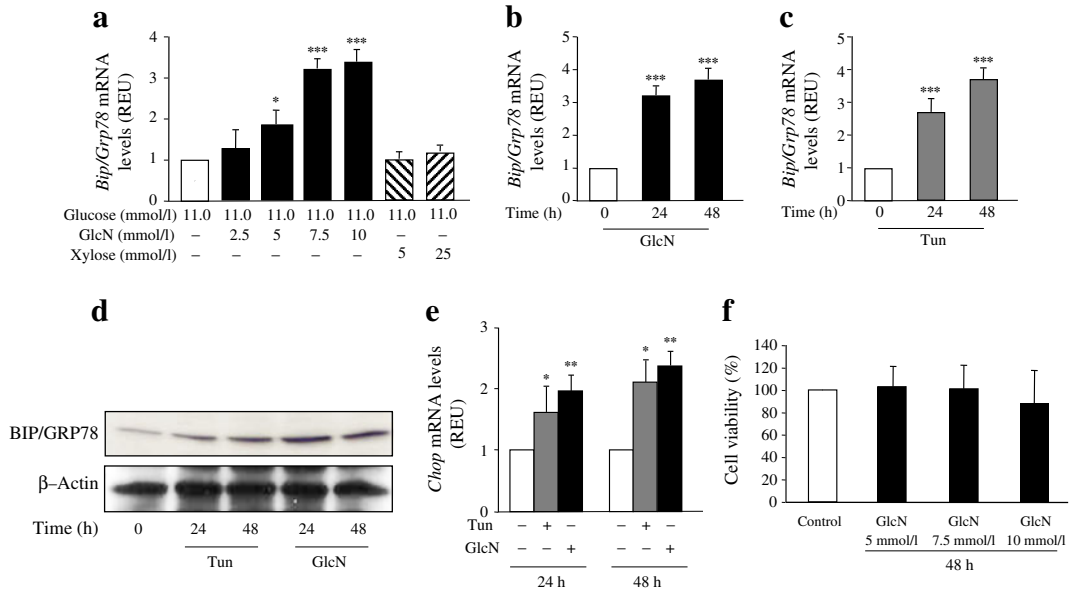

Fig. 1 Glucosamine induces ER stress but does not affect cell viability in INS-1E cells. **a** INS-1E cells were treated with the indicated concentrations of glucosamine (GlcN) or xylose, or (**b, d, e**) with 7.5 mmol/l glucosamine or (**c, d, e**) 0.5 μg/ml tunicamycin (Tun) for times as indicated. *Bip/Grp78* (**a–c**) and *Chop* (**e**) mRNA was determined by real-time RT-PCR analysis of total RNA isolated from INS-1E, using cyclophilin as internal standard. mRNA levels in treated cells are relative expression units (REU) to those in control cells. Values are mean±SD; $n=6$; *$p<0.05$, **$p<0.01$ and ***$p<0.001$. **d** INS-1E cells treated with 0.5 μg/ml tunicamycin or 7.5 mmol/l glucosamine for the indicated times were solubilised and equal amounts of protein (40 μg/sample) were analysed by western blotting using BIP/GRP78- or β-actin-specific antibodies, with BIP and actin from the same gel; $n=3$. **f** MTT assay for cell viability (48 h treatment) in INS-1E cells; results are percentage of the control ($n=3$)

through a glucosamine intermediate. Glucosamine can promote the *O*-GlcNAc modification of intracellular proteins. *O*-GlcNAc levels can also be increased by treatment of cells with *O*-(2-acetamido-2-deoxy-D-glucopyranosylidene) amino-*N*-phenylcarbamate (PUGNAc), an inhibitor of *O*-GlcNAcase. However, PUGNAc treatment did not promote ER stress (Fig. 2a). Thus, we cannot conclude that glucosamine causes ER stress via increased protein *O*-GlcNAc levels, although this mechanism cannot be ruled out.

Chemical chaperones are a group of compounds that can stabilise protein conformation and improve ER folding capacity. We sought to test whether ER stress induced by glucosamine and high glucose in beta cells is, in fact, alleviated by chemical chaperones. As shown in Fig. 2a–e, 4-phenyl butyric acid (PBA) was able to inhibit activation of glucosamine-, high glucose- (and tunicamycin-) induced ER stress markers. Therefore, PBA could be used to investigate the causal relationship between glucosamine-induced ER stress and beta cell dedifferentiation (see below).

To evaluate whether glucosamine- and high glucose-induced ER stress could be mediated by oxidative stress, INS-1E cells were pretreated with the glutathione precursor *N*-acetylcysteine (NAC) (Fig. 2a–c). NAC was not able to inhibit the glucosamine- and high glucose-induced increase of *Bip* and *Chop* mRNA, suggesting that glucosamine- and high glucose-induced ER stress was not dependent on oxidative stress in INS-1E beta cells.

Glucosamine-induced ER stress inhibits differentiation of INS-1E To examine the effects of HBP activation on beta cell function, we examined the expression of two beta cell markers, *Glut2* and *Ins1*. Glucosamine treatments, which are able to trigger ER stress, downregulated the expression of *Glut2* (Fig. 3a, b) and *Ins1* (Fig. 3c). To gain insights into the mechanism of downregulation of *Glut2* and *Ins1*, we analysed the expression of a transcriptional regulator of both genes, the homeobox transcription factor *Pdx1*. As shown in Fig. 3d, *Pdx1* was downregulated by glucosamine treatment. These results suggest that *Glut2* and *Ins1* were transcriptionally downregulated by glucosamine-induced ER stress and that the downregulation of *Pdx1* participated in this effect.

To test the functionality of the beta cell following glucosamine-induced ER stress, we measured GSIS in control and glucosamine-treated INS-1E cells. In comparison with untreated cells, glucosamine-treated cells had a significantly reduced GSIS (Fig. 3e), showing that glucosamine alters the insulin secretory response of normal beta cells to glucose.

The glucosamine-induced dedifferentiation of INS-1E cells is suppressed by the chemical chaperone PBA To establish a causal relationship between glucosamine-induced ER stress and the decreased differentiation of INS-1E cells, we used pre-treatment with PBA, which alleviated the

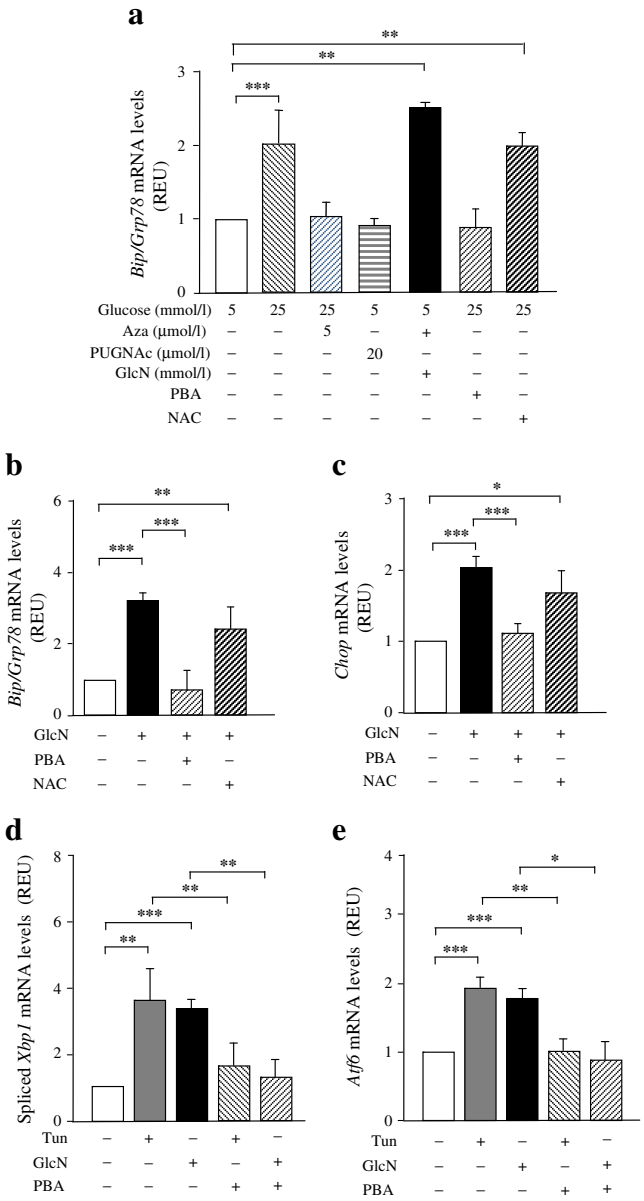

Fig. 2 High glucose induces ER stress and UPR through activation of the hexosamine pathway in INS-1E cells. High glucose-/glucosamine (GlcN)-induced ER stress is reversed by the chemical chaperone PBA, but not by the antioxidant NAC. **a** INS-1E cells were pre-treated or not with 5 μmol/l azaserine (Aza) for 20 min, or (**a**–**e**) with 2.5 mmol/l PBA or (**a**–**c**) 1 mmol/l NAC for 24 h, followed by 24 h culture in the presence of glucose, PUGNAc or GlcN (**a**) as indicated, or of 7.5 mmol/l glucosamine (**b**–**e**) or 0.5 μg/ml tunicamycin (Tun) (**d**, **e**) for 24 h. *Bip/Grp78* (**a**, **b**), *Chop* (c), spliced *Xbp1* (**d**) and *Atf6* (**e**) mRNA in treated cells was determined by real-time RT-PCR analysis using cyclophilin as internal standard and is quantified in relative expression units (REU) vs control cells; values mean±SD; $n=5$; *$p<0.05$, **$p<0.01$, ***$p<0.001$

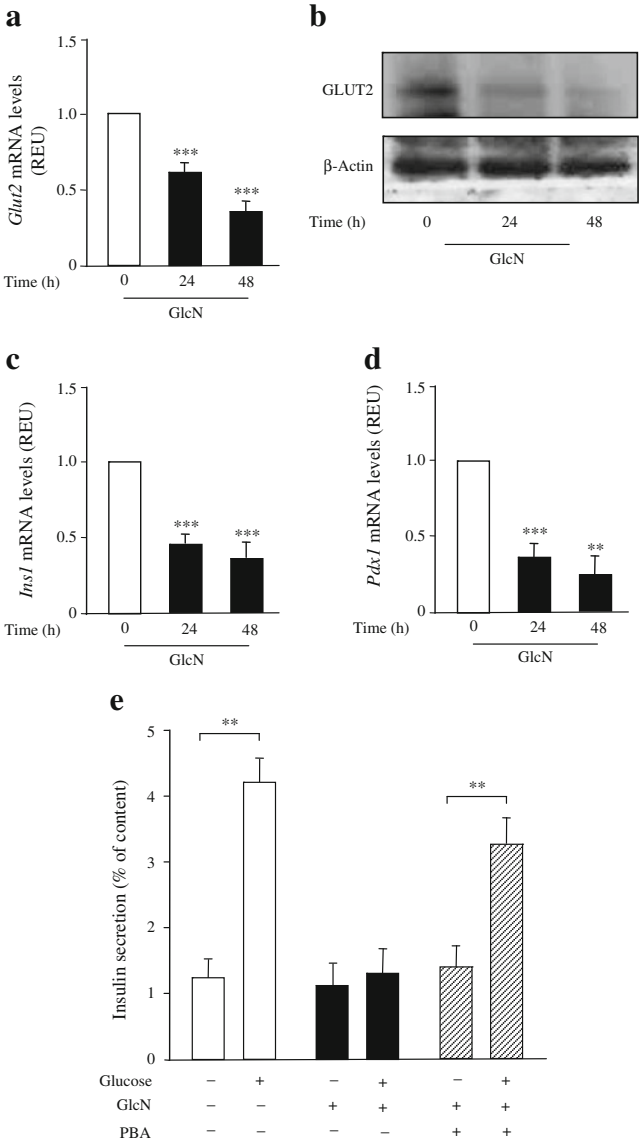

Fig. 3 Effects of glucosamine on beta cell-associated gene expression and glucose-induced insulin secretion in INS-1E cells. **a**–**d** INS-1E cells were treated with 7.5 mmol/l glucosamine (GlcN) for times indicated or (**e**) for 24 h. *Glut2* (**a**), *Ins1* (**c**) and *Pdx1* (**d**) mRNA was determined by real-time RT-PCR analysis of total RNA isolated from INS-1E cells, using cyclophilin as internal standard. mRNA levels in treated cells are quantified as relative expression units (REU) vs control cells; values are mean±SD; $n=5$. **b** Total proteins (40 μg/sample) were analysed by western blotting using GLUT2- or β-actin-specific antibodies ($n=4$). **e** Glucosamine inhibited the insulin secretory response to 30 min incubation with 20 mmol/l glucose. This inhibition was prevented by pretreatment with 2.5 mmol/l PBA for 24 h. GSIS was assayed by RIA in the culture medium; values are mean±SD; $n=4$. **$p<0.01$ and ***$p<0.001$

glucosamine-induced ER stress (Fig. 2b–e). PBA reversed the effect of glucosamine on *Glut2* mRNA (Fig. 4a), *Ins1* mRNA (Fig. 4b), *Pdx1* mRNA (Fig. 4c) and GSIS (Fig. 3e). These results indicate that glucosamine-induced ER stress causally decreases differentiation of INS-1E cells. Since oxidative stress is another important determinant of beta cell damage, we checked for its involvement in glucosamine-induced ER stress. However, pre-treatment with NAC did not prevent the glucosamine-induced down-regulation of beta cell markers (Fig. 4a–c).

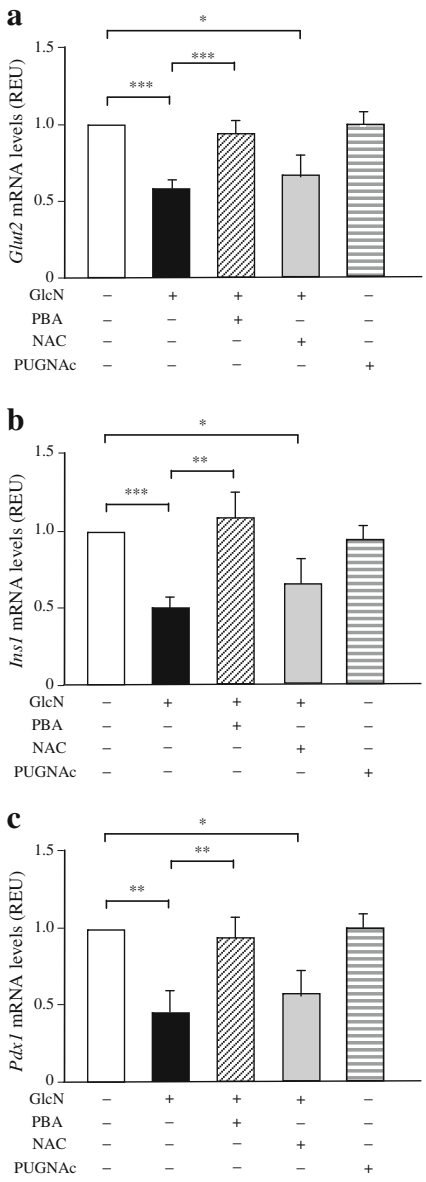

Fig. 4 PBA, but not NAC reversed the dedifferentiating effect of glucosamine. INS-1E cells were pre-treated or not with 2.5 mmol/l PBA or 1 mmol/l NAC for 24 h and then cultured in the presence of 7.5 mmol/l glucosamine (GlcN) or 20 μmol/l PUGNAc for 24 h. **a** *Glut2*, (**b**) *Ins1* and (**c**) *Pdx1* mRNA was determined by real-time RT-PCR analysis of total RNA isolated from INS-1E cells, using cyclophilin as internal standard. mRNA levels in treated cells are quantified as relative expression units (REU) vs control cells; values are mean±SD; $n=3$; *$p<0.05$, **$p<0.01$, ***$p<0.001$

Since chemical chaperones prevented glucosamine-induced ER stress and glucosamine-induced downregulation of *Ins1*, *Glut2* and *Pdx1* mRNA, we sought to determine whether PUGNAc, which was unable to induce ER stress, was also unable to induce beta cell dedifferentiation. As shown in Fig. 4a–c, treatment of INS-1E cells with PUGNAc did not cause dedifferentiation, thus strengthening the notion that ER stress was the cause of loss of differentiation.

The glucosamine-induced dedifferentiation of INS-1E cells is mediated by activation of the mitogen-activated protein kinase/ERK kinase–ERK pathway To obtain insights into the signal transmission pathway linking glucosamine-induced ER stress and beta cell dedifferentiation, we analysed the effect of specific inhibitors of pathways emanating from the stressed ER [28]. We began by using SB203580 to inhibit p38 mitogen-activated protein kinase (MAPK). SB203580 pretreatment had no effect on glucosamine-induced *Ins1* and *Pdx1* mRNA downregulation evaluated by real-time RT-PCR (not shown). Next, we used U0126, a specific inhibitor of MAPK/ERK kinase (MEK)1/2. In this case, U0126 not only completely reversed the effect of glucosamine, but even increased mRNA expression of *Ins1*, *Glut2* and *Pdx1* in the control condition (Fig. 5a). Therefore, it appears that MEK1/2, probably through phosphorylation of ERK1/2, exerts an inhibitory effect on *Ins1* and *Glut2* expression under basal conditions and following glucosamine treatment. In addition to this inhibitory effect, MEK1/2 also seems to contribute to decreased expression of *Pdx1*.

Next, we sought to determine whether glucosamine treatments activated ERK1/2 and whether U0126 prevented such activation. As shown in Fig. 5b, c, glucosamine induced an approximately twofold increase in phosphorylated ERK1/2 at 24 h (the effect being evident as early as 6 h and lasting at least 48 h, data not shown). PBA blocked ERK activation by glucosamine. U0126 not only prevented the increase of phosphorylated ERK1/2, but also inhibited the basal levels of activation of ERK1/2. Notably, BIP induction by glucosamine was not affected by U0126 pretreatment, indicating that U0126 did not prevent ER stress (Fig. 5d). Moreover, U0126 almost completely restored glucosamine-inhibited GSIS (Fig. 5e). Finally, immunofluorescence experiments confirmed that U0126 was not only able to prevent the downregulation of total insulin levels (the antibodies used react with insulin and proinsulin), but also to increase this level above the control value (Fig. 5f–g).

High glucose-induced ER stress displays similar effects to glucosamine-induced ER stress As shown in Fig. 6, high glucose-induced ER stress was also able to dedifferentiate INS-1E cells (*Glut2*, *Ins1* and *Pdx1* mRNA). These effects were reversed by azaserine, PBA and U0126, suggesting that they were dependent on increased HBP flux, ER stress and ERK activation, respectively; however, the effects were not reversed by NAC, suggesting that they were independent of oxidative stress. GSIS was inhibited by high glucose, an effect that was reversed by azaserine, PBA and U0126, but not by NAC (Fig. 6d).

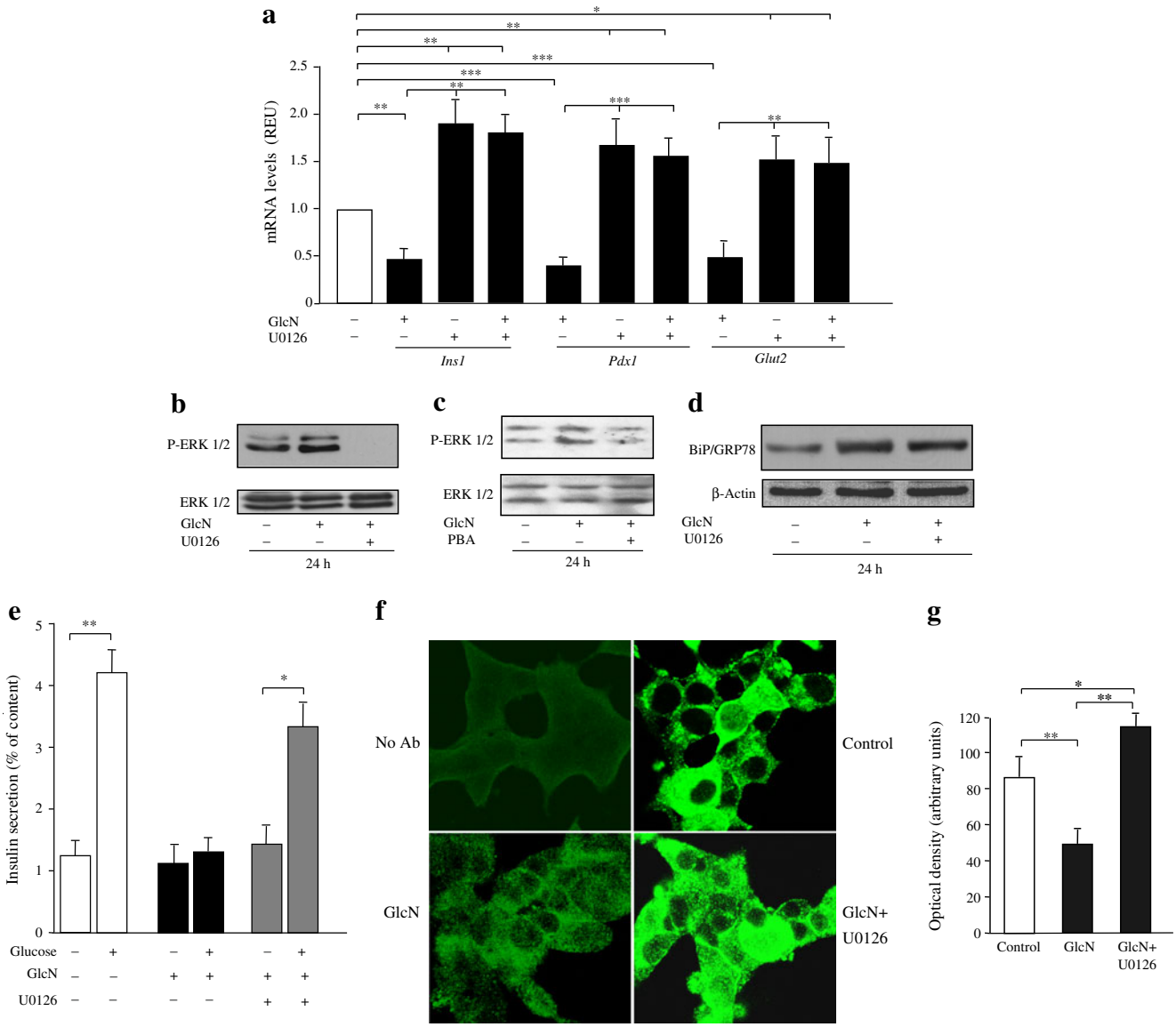

Fig. 5 Role of phosphorylation of ERK 1/2 on glucosamine-induced dedifferentiation in INS-1E cells. INS-1E cells were pretreated or not with 10 μmol/l U0126 for 1 h (**a**, **b**, **d**, **e**) and then treated (**a–f**) with 7.5 mmol/l glucosamine (GlcN) for 24 h. **a** mRNA was determined by real-time RT-PCR analysis of total RNA isolated from INS-1E cells, using cyclophilin as internal standard. mRNA levels in treated cells are quantified as relative expression units (REU) vs control cells; values are mean±SD; $n=3$; *$p<0.05$, **$p<0.01$, ***$p<0.001$. **b–d** Cells were solubilised and equal amounts of proteins (40 μg/sample) were analysed by western blotting using antibodies to phosphorylated (P)-ERK 1/2 and ERK 1/2 (**b, c**), and (**d**) to BIP/GRP78 or β-actin ($n=5$). **e** Glucose-stimulated insulin release was assayed by RIA in the culture medium; values are mean±SD; $n=4$; *$p<0.05$, **$p<0.01$. **f** INS-1E cells were stained with antibodies (Ab) against insulin (green). Following glucosamine treatment, the signal for insulin decreased, compared with untreated control cells. However, pre-treatment for 1 h with 10 μmol/l U0126 not only prevented the decrease, but also increased insulin levels above those of control. **g** Quantification of three different experiments was performed with the software package of a confocal microscope (LSM 510 META; Zeiss, Oberkochen, Germany) *$p<0.05$, **$p<0.01$

Glucosamine induces ER stress and dedifferentiates primary mouse islets in a manner that is dependent on ER stress and ERK Next, we sought to determine whether the dedifferentiating effect of glucosamine was also present in primary mouse islets. To this end, we first evaluated whether glucosamine was able to induce ER stress in this system. As shown in Fig. 7a, b, 7.5 mmol/l glucosamine induced *Bip* and *Chop* mRNAs with a time course similar to that seen in INS-1E cells. Thus, at 24 h the effect of glucosamine was already maximal (Fig. 7a, b). Next, we investigated the effect of glucosamine on beta cell genes *Glut2* and *Ins1*. In a manner that was reciprocal to *Bip* and

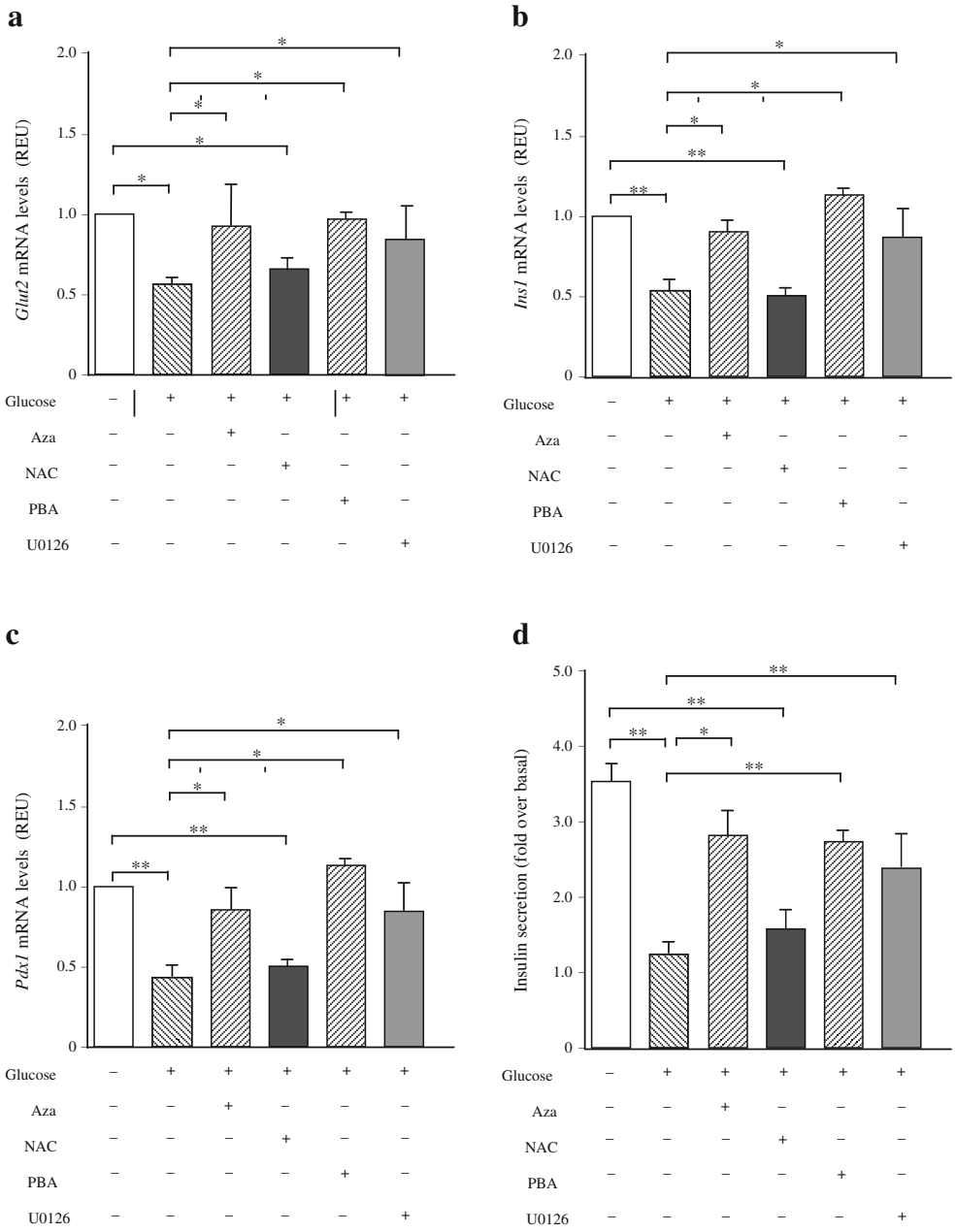

Fig. 6 High glucose-induced ER stress displays similar effects to those of glucosamine-induced ER stress. INS-1E cells were pre-treated or not with 5 μmol/l azaserine (Aza) for 20 min, 10 μmol/l U0126 for 1 h, and 2.5 mmol/l PBA and 1 mmol/l NAC for 24 h, followed by 24 h culture in the presence of 25 mmol/l glucose. mRNA for *Glut2* (**a**), *Ins1* (**b**) and *Pdx1* (**c**) was determined by real-time RT-PCR analysis of total RNA isolated from INS-1E cells, using cyclophilin as internal standard. mRNA levels in treated cells are quantified as relative expression units (REU) vs control cells; values are mean±SD; $n=3$. **d** GSIS was assayed by RIA in the culture medium; values are mean±SD; $n=4$. 7*$p<0.05$, **$p<0.01$, ***$p<0.001$

Chop mRNA induction, *Glut2* and *Ins1* mRNA downregulation was maximal as early as 24 h (Fig. 7c, d), again mimicking the results obtained in INS-1E cells. Also in primary islets, the inhibitory effect of glucosamine on *Glut2* and *Ins1* mRNA is likely to have been transcriptional, as glucosamine also downregulated *Pdx1* mRNA (Fig. 7e). Moreover, GSIS was reduced in islets treated with glucosamine, suggesting that there was also a functional defect in the secretion machinery of islets (Fig. 7f). Finally, these effects were dependent on phosphorylation of ERK, since they were reversed by pretreatment with U0126 (Fig. 7g, h).

Fig. 7 Effects of glucosamine in isolated mice islets. Islets isolated from 6-month-old mice were pre-treated or not with 2.5 mmol/l PBA for 24 h (**f**) or with 10 μmol/l U0126 for 1 h (**g, h**), followed by treatment for 1 day (**a–h**) with 7.5 mmol/l glucosamine (GlcN). **a** *Bip/Grp78*, (**b**) *Chop*, (**c**, **g**) *Glut2*, (**d**, **g**) *Ins1* and (**e**, **g**) *Pdx1* mRNA was determined by real-time RT-PCR analysis of total RNA isolated from mice islets, using cyclophilin as internal standard. mRNA levels in treated cells are quantified as relative expression units (REU) vs control; values are mean±SD; $n=4$; *$p<0.05$, **$p<0.01$ and ***$p<0.001$. **f**, **h** GSIS was examined over 30 min with batches of 20 islets, comparing 3.3 mmol/l with 20 mmol/l (+) glucose. Islets were subsequently collected by centrifugation at 1500 *g* and supernatant fractions assayed for insulin content by RIA. Values are mean±SD; $n=3$; **$p<0.01$

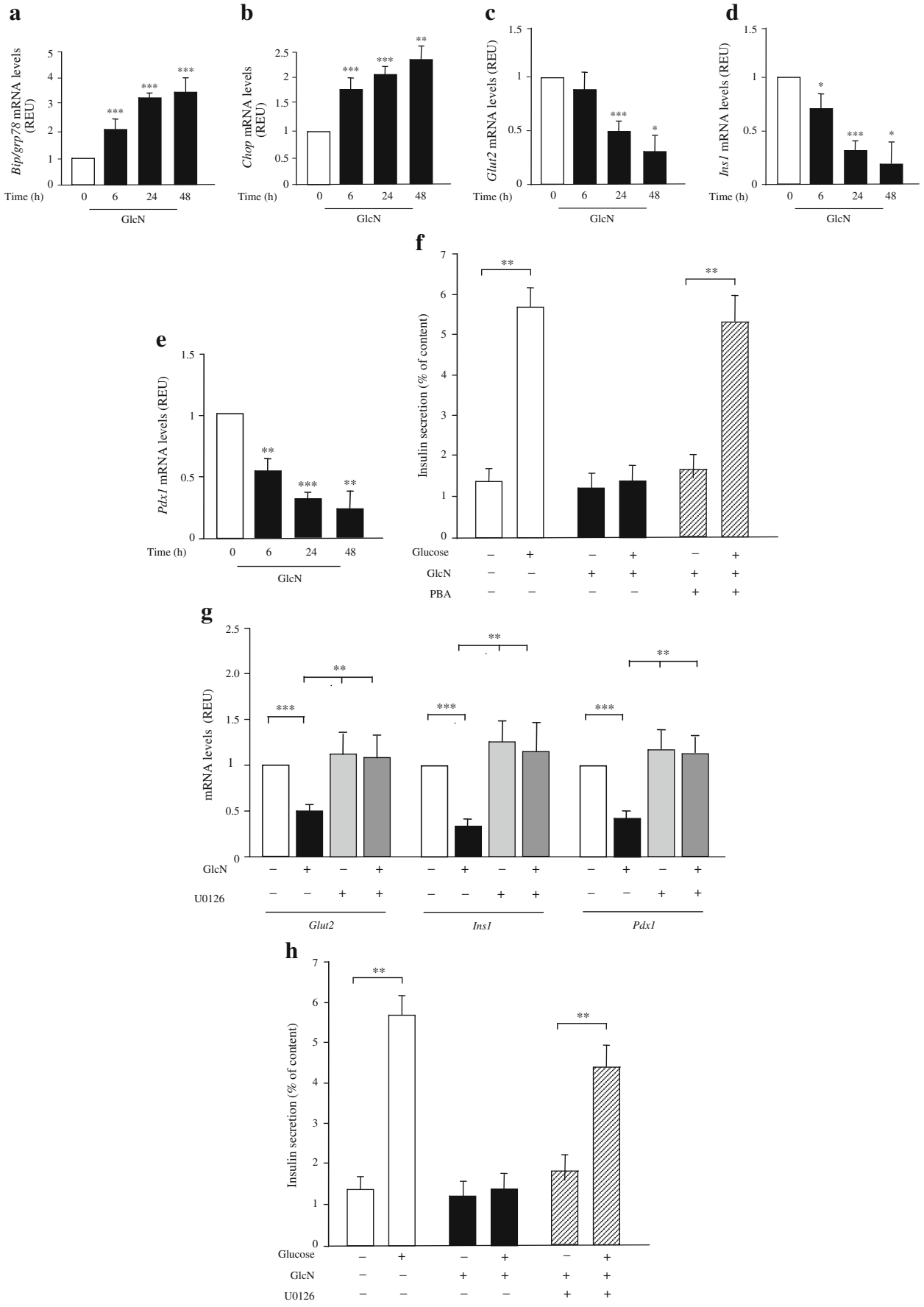
a
Bip/grp78 mRNA levels (REU)
Time (h) 0 6 24 48
GlcN
b
Chop mRNA levels (REU)
Time (h) 0 6 24 48
GlcN
c
Glut2 mRNA levels (REU)
Time (h) 0 6 24 48
GlcN
d
Ins1 mRNA levels (REU)
Time (h) 0 6 24 48
GlcN
e
Pdx1 mRNA levels (REU)
Time (h) 0 6 24 48
GlcN
f
Insulin secretion (% of content)
Glucose
GlcN
PBA
g
mRNA levels (REU)
GlcN
U0126
Glut2
Ins1
Pdx1
h
Insulin secretion (% of content)
Glucose
GlcN
U0126

Discussion

In this study, we show that glucosamine and high glucose induced ER stress in INS-1E cells and in murine islets. As a result, the expression of beta cells markers was decreased and GSIS was inhibited. These deleterious consequences of glucosamine and high glucose treatment were fully prevented by the chemical chaperone PBA, but not by the antioxidant NAC. The effect of glucosamine- and high glucose-induced ER stress on beta cell differentiation and function appears to be mediated by the MEK–ERK pathway.

The declining function and mass of the pancreatic beta cells is central to the progression of type 2 diabetes. While it is well established that dyslipidaemia and hyperglycaemia contribute to beta cell dysfunction [1, 2], the molecular mechanisms implicated are far less clear. In particular, the adverse action of glucose on beta cells is much less well understood, being slower and more subtle than that of fatty acids, which cause strong ER stress and subsequent apoptosis. High glucose has been reported to cause generation of ROS [4, 5], activation of ER stress [6–8] and increase in the HBP flux [9]. Under physiological conditions, only 1–3% of intracellular glucose enters the hexosamine pathway; however, the flux increases with glucose concentration [9]. Increased HBP flux, in turn, causes hyper-O-GlcNAc of proteins [10], oxidative stress [11] and ER stress, although this last mechanism has been demonstrated in cells other than beta cells [12, 29].

We have demonstrated that glucose and glucosamine promote ER stress in beta cells. From our data, we cannot conclude that glucosamine causes ER stress via increased protein O-GlcNAc levels, although this mechanism cannot be ruled out. In fact, data from the literature support the existence of mechanisms that are dependent on [30] and independent of [31] protein O-GlcNAc. Our results also suggest that a glucosamine intermediate is involved in ER stress induction, as inhibition of glutamine amidotransferases, including GFAT, by azaserine blocked ER stress induction by high glucose but not by glucosamine.

ER stress is recognised as an important determinant of type 2 diabetes, and is a central feature of peripheral insulin resistance, acting by inhibiting insulin receptor signalling. However, ER stress also plays an important role in the beta cell failure that precipitates type 2 diabetes. Beta cells, like plasma cells and thyroid cells, have a high protein load [32, 33], synthesising large quantities of (a single) protein. Proinsulin represents up to 20% of the total mRNA and 30–50% of the total protein synthesis of the beta cell [18, 19]. These percentages increase further, when considering only cargo (secretory and membrane) proteins synthesised by the beta cell. In addition, glucose stimulates proinsulin translation [20], and increases the stability of pre-proinsulin and transcription of the insulin gene [21, 22], further increasing the protein load. Therefore, beta cells are highly susceptible to ER stress.

The ER stress induced by high glucose/glucosamine is mild, in contrast to that induced by fatty acids and Ca^{2+}-perturbing drugs. Accordingly, we did not detect a significant effect of glucosamine on the viability of INS-1E cells, while ER stress induced by fatty acids [17] and the Ca^{2+}-perturbing drug cyclopiazonic acid [34] is followed by massive apoptosis. However, the activation of HBP flux, even in the absence of relevant apoptosis, has deleterious effects on beta cells, causing ER stress and inhibiting beta cell differentiation. High glucose-/glucosamine-induced ER stress and beta cell dedifferentiation are causally linked, as demonstrated by the effect of PBA. Indeed, pretreatment with PBA prevented ER stress and dedifferentiation of beta cells. In general, adaptation or apoptosis are believed to be the major outcomes of ER stress. However, dedifferentiation has recently been identified as a new response to ER stress. It has been shown that ER stress dedifferentiates chondrocytes, downregulating collagen II and aggrecan [23]. In vivo, in transgenic mice expressing mutant collagen X, ER stress altered chondrocyte differentiation [24]. Chondrocytes survive ER stress, but terminal differentiation is interrupted. Thyroid cells subjected to ER stress downregulate thyroid-specific markers and their transcriptional factors [25]. Dedifferentiation may constitute a new tactic for survival, since cells avoid energy expenditure for the expression of genes that, in this condition, are unnecessary or even dispensable. Moreover, in all cited cases [23–25], as well as in the case of beta cells (this study), the differentiation genes encode cargo proteins, resulting in a reduction of ER-specific protein load. This represents a selective and long-term downregulation, which is temporally distinct from the general and short-term shut-off of protein synthesis elicited by (PKR)-like endoplasmic reticulum kinase (PERK) [35]. The mechanism of this downregulation is, at least in part, transcriptional, since downregulation of *Ins1* and *Glut2* is accompanied by the coordinate downregulation of *Pdx1*.

Our results indicate that ER stress induced by HBP flux triggers signalling via the MEK–ERK pathway to elicit dedifferentiation of beta cells. It is well known that glucose regulates insulin transcription. Acute exposure of beta cells to high glucose stimulates insulin transcription, while chronic exposure to high glucose results in inhibition of the insulin gene promoter activity. Both effects are mediated by phosphorylation of ERK1/2 [36]. Downstream of ERK1/2 there are several factors that bind to the insulin gene promoter to enhance transcription in response to glucose [37]. Pancreatic and duodenal homeobox 1 (PDX1) and beta cell E-box transcriptional activator

2 (BETA2) synergistically activate insulin gene transcription [38]. v-Maf musculoaponeurotic fibrosarcoma oncogene family, protein A (avian) (MAFA) also contributes to glucose responsiveness [39]. Negative regulators of insulin promoter activity include Jun and the CCAAT/enhancer binding protein β (C/EBP-β). These transcription factors are increased in beta cells during prolonged exposure to low and high glucose, respectively [40, 41]. ERK1 and 2 are activated in pancreatic beta cells by stimulatory concentrations of glucose, this activation being Ca^{2+}-dependent [42, 43]. A rise in intracellular Ca^{2+} is secondary to glucose metabolism and cell depolarisation. Moreover, activation of ERK1/2 by glucose is sensitive to inhibitors of calmodulin and the class 2B Ca^{2+}/calmodulin-dependent phosphatase, calcineurin [44]. Hence, calcineurin is an upstream regulator of the ERK1/2 pathway in pancreatic beta cells. More recently a possible mechanism linking glucose, Ca^{2+} and ERK activation has been elucidated. The protein phosphatase calcineurin selectively dephosphorylates kinase suppressor of Ras 2 (KSR2) in response to Ca^{2+} signals, regulating KSR2 localisation and ERK scaffold activity [45].

However, besides Ca^{2+}- and calcineurin-mediated mechanisms, our study suggests that ER stress may play a role. This may occur specifically during chronic hyperglycaemia. Thus, it is known that chronic challenge of islets with high glucose causes a reduction of Ca^{2+} influx induced by glucose and diazoxide compared with control islets and, moreover, does not lead to detectable changes in the intracellular Ca^{2+} concentration [46]. Therefore, in chronic hyperglycaemia, the Ca^{2+}-mediated mechanisms of ERK activation are likely to be much less involved. Instead, prolonged exposure of beta cells to high glucose or glucosamine induces ER stress. Following the stress, ERK is activated through inositol-requiring 1 (IRE1)-dependent mechanisms [27]. This long term ERK activation may inhibit proinsulin transcription by the already described, mainly post-translational mechanisms. BETA2, PDX1, MAFA, NFAT and C/EBP-β are ERK1/2 substrates [36, 47, 48]. The latter three associate with the insulin gene promoter in an ERK1/2-dependent manner [36]. Finally, the transactivating activities of BETA2 and PDX1 depend at least partly on ERK1/2 activity [49]. Moreover, the present study suggests that, in addition to those known mechanisms in the regulation of insulin transcription, inhibition (probably transcriptional) of an important beta cell transcriptional factor, PDX1, may also play a role.

Interestingly, U0126 not only prevented the glucosamine stimulation of ERK1/2 phosphorylation, but also inhibited the phosphorylation of ERK1/2 present in the basal condition. This effect is paralleled by prevention of the inhibitory effect of glucosamine on *Ins1* and *Pdx1* mRNA, and on total insulin protein (as detected by immunofluorescence), and also by an increase of these mRNAs and total insulin protein levels above those present in basal conditions. It has been proposed recently that cells with a high protein load, such as beta cells, have a level of 'physiological' UPR activation that balances the high protein load with the folding capability [50]. It is conceivable that this 'physiological' UPR causes a certain level of ERK activation. This, in turn, may basally inhibit insulin transcription. In this model, insulin load and 'physiological' UPR activation exert a feedback loop at the level of insulin transcription, in addition to the loop at the translational level, which is operated by PERK–eukaryotic translation initiation factor 2A (eIF2α).

Acknowledgements This work was supported by grant 2006069102_004 of MIUR to B. Di Jeso, as well as by the EFSD and the European Community's PREPOBEDIA (201681). The financial support of Telethon, Italy to F. Beguinot is acknowledged.

Contribution statement AL, LU, AST, CN, LP, DDL, GN, CG, FB, CM analysed the data. AL, LU, AST, CN, LP, DDL, GN, CG, FB, CM revised the article critically. BDJ conceived and designed the study, and wrote the article. All authors approved the final version of the paper to be published.

Duality of interest The authors declare that there is no duality of interest associated with this manuscript.

References

1. Donath MY, Halban PA (2004) Decreased beta-cell mass in diabetes: significance, mechanisms and therapeutic implications. Diabetologia 47:581–589
2. Kaiser N, Leibowitz G, Nesher R (2003) Glucotoxicity and beta-cell failure in type 2 diabetes mellitus. J Pediatr Endocrinol Metab 16:5–22
3. Rhodes CJ (2005) Type 2 diabetes—a matter of beta-cell life and death? Science 307:380–384
4. Robertson RP (2004) Chronic oxidative stress as a central mechanism for glucose toxicity in pancreatic islet cells in diabetes. J Biol Chem 279:42351–42354
5. Kaneto H, Nakatani Y, Kawamori D et al (2005) Role of oxidative stress, endoplasmic reticulum stress, and c-Jun N-terminal kinase in pancreatic beta cell dysfunction and insulin resistance. Int J Biochem Cell Biol 37:1595–1608
6. Cnop M, Welsh N, Jonas JC, Jorns A, Lenzen S, Eizirik DL (2005) Mechanisms of pancreatic β-cell death in type 1 and type 2 diabetes: many differences, few similarities. Diabetes 54:S97–S107
7. Elouil H, Bensellam M, Guiot Y et al (2007) Acute nutrient regulation of the unfolded protein response and integrated stress response in cultured rat pancreatic islets. Diabetologia 50:1442–1452
8. Eizirik DL, Cardozo AK, Cnop M (2008) The role for endoplasmic reticulum stress in diabetes mellitus. Endocr Rev 29:42–61
9. Hanover JA, Lai Z, Lee G, Lubas WA, Sato SM (1999) Elevated O-linked *N*-acetylglucosamine metabolism in pancreatic beta-cells. Arch Biochem Biophys 362:38–45

10. Park J, Kwon H, Kang Y, Kim Y (2007) Proteomic analysis of O-GlcNAc modifications derived from streptozotocin and glucosamine induced beta-cell apoptosis. J Biochem Mol Biol 40:1058–1068
11. Kaneto H, Xu G, Song KH et al (2001) Activation of the hexosamine pathway leads to deterioration of pancreatic beta-cell function through the induction of oxidative stress. J Biol Chem 276:31099–31104
12. Qiu W, Kohen-Avramoglu R, Mhapsekar S, Tsai J, Austin RC, Adeli K (2005) Glucosamine-induced endoplasmic reticulum stress promotes ApoB100 degradation: evidence for Grp78-mediated targeting to proteasomal degradation. Arterioscler Thromb Vasc Biol 25:571–577
13. Harmon JS, Stein R, Robertson RP (2005) Oxidative stress-mediated, post-translational loss of MafA protein as a contributing mechanism to loss of insulin gene expression in glucotoxic cells. J Biol Chem 280:11107–11113
14. Oyadomari S, Araki E, Mori M (2002) Endoplasmic reticulum stress-mediated apoptosis in pancreatic beta cells. Apoptosis 7:335–345
15. Fonseca SG, Burcin M, Gromada J, Urano F (2009) Endoplasmic reticulum stress in beta cells and development of diabetes. Curr Opin Pharmacol 9:763–770
16. Cnop M, Ladriere L, Hekerman P et al (2007) Selective inhibition of eukaryotic translation initiation factor 2 alpha dephosphorylation potentiates fatty acid-induced endoplasmic reticulum stress and causes pancreatic beta cell dysfunction and apoptosis. J Biol Chem 282:3989–3997
17. Cunha DA, Hekerman P, Ladrière L et al (2008) Initiation and execution of lipotoxic ER stress in pancreatic beta cells. J Cell Sci 121:2308–2318
18. van Lommel L, Janssens K, Quintens R et al (2006) Probe-independent and direct quantification of insulin mRNA and growth hormone mRNA in enriched cell preparations. Diabetes 55:3214–3220
19. Schuit FC, Kiekens R, Pipeleers DG (1991) Measuring the balance between insulin synthesis and insulin release. Biochem Biophys Res Commun 178:1182–1187
20. Wicksteed B, Uchizono Y, Alarcon C, McCuaig JF, Shalev A, Rhodes CJ (2007) A cis-element in the 5′ untranslated region of the preproinsulin mRNA (ppIGE) is required for glucose regulation of proinsulin translation. Cell Metab 5:221–227
21. Leibiger B, Moede T, Schwarz T et al (1998) Short-term regulation of insulin gene transcription by glucose. Proc Natl Acad Sci USA 95:9307–9312
22. German M, Ashcroft S, Docherty K et al (1995) The insulin gene promoter. A simplified nomenclature. Diabetes 44:1002–1004
23. Yang L, Carlson SG, McBurney D, Horton WE Jr (2005) Multiple signals induce endoplasmic reticulum stress in both primary and immortalized chondrocytes resulting in loss of differentiation, impaired cell growth, and apoptosis. J Biol Chem 280:31156–31165
24. Tsang KY, Chan D, Cheslett D et al (2007) Surviving endoplasmic reticulum stress is coupled to altered chondrocyte differentiation and function. PLoS Biol 5:568–585
25. Ulianich L, Garbi C, Treglia AS et al (2008) ER stress is associated with dedifferentiation and an epithelial-to-mesenchymal transition-like phenotype in PC Cl3 thyroid cells. J Cell Sci 121:477–486
26. De Vitis S, Treglia AS, Ulianich L et al (2011) Tyr phosphatase-mediated P-ERK inhibition suppresses senescence in EIA + v-raf transformed cells, which, paradoxically, are apoptosis-protected in a MEK-dependent manner. Neoplasia 13:120–130
27. Di Jeso B, Park YN, Ulianich L et al (2005) Mixed-disulfide folding intermediates between thyroglobulin and endoplasmic reticulum resident oxidoreductases ERp57 and protein disulfide isomerase. Mol Cell Biol 25:9793–9805
28. Nguyên DT, Kebache S, Fazel A et al (2004) Nck-dependent activation of extracellular signal-regulated kinase-1 and regulation of cell survival during endoplasmic reticulum stress. Mol Biol Cell 15:4248–4260
29. Raciti GA, Iadicicco C, Ulianich L et al (2010) Glucosamine-induced endoplasmic reticulum stress affects GLUT4 expression via activating transcription factor 6 in rat and human skeletal muscle cells. Diabetologia 53:955–965
30. Vosseller K, Wells L, Lane MD, Hart GW (2002) Elevated nucleoplasmic glycosylation by O-GlcNAc results in insulin resistance associated with defects in Akt activation in 3T3–L1 adipocytes. Proc Natl Acad Sci USA 99:5313–5318
31. Robinson KA, Ball LE, Buse MG (2007) Reduction of *O*-GlcNAc protein modification does not prevent insulin resistance in 3T3-L1 adipocytes. Am J Physiol Endocrinol Metab 292: E884–E890
32. Di Jeso B, Ulianich L, Pacifico F et al (2003) Folding of thyroglobulin in the calnexin/calreticulin pathway and its alteration by loss of Ca^{2+} from the endoplasmic reticulum. Biochem J 370:449–458
33. Di Jeso B, Pereira R, Consiglio E, Formisano S, Satrustegui J, Sandoval IV (1998) Demonstration of a Ca^{2+} requirement for thyroglobulin dimerization and export to the Golgi complex. Eur J Biochem 252:583–590
34. Pirot P, Naamane N, Libert F et al (2007) Global profiling of genes modified by endoplasmic reticulum stress in pancreatic beta cells reveals the early degradation of insulin mRNAs. Diabetologia 50:1006–1014
35. Harding H, Zhang Y, Ron D (1999) Translation and protein folding are coupled by an endoplasmic reticulum resident kinase. Nature 397:271–274
36. Lawrence MC, McGlynn K, Park BH, Cobb MH (2005) ERK1/2-dependent activation of transcription factors required for acute and chronic effects of glucose on the insulin gene promoter. J Biol Chem 280:26751–26759
37. Ohneda K, Ee H, German M (2000) Regulation of insulin gene transcription. Semin Cell Dev Biol 11:227–233
38. Frayling TM, Evans JC, Bulman MP (2001) Beta cell genes and diabetes: molecular and clinical characterization of mutations in transcription factors. Diabetes 1:S94–S100
39. Olbrot M, Rud J, Moss LG, Sharma A (2002) Identification of beta cell-specific insulin gene transcription factor RIPE3b1 as mammalian MafA. Proc Natl Acad Sci USA 99:6737–6742
40. Lu M, Seufert J, Habener JF (1997) Pancreatic beta cell-specific repression of insulin gene transcription by CCAAT/enhancer-binding protein beta. Inhibitory interactions with basic helix–loop–helix transcription factor E47. J Biol Chem 272:28349–28359
41. Inagaki N, Maekawa T, Sudo T, Ishii S, Seino Y, Imura H (1992) c-Jun represses the human insulin promoter activity that depends on multiple cAMP response elements. Proc Natl Acad Sci USA 89:1045–1049
42. Khoo S, Cobb MH (1997) Activation of mitogen-activating protein kinase by glucose is not required for insulin secretion. Proc Natl Acad Sci USA 94:5599–5604
43. Briaud I, Lingohr MK, Dickson LM, Wrede CE, Rhodes CJ (2003) Differential activation mechanisms of Erk-1/2 and p70 (S6K) by glucose in pancreatic beta-cells. Diabetes 52:974–983
44. Arnette D, Gibson TB, Lawrence MC et al (2003) Regulation of ERK1 and ERK2 by glucose and peptide hormones in pancreatic beta cells. J Biol Chem 278:32517–32525
45. Dougherty MK, Ritt DA, Zhou M et al (2009) KSR2 is a calcineurin substrate that promotes ERK cascade activation in response to calcium signals. Mol Cell 34:652–662

46. Khaldi MZ, Guiot Y, Gilon P, Henquin JC, Jonas JC (2004) Increased glucose sensitivity of both triggering and amplifying pathways of insulin secretion in rat islets cultured for 1 wk in high glucose. Am J Physiol Endocrinol Metab 287:E207–E217
47. Piwien-Pilipuk G, Galigniana MD, Schwartz J (2003) Subnuclear localization of C/EBP is regulated by growth hormone and dependent on MAPK. J Biol Chem 278:35668–35677
48. Yang TT, Xiong Q, Graef IA, Crabtree GR, Chow CW (2005) Recruitment of the extracellular signal-regulated kinase/ribosomal S6 kinase signaling pathway to the NFATc4 transcription activation complex. Mol Cell Biol 25:907–920
49. Khoo S, Griffen SC, Xia Y, Baer RJ, German MS, Cobb MH (2003) Regulation of insulin gene transcription by extracellular-signal regulated protein kinases (ERK) 1 and 2 in pancreatic beta cells. J Biol Chem 278:32969–32977
50. Rutkowski DT, Hegde RS (2010) Regulation of basal cellular physiology by the homeostatic unfolded protein response. J Cell Biol 189:783–794

Francesco Beguinot and Cecilia Nigro

Dipartimento di Biologia e Patologia Cellulare e Molecolare & Istituto di Endocrinologia ed Oncologia Sperimentale del CNR – Federico II University of Naples, Italy

Corresponding author: beguino@unina.it

Title: **Measurement of Glucose Homeostasis in vivo: Glucose and Insulin Tolerance Tests**

Running title: Glucose and insulin tolerance tests

Summary

The feasibility of investigating glucose tolerance and insulin action and secretion *in vivo* in mouse models has provided major insights into both type 2 diabetes pathogenesis and the identification of novel strategies to treat this common disorder. When initial studies provide evidence for altered levels of insulin and/or glucose in the animal blood, a number of well-characterized tests can be adopted to estimate glucose homeostasis, insulin action and secretion *in vivo.* These tests include model assessments, glucose and insulin sensitivity studies and glucose clamps. None of them can be considered appropriate under all circumstances and there is significant variation in their complexity, technical ease and invasiveness. Thus, while the euglycaemic hyperinsulinemic clamp represents the gold standard for measuring *in vivo* insulin action, less labour-intensive as well as invasive techinques are usually considered as the initial approach to evaluate glucose homeostasis. This section will focus on glucose and insulin tolerance tests. The clamp technique is described in section 2b.

Keywords: Type 2 diabetes, insulin resistance, insulin sensitivity, mouse phenotyping, insulin secretion.

1. Introduction

Insulin represents the major regulator of glucose homeostasis ***(1)***. The post-prandial rise in plasma insulin enables appropriate disposal of blood glucose in the absorptive state, while the fall in plasma insulin contributes to maintaining euglycaemia in the post-absorptive state and during starvation ***(2)***. In all mammals, these normal fluctuations in insulin levels are dependent upon the ability of pancreatic beta-cells to respond to changes in plasma glucose levels by modulating insulin secretion ***(3)***.

Type 2 diabetes is the most common abnormality of glucose homeostasis and the most frequent endocrine disorder ***(4)***. Current evidence indicates that, in the years preceeding type 2 diabetes onset, a progressive deterioration of insulin sensitivity in liver and peripheral tissues and of beta-cell insulin secretion occurs (Fig.1). This leads to increasingly abnormal glucose tolerance and, finally, to type 2 diabetes ***(5)***. How these abnormalities are generated and become established remain

ultimately unclear, but tremendous interest to solve this problem has accumulated also due to the epidemic diffusion of type 2 diabetes. This circumstance has strengthened the motivation to adopt the convenient mouse model for dissecting the genetic and the molecular causes of type 2 diabetes.

In mice as in humans, derangement in glucose homeostasis is often suspected on the bases of elevated plasma insulin or glucose levels. These abnormalities can be further investigated in the mouse by methodologies similar to those commonly used in humans, including measurements of fasting and post-load glucose and insulin levels, glucose and insulin sensitivity tests and the more invasive clamps (TABLE I). These different approaches correlate quite well and may enable both an accurate characterization of glucose tolerance, i.e., the ability to rescue basal glycaemia upon a load, and identification of major reasons for derangement in glucose homeostasis.

An important and general consideration when assessing glucose tolerance, plasma insulin or glucose concentrations in mice (as well as in humans) is that the conditions under which these variables are measured must be carefully taken into account, as they are affected by a number of physiological and environmental factors in addition to pathological situations. These include physical activity levels, the time of the day and stress. For example, stress-induced increase in catecholamines and cortisol levels can enhance liver glucose production and affect the assessment of glucose tolerance ***(6)***. Also, mice usually exhibit higher cortisol levels in the evening, leading to increased glucose production. Finally, as for many other tests used in the endocrinological assessment of the mouse phenotype, the validity of results obtained is largely dependent on methods of animal husbandry. Adequate experience of the personnel performing the tests is key to reduce the anxietly levels of the mice both before and during the experiments. Reference values for metabolite and hormone levels in many mouse strains are available through the Jackson Laboratories web site (http://www.jacksonlaboratory.com).

2. Material

2.1 Detection of blood glucose concentrations

1. Blood glucose monitor and associated test strips for glucose measurement (e.g., Accu-Check Active, Roche Diagnostics).
2. Low and high-level glucose control solutions (e.g., Accu-Check Active glucose control solutions, Roche Diagnostics; low concentration: 50 mg/dL, reference range 42 to 72 mg/dL, and high concentration: 300 mg/dL, reference range 290 to 328 mg/dL).
3. Scalpel blade.

2.2 Detection of insulin concentration

1. Mouse serum or plasma.
2. Microtiter plate shaker.
3. Microtiter plate washer.
4. Plate reader with 450 nm reading capability.
5. Ultrasensitive Mouse Insulin ELISA kit (e.g. Mercodia).

2.3 Oral glucose tolerance test

1. 20% (w/v) aqueous glucose solution.
2. Animal scale.
3. Blood glucose monitor and test strips for glucose measurement (e.g. Accu-Check Active, Roche Diagnostics).
4. Scalpel blade.
5. 1-mL syringe (e.g. Terumo) and 22-G ball-tip needle (e.g. Popper and Sons).
6. Timer.

2.4 Intraperitoneal insulin tolerance test

1. Animal scale.
2. Blood glucose monitor and test strips for glucose measurement (e.g. Accu-Check Active, Roche Diagnostics).
3. Fast-acting insulin solution.
4. Scalpel blade.
5. 1-mL syringe (e.g. Terumo) and 25-G x 5/8-in. Needles (e.g. Terumo).
6. Timer.

4. Methods

4.1 Determination of glycaemia by glucose monitor

Blood glucose concentration is often the first parameter to be determined when defining the metabolic phenotype, as abnormalities are indicative of alterations in glucose homeostasis. Blood glucose can be assayed on plasma or serum samples, which is usually achieved by enzymatic methods using either hexokinase or glucose oxidase. Whether performed manually or authomatically, this approach is specially useful when samples are to be frozen and/or analyzed at a later point in time. Alternatively, glucose concentration can be conveniently determined on whole blood using the portable glucose monitors designed for human diabetes self-control. These devices are inexpensive, easy to use and provide fast and reliable results from very small volumes of blood. The protocol below describes the use of the Accu-Chek Active blood glucose monitor from Roche Diagnostics. Other widely used monitors include the HemoCue Glucose (HemoCue), BD Logic Blood Glucose Monitor (BD), Precision Xtra (Abbott) and One Touch Ultra (LifeScan).

1. Calibrate the blood glucose monitor as described in the manufacturer's user manual of the device, and repeat calibration each time a new box of test strips is used (*see* **Note 1**).
2. Using the low and the high-level glucose control solutions, execute a performance check on the monitor as described in the manufacturer's user manual of the device. This routine should be repeated each time a new box of test strips is used, or if uncertain of the monitor performance. Use the same lot of test strips for one experiment as intra-lot variations can occur (*see* **Note 1**).
3. Insert a new test strip in the device.
4. Draw an approximately 3 μL blood drop from a mouse by notching the lateral tail vein 1-2 cm from the tip using a scalpel blade and apply the drop to the test strip by touching the strip directly to the bleeding tail wound.
5. Read and record the test result (*see* **Note 2**).
6. Facilitate blood clotting by applying gentle mechanical pressure to the tail wound and return the mouse in its cage.

3.2 Determination of insulinemia by ELISA

For measuring the plasma insulin concentration we recommend the use of the Ultrasensitive Mouse Insulin ELISA by Mecordia. The assay is based on a solid-phase direct sandwich ELISA and adopts two monoclonal antibodies against separate epitopes of the insulin molecule. Sample insulin is immobilized by the first antibody bound to the assay well, followed by labelling with peroxidase-conjugated antibodies. The bound insulin is then revealed colorimetrically. Other commercially available ELISA kits for measuring insulin in small volumes include the Linko Research kit.

1. Pipet calibrator 0 (25 μL) into each well of a 96-well microtiter plate coated with mouse insulin antibody.
2. Pipet calibrators (5 μL) and mouse serum or plasma (5 μL) into duplicate wells of the antibody-coated microtiter plate (*see* **Note 3**).
3. Add 50 μL of antibody-enzyme conjugate reagent to each well (the reagent is prepared by diluting the concentrated antibody-enzyme conjugate provided with the commercial kit as specified in the manufacturer's instructions.
4. Incubate on a shaker for 2h at room temperature (18° – 25°C).
5. Aspirate the reaction volume, add 350 μL of wash buffer to each well and aspirate completely. Repeat this procedure five more times. The wash buffer is prepared by diluting the concentrated wash buffer provided with the commercial kit as specified in the kit manufacturer's instructions).
6. After the last wash, invert the plate and tap firmly against absorbent paper.
7. Add 200 μL of TMB substrate reagent (provided with the kit) to each well (light-sensitive reagent).
8. Incubate 30 min at room temperature.
9. Add 50 μL stop solution.
10. Place the plate on the shaker for about 10 sec to enable adequate mixing of substrate and stop reagents.
11. Measure the absorbance at 450 nm and compute results according to the kit manufacturer's instructions (for manual calculation, plot the calibrators on a log-log or log-in paper and read the insulin concentrations for each sample from the curve).
12. If the insulin concentration exceeds the value of the highest calibrator, dilute the sample ten-fold with 0.9% NaCl and repeat the analysis.

3.3 Oral glucose tolerance test

The oral glucose tolerance test (OGTT) enables an estimate of the clearance of a standard bolus of glucose. At variance from the intraperitoneal glucose tolerance test (IPGTT) described in 3.4, the OGTT is based on orally administered glucose, so that its clearance is also determined by intestinal factors. Animals tested by OGTT are starved for 14-16 h, followed by glucose administration by gavage and blood or plasma glucose measurement through the following 3h. The oral gavage techniques is fully described in ***(7)***. In each experimental setting, two trained persons should cooperate with one of them only performing the gavage in the entire group of animals. In order to achieve interpretable results, it is advisable that no more than 16 mice are treated in each experimental setting. Accordingly, accurate experimental design to divide the animal group is necessary.

1. Fast mice for 14-16 h (overnight) with constant access to drinking water.

2. On the following day, at 8:00 A.M., place each mouse in a fresh cage with access to water and identify each cage with the mouse number.
3. Record the weight of each mouse.
4. Calculate and record the volume of the 20% glucose solution required for oral gavaging of 2g of glucose/kg (oral injection volume 10 μL/g body weight).
5. Prepare strips for glucose measurements, record sheets, and a 1mL syringe for each animal containing the calculated glucose to be gavaged. One ball-tip needle can be used through the entire experiment, switching it between the different syringes upon fast external rinsing with 70% ethanol and water.
6. Calibrate the blood glucose monitor as described in 3.1.
7. Determine the basal glucose concentration in each mouse (T_0) by removing one mouse at a time, placing it on the top of its cage and drawing blood from the lateral vein of the tail as previously outlined in 3.1. Place the blood sample on the test strip of the glucose monitor, read and record the result. Facilitate blood clotting on the tail incision as previously described and return the mouse in its cage.
8. After the basal glucose concentrations has been determined in all mice, perform gavaging and administer the glucose load to each mouse, maintaining a 30-60 sec interval between animals, depending on the size of the experimental group. Start the timer upon the first mouse has been gavaged. It takes at least 30 seconds for an experienced investigator to perform gavaging and blood glucose determination (*see* **Note 4**).
9. At T_{15}, measure the blood glucose again, starting with the first mouse gavaged and maintaining the same time interval until all of the mice in the experimental group have been assesed. To enable rebleeding, remove the clot from the incision and massage the tail as needed to enable sufficient blood flow.
10. Repeat this procedure at T_{30}, T_{60}, T_{90}, T_{120}, T_{150}, T_{180} (*see* **Note 5**).
11. At the end of the experiment, return mice in their original cages and make sure that none of them is beeding. Also, make sure that animals food and drinking water is available again.
12. Data are usually plotted as glucose values versus time. Statistical treatment of the data can be simplified by calculating, for each mouse, areas under the curves as in ***(8)***.

3.4 Intraperitoneal glucose tolerance test

The intraperitoneal glucose tolerance test (IPGTT) measures the clearance of an intraperitoneally-injected glucose load by tissues. Compared to the OGTT, IPGTT does not address the intestinal phase of glucose absorption and is, therefore, a less physiological test. The procedure is very similar to that used for OGTT with the exception that the glucose load is injected intraperitoneally rather than by gavaging (*see* **Note 6**). Accordingly, matherials and methods will not be outlined again. Please refer to 3.3 for details (*see* **Note 7**). Same as for oral administration, a 2g glucose/kg load should be used, with an intraperitoneal injection volume of 10μL/g body weight. The same considerations on timing and group size apply to IPGTT and to OGTT (see 3.3).

3.5 Intraperioneal insulin tolerance test

The intraperitoneal insulin tolerance test (IPITT) measures glucose levels upon administration of a standard insulin bolus, providing an estimate of the insulin sensitivity of the animal. Animals are fasted for 14 to 16 h and subjected to intraperitoneal insulin loading. Blood glucose levels are measured at different time points through the following 90 min.

As for glucose tolerance studies, experimental design of IPITT studies must take into serious consideration the size of the experimental sample. Again, it is advisable that no more than sixteen animals are examined during the same experimental set-up with two trained personnel units each of which is attributed specific roles in the experiment. To minimize technical variation, insulin should be injected by the same unit of personnel to all of the mice.

1. Fast mice for 14-16 h (overnight) with constant access to drinking water.
2. On the following day, at 8:00 A.M., place each mouse in a fresh cage with access to water and identify each cage with the mouse number.
3. Record the weight of each mouse.
4. Calculate and record the volume of insulin solution required for an intraperitoneal injection of 0.5 IU/kg in an injection volume of 3.6 μL/g body weight.
5. Prepare the 1 mL insulin syringes and 25-G x 5/8-in. needles with the calculated volumes for each animal in the experiment. Prepare experiment record sheets and test strips for glucose measurement (*see* **Note 8**).
6. Calibrate the glucose monitor with the standard strip.
7. Determine the basal glucose levels in each mouse by removing one mouse at a time from its cage, placing it on the top of the cage and drowing blood from the lateral vein of the tail as outlined in 3.1. Facilitate blood cloting as described under in 3.1.
8. Inject insulin intraperitoneally in each mouse at 30-60 sec interval between animals, depending on the size of the experimetal group. Start the timer when the first mouse is injected (*see* **Note 9**).
9. At T_{15}, determine blood glucose again, starting with the first mouse injected and using the same interval adopted for injection, until all the mice in the experimental group have been measured. To restart bleeding, gently remove the clot from the incision and massage the tail as needed to increase the blood flow.
10. Repeat the above sequence at T_{30}, T_{60} and T_{90} after insulin injection. If at any time during implementation of the protocol, blood glucose falls below 36 mg/dL, the value must be confirmed. If confirmed, the mouse must be rescued by injecting 0.5-1.0 g glucose/kg from a 20% glucose solution as hypoglycaemia might be otherwise lethal (*see* **Note 10**).
11. Data are usually presented by plotting glucose values versus time. If mice significantly differ in their basal glucose levels, plotting % of basal value versus time may represent a valid alternative.
12. Calculation of areas under the curve may provide additional information, especially if the initial and the late phases (the last 90-60 min, when counterregulatory hormones start playing a major role) are analyzed separately.

4. Notes

1. The small size of the blood volume of a normal mouse requires high sensitivity of all of the procedures adopted to assay circulating metabolites. This requirement is particularly strict in the case of glucose as the accomplishment of several metabolic tests needs repeated sampling over short periods of time.
2. For very low (<2mM) or very high glucose levels (reported upper limit for the Accu-Check monitor is 33.3 mM) use of alternative methods to confirm readings is highly advisable.
3. Fasting insulin levels in many mouse strains are close to the sensitivity limit of most commercially available kits (0.2 μg/L for the Mercodia kit). Attention must be payed to the storage conditions of the serum /plasma samples and their freeze-thaw cycles. Also, the upper level detection limits of many commercial kits (7 μg/L for the Mercodia kit) are relatively low compared to the insulin levels which may be achieved in certain experimental conditions. This circumstance may require adequate dilution of the samples and re-test.
4. Correct oral gavaging is essential and must be performed by experienced personnel to avoid tracheal instead of oesophagus gavaging.
5. After the load (T_{15}), blood glucose is expected to increase 1.5 to 2-fold, followed by a slow return toward the basal values. However, in insulin-resistant states, peak glucose concentration is usually higher and return to basal slower. The kinetics of blood glucose excursion resembles that occurring during IPGTT, although glucose peak is usually reached later, it is somewhat more blunted and the return toward the basal condition is slower. During all tolerance tests, changes in glucose and insulin levels are dynamic. Therefore, the number of animals used in each experimental group must be small enough to precisely respect of the scheduled timetable, perticularly during the initial phases of the study where the most rapid changes occurs (tipically the T_0 to T_{30} in the glucose tolerance tests).
6. An important technical concern, specially with obese mice, is that the glucose solution may end up to be injected in the adipose depots, slowing absorption. This circumstance may offer reasons for even greater concern when animals with large difference in the amount of fat tissue are compared. Since direct possibilities to clarify this issue are scarce, efforts must be devoted at the time of data analysis to identify unresponsive animals.
7. Initial glucose peaks during IPGTT should be at least 2-fold higher than baseline levels but can be even 10-fold higher depending on the particular experimental set-up, including the mouse genetic background. When insulin is measured in addition to glucose, values usually follow the changes in glycaemia. On the other hand, a significant increase in peak glucose (T_0-T_{30}) may be indicative of defective beta-cell function.
8. For some mouse strains, the insulin dose recommended in the above protocol may be too high and result in severe, even lethal hypoglycaemia. Since this circumstance is somewhat impredictable, it is advisable that a preliminary test with a small number of mice is implemented to assess the insulin sensitivity of the particular mouse strain unders study. From a practical perspective it is also advisable that only freshly prepared insulin solutions are used, as this will prevent excessive binding to the test tube walls and the syringe.

9. As in the case of IPGTT, adiposity may create reasons for concern when data from IPITT are to be analyzed, specially if study groups differ significantly for abdominal fat (see under Protocol 4).
10. Upon insulin injection, blood glucose typically falls from the basal levels until T_{30}, after which it tends to stabilize and slowly returns toward basal levels. Slower recovery from hypoglycaemia may indicate failure of the counter-regulatory system and or impaired glucose production.

References

1. Pickup J.C., Williams G. (2005) Textbook of Diabetes: selected chapters, 3rd edn. Blackwell Publishing, Oxford.
2. Saltiel A.R., Kahn C.R. (2001) Insulin signalling and the regulation of glucose and lipid metabolism. Nature 414, 799-806.
3. Andrali S.S., Sampley M.L., Vanderford N.L. et al. (2008) Glucose regulation of insulin gene expression in pancreatic beta-cells. Biochem J. Oct 1 415(1), 1-10.
4. Sicree R., Shaw J., Zimmet (2009) The Global Burden: Diabetes and Impaired Glucose Tolerance. Diabetes Atlas, IDF. 4. International Diabetes Federation, Brussels.
5. Cavaghan M.K., Ehrmann D.A. et al. (2000) Interaction between insulin resistance and insulin secretion in the development of glucose intolerance. J. Clin. Invest. 106, 329-333.
6. Vranic M., Miles P., Rastogi K. et al. (1991) Effect of stress on glucoregulation in physiology and diabetes. Adv Exp Med Biol. 291, 161-83.
7. Hedrich, H. (ed.) (2004) The Laboratory mouse. Elsevier Academic Press, London.
8. Heikkinen, S., Argmann, C.A., Champy, M.F. et al. (2007) Evaluation of glucose homeostasis. Curr Protoc Mol Biol Chapter 29: Unit 29B.3.

Table 1
Basic methods used to assess insulin sensitiviy and glucose tolerance[1]

Test	Sample	Method
FPG and FPI	One 50 μL blood sample	Overnight or 4h fasting glucose and insulin measurements
OGTT	Eight 3 μL blood samples	Overnight fast and glucose measurement after oral glucose load
IPGTT	Eight 3 μL blood samples	Overnight fast and glucose measurements after I.P. glucose load
IPITT	Six 3 μL blood samples	Overnight fast and glucose measurements after I.P. glucose load

FPG, fasting plasma glucose; FPI, fasting plasma insulin; OGTT, oral glucose tolerance test; IPGTT, intaperitoneal glucose tolerance test; IPITT, intraperitoneal insulin tolerance test; I.P., intraperitoneal.

Major pathophysiological abnormalities leading to impaired glucose tolerance

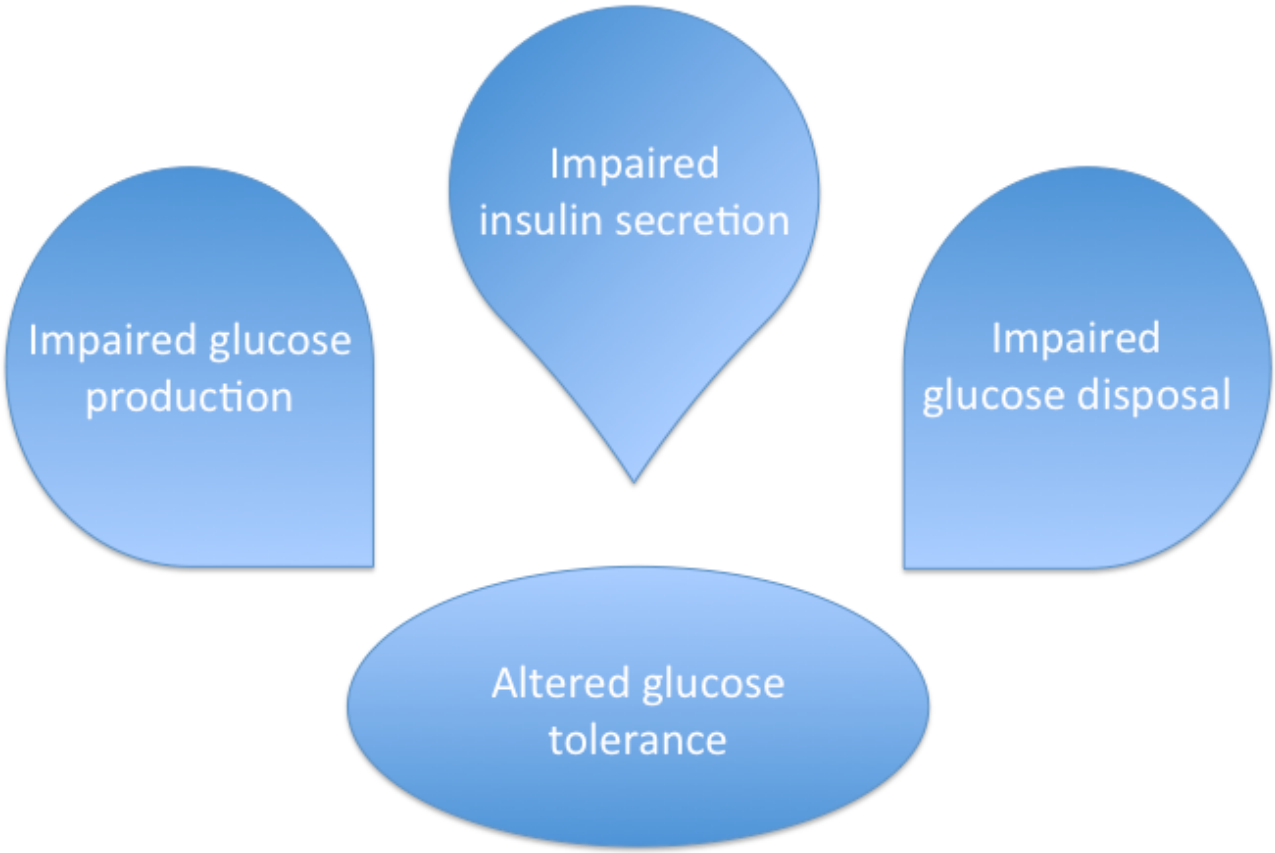

Diabetologia (2010) 53:1482–1492
DOI 10.1007/s00125-010-1732-x

ARTICLE

Hepatocyte nuclear factor (HNF)-4α-driven epigenetic silencing of the human *PED* gene

P. Ungaro · R. Teperino · P. Mirra · M. Longo · M. Ciccarelli · G. A. Raciti · C. Nigro · C. Miele · P. Formisano · F. Beguinot

Received: 1 February 2010 / Accepted: 25 February 2010 / Published online: 16 April 2010
© Springer-Verlag 2010

Abstract
Aims/hypothesis Overexpression of *PED* (also known as *PEA15*) determines insulin resistance and impaired insulin secretion and may contribute to progression toward type 2 diabetes. Recently, we found that the transcription factor hepatocyte nuclear factor (HNF)-4α binds to *PED* promoter and represses its transcription. However, the molecular details responsible for regulation of *PED* gene remain unclear.
Methods Here we used gain and loss of function approaches to investigate the hypothesis that HNF-4α controls chromatin remodelling at the *PED* promoter in human cell lines.
Results HNF-4α production and binding induce chromatin remodelling at the −250 to 50 region of *PED*, indicating that remodelling is limited to two nucleosomes located at the proximal promoter. Chromatin immunoprecipitation assays also revealed concomitant HNF-4α-induced deacetylation of histone H3 at Lys9 and Lys14, and increased dimethylation of histone H3 at Lys9. The latter was followed by reduction of histone H3 Lys4 dimethylation. HNF-4α was also shown to target the histone deacetylase complex associated with silencing mediator of retinoic acid and thyroid hormone receptor, both at the *PED* promoter, and at *GRB14* and *USP21* regulatory regions, leading to a reduction of mRNA levels. Moreover, HNF-4α silencing and *PED* overexpression were accompanied by a significant reduction of hepatic glycogen content.
Conclusions/interpretation These results show that HNF-4α serves as a scaffold protein for histone deacetylase activities, thereby inhibiting liver expression of genes including *PED*. Dysregulation of these mechanisms may lead to upregulation of the *PED* gene in type 2 diabetes.

Keywords Chromatin remodelling · HNF-4α · Insulin resistance · PED · Type 2 diabetes

Abbreviations

ChIP	Chromatin immunoprecipitation
ECL	Electrochemiluminescence
$HeLa_{HNF\text{-}4\alpha}$	HeLa cells overproducing exogenous HNF-4α
$HepG2_{HNF\text{-}4\alpha\text{-}sh}$	HepG2 cells subjected to silencing of the endogenous HNF-4α
H3K4	Histone H3 Lys4
H3K9	Histone H3 Lys9
HNF	Hepatocyte nuclear factor
HRE	HNF-4α response element
MNase	Micrococcal nuclease
panSMRT	Regions common to SMRTα and SMRTβ
PED	Phosphoprotein enriched in diabetes
shRNA	Short hairpin RNA
siRNA	Short interfering RNA
SMRT	Silencing mediator of retinoic acid and thyroid hormone receptor

P. Ungaro and R. Teperino contributed equally to the present study.

Electronic supplementary material The online version of this article (doi:10.1007/s00125-010-1732-x) contains supplementary material, which is available to authorised users.

P. Ungaro (✉) · R. Teperino · P. Mirra · M. Longo · M. Ciccarelli · G. A. Raciti · C. Nigro · C. Miele · P. Formisano · F. Beguinot
Dipartimento di Biologia e Patologia Cellulare e Molecolare "L. Califano" & Istituto di Endocrinologia ed Oncologia Sperimentale del CNR, Università di Napoli Federico II,
Via Sergio Pansini, 5,
Naples 80131, Italy
e-mail: pungaro@ieos.cnr.it

Introduction

Recent genetic studies [1–3] have considerably expanded the list of known genes that may cause a predisposition to diabetes. However, it remains largely unclear how these genes determine the development of type 2 diabetes. Phosphoprotein enriched in diabetes (PED, also known as phosphoprotein enriched in astrocytes-15 [PEA15]) is a scaffold cytosolic protein widely produced in human tissues [4, 5]. Early studies indicated that PED has an important role in controlling glucose disposal by impacting on protein kinase C signalling [5, 6]. It was later found that PED is commonly overproduced in individuals with type 2 diabetes as well as in their euglycaemic offspring [5, 7]. In these persons PED overproduction causes insulin resistance in GLUT4-mediated glucose disposal. Studies in tissue-specific transgenics and in null mice have indicated that the upregulation of PED observed in type 2 diabetic patients might also contribute to impaired beta cell function [7]. PED cellular levels are regulated by ubiquitinylation and proteosomal degradation [8], but run-on experiments in cultured cells from type 2 diabetic patients have demonstrated that, at least in part, the overproduction observed in these participants is caused by transcriptional abnormalities [5]. The molecular details responsible for these abnormalities and how the *PED* gene is regulated remain unclear. Moreover, the role of PED in liver glucose metabolism has been less extensively investigated.

We have recently demonstrated that the hepatocyte nuclear factor (HNF)-4α (NR2A1), a highly conserved member of the nuclear receptor superfamily involved in the control of glucose homeostasis [9, 10], regulates transcription of the *PED* gene by binding to a *cis*-regulatory element of the *PED* promoter and represses its transcription [11].

HNF-4α is essential for hepatocyte differentiation at the developmental and the functional levels [12], as well as for accumulation of hepatic glycogen stores and generation of normal hepatic epithelium [13]. Point mutations in HNF-4α impair liver and pancreatic regulation of glucose homeostasis and cause maturity onset diabetes of the young type 1. More recently, genetic and biochemical evidence has been generated indicating that HNF-4α may also have a role in the development of more common forms of type 2 diabetes [14–16], but understanding of the underlying mechanisms is incomplete.

The ability of nuclear receptors to induce specific transcription events depends on their recruitment of chromatin remodelling cofactors and enzymes, and on the assembly of the basal transcription machinery [17]. In the absence of ligand, nuclear receptors recruit co-repressors such as silencing mediator of retinoic acid and thyroid hormone receptor (SMRT) and nuclear receptor co-repressor. These, in turn, bind repressive enzymes such as the histone deacetylases and histone methyltransferases, specifically controlling the methylation state of lysine 9 at histone H3 and certain chromatin remodelling events.

Increasing evidence now indicates that chromatin remodelling is an important mechanism enabling transcription regulation [18]. Chromatin remodelling occurs through different mechanisms. One is the covalent modification of histone tails, including acetylation, methylation and phosphorylation [19]. These changes also affect the ability of chromatin to interact with transcription factors and the basal transcription machinery [20]. Acetylation and methylation of lysine residues at H3 and H4 amino termini represent the most common modifications. Indeed, increased acetylation induces transcriptional activation [21], while reduced acetylation usually signals transcriptional repression [22, 23]. Methylation of H3 lysine 9 is also associated with transcriptional repression [24].

In this work, we have investigated the molecular mechanisms responsible for HNF-4α-dependent silencing of *PED* expression in liver. We show that by causing epigenetic changes at the *PED* gene, HNF-4α controls transcriptional activity of *PED* and may affect glucose metabolism in liver.

Methods

Materials Media, sera and antibiotics for cell culture, and the lipofectamine reagent were purchased from Invitrogen (Paisley, UK). Goat polyclonal HNF-4α and acetyl-histone H3 (K9/K14) and rabbit polyclonal SMRTe antibodies were from Santa Cruz Biotechnology (Santa Cruz, CA, USA). Mouse monoclonal histone H3 Lys9 (H3K9) and rabbit monoclonal histone H3 Lys4 (H3K4) antibodies were from Abcam (Cambridge, UK). The PED antibody, the pCDNA3/HNF-4α expression vector and the HNF-4α-specific short hairpin RNA (shRNA) plasmid have been previously described [11]. All short interfering RNAs (siRNAs) were chemically synthesised by Ambion (Austin, TX, USA) as oligonucleotide duplexes. siRNA target sequences for silencing mediator for retinoid and thyroid hormone receptors (SMRT) were directed at regions common to SMRTα and SMRTβ (panSMRT) [25]. As non-specific siRNA controls, the Ambion Silencer 2 negative control was used.

Western blot and electrochemiluminescence (ECL) reagents were from Thermo Scientific (Rockford, Illinois, USA). All other reagents were from Sigma (St Louis, MO, USA).

Animal studies, cell culture, transfections, RT-PCR and western blot assay The PED transgenic mice and cellular models generation have been previously described [11, 26]. Total RNA extraction, cDNA synthesis, real-time PCR and

western blot analysis were performed as described in [11]. Antibodies against SMRT, HNF-4α, PED and actin were used for detection of proteins. All the experiments involving animals were approved by the Local Ethics Committee and conducted in accordance with the Principles of Laboratory Care.

Formaldehyde-assisted isolation of regulatory elements Whole cells were fixed in growth medium by addition of 37% (vol./vol.) formaldehyde to a final concentration of 1% (vol./vol.) formaldehyde for 10 min. The fixed cells were resuspended in nuclear lysis buffer containing 50 mmol/l Tris–HCl (pH 8.0), 10 mmol/l EDTA, 0.8% (wt/vol.) sodium dodecyl sulphate, 1 mmol/l phenyl methyl sulfonyl fluoride and inhibitors cocktail (Sigma), and then incubated on ice for 10 min. The extracts were then sonicated (Misonix 3000) and microcentrifuged for 10 min at 16,000 *g* and 4°C. Protein-free DNA was then analysed by SYBR Green real-time PCR [27]. The primer sets used are shown in Electronic supplementary material (ESM) Table 1. The amount of PCR product (representing nucleosome-free DNA) was plotted as a percentage of the input DNA representing total cellular DNA.

Micrococcal nuclease protection assay Nuclei were isolated from 1×10^8 of the following cells: HeLa wild-type, HeLa overproducing exogenous HNF-4α ($HeLa_{HNF\text{-}4\alpha}$) HepG2 and HepG2 subjected to silencing of the endogenous HNF-4α ($HepG2_{HNF\text{-}4\alpha\text{-}sh}$). Isolated nuclei were suspended in 1 ml of wash buffer (10 mmol/l Tris–HCl, pH 7.4, 15 mmol/l NaCl, 50 mmol/l KCl, 0.15 mmol/l spermine, 0.5 mmol/l spermidine and 8.5% [wt/vol.] sucrose) and digested with 120 U of micrococcal nuclease (MNase) for 30 min at 37°C. The purified DNA was quantified and identified on an agarose gel, and subsequently amplified by PCR using the C, D and F primer sets. An aliquot of undigested DNA was obtained as a control of total cellular DNA quality.

Chromatin immunoprecipitation and re-chromatin immunoprecipitation assay procedures Chromatin immunoprecipitation (ChIP) assay was performed as previously described [11]. Sheared chromatin samples were taken as input control or used for immunoprecipitation with the following antibodies: acetyl-histone H3 (sc-8655), dimethylated histone H3 at lysine 9 (H3K9me2; ab-1220), H3K4me2 (ab-7766), HNF-4α (sc-6556), SMRTe (sc-1612) and normal rabbit IgG as a negative control. DNA fragments were recovered and subjected to real-time PCR amplification using primer sequences described in Table 1.

For re-chromatin immunoprecipitation (Re-ChIP) assay, immunoprecipitates with the first antibody were eluted in 50 µl of dithiothreitol 10 mmol/l, diluted tenfold in ChIP dilution buffer supplemented with protease inhibitors and immunoprecipitated with the second antibody. Following immunoprecipitation, samples were processed as described for ChIP assay [11] and eluted DNA was amplified by real-time PCR with specific oligos.

Trichostatin A treatment of cells HepG2 cells were seeded in 10 cm dishes at a density of 1×10^6 cells 1 day before drug treatment. The cells were treated with 330 nmol/l trichostatin A (Sigma-) for 1 day, and total RNA and chromatin were prepared as described before.

Hepatic glycogen measurement Cells and tissues were solubilised in 0.1% (wt/vol.) sodium dodecyl sulphate and then further incubated with 1:1 saturated Na_2SO_4 and 95% (vol./vol.) ethanol. The pellets were rehydrated, and 5% (vol./vol.) phenol and H_2SO_4 were added. Finally, absorbance at 490 nm was measured. Results are expressed as micrograms of glycogen per milligram of protein or tissues.

Statistical procedures Statistical analysis was performed with a software package (StatView 5.0; Abacus Concepts, Berkley, CA, USA) using the Student's *t* test. Values of $p<0.05$ were considered statistically significant.

Results

HNF-4α induces DNA remodelling and nucleosome positioning at the PED promoter As previously reported, HeLa cells feature high expression of the *PED* gene, while very low expression was found in the HepG2 cells [11]. Expression of the *PED* silencer HNF-4α is inversely related to that of *PED* in these cells [11]. Thus, these cell lines represent an attractive model to investigate the molecular mechanisms responsible for HNF-4α regulation of *PED* gene transcription. To investigate changes induced by HNF-4α in chromatin structure across the *PED* promoter, we isolated nucleosome-free chromatin DNA from HeLa cells (either wild-type or expressing an *HNF-4α* [also known as *HNF4A*] cDNA) and from HepG2 cells (wild-type and expressing an *HNF-4α* shRNA) by performing a formaldehyde-assisted isolation of regulatory elements assay [28]. The DNA fragments were amplified using seven sets of PCR primers, covering consecutive 100 bp regions positioned at −500 to 300 in the *PED* gene (Fig. 1a, ESM Table 1) and PCR amplification was monitored by SYBR green incorporation [29]. The amount of DNA amplified (nucleosome-free DNA) was plotted as percentage of the input DNA representing total cellular DNA.

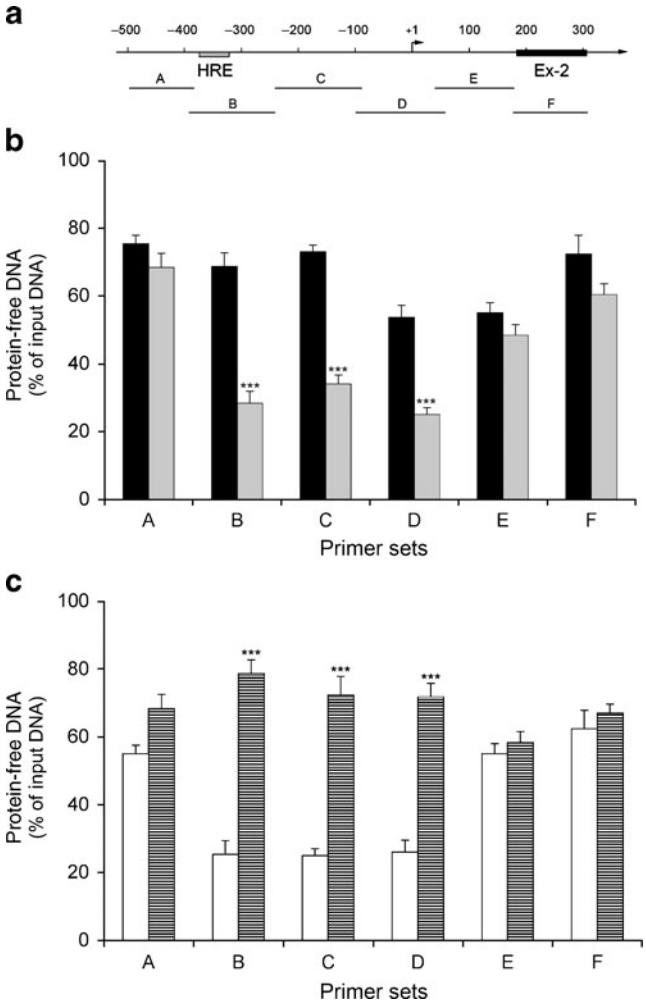

Fig. 1 Enrichment of regulatory DNA across 0.8 kb of *PED* gene using formaldehyde-assisted isolation of regulatory elements. **a** Schematic representation of *PED* showing the HRE, the transcription start site, the exon 2 position and the DNA fragments amplified by primer sets A to F. **b** Protein-free DNA was extracted from HeLa (black bars) and $HeLa_{HNF\text{-}4\alpha}$ (grey bars), and (**c**) from HepG2 (white bars) and $HepG2_{HNF\text{-}4\alpha\text{-}sh}$ (striped bars) cells as described above and analysed by real-time PCR using the indicated primers. The mean and standard errors of at least three independent experiments each performed in triplicate are shown. Statistical significance was determined by *t* test (two-tailed) analysis; ***$p<0.001$

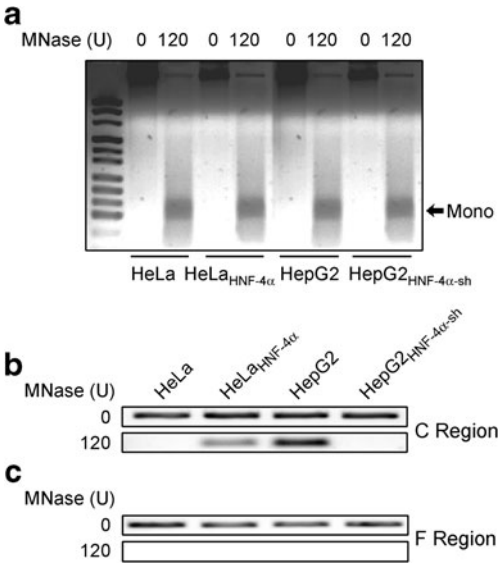

Fig. 2 Accessibility of *PED* gene regions to MNase digestion. HeLa, $HeLa_{HNF\text{-}4\alpha}$, HepG2 and $HepG2_{HNF\text{-}4\alpha\text{-}sh}$ nuclei were digested with 120 U of MNase for 30 min, which extensively digests the linker and nucleosome-free regions. **a** Representative image of digested nucleosomes separated on a 2% agarose gel before purification. First lane contains a DNA marker ladder. The arrow indicates mononucleosomes. **b** PCR amplification with primer sets from Fig. 1a as indicated using mononucleosomal DNA (bottom rows) and genomic DNA as positive control (top rows) for C region and (**c**) F region. The PCR products are shown for each primer set after agarose gel electrophoresis. Photographs are representative of three (**a**) and four (**b**, **c**) independent experiments

In $HeLa_{HNF\text{-}4\alpha}$, the amount of nucleosome-free DNA across the examined regions ranged from 25 to 65% compared with untransfected HeLa cells showing higher free DNA amounts (Fig. 1b). $HepG2_{HNF\text{-}4\alpha\text{-}sh}$ featured high levels and low reduction of nucleosome-free DNA, compared with untransfected HepG2 cells exhibiting high expression levels of HNF-4α and reduced free DNA across the −500 to 300 region of the *PED* gene (Fig. 1c). In $HeLa_{HNF\text{-}4\alpha}$ and HepG2 cells, three regions were found to be associated with reduced levels of free DNA. These corresponded to the HNF-4α response element (HRE; at −350, region B), its immediate proximity (−200, region C) and the proximity of the *PED* transcription start site (−50, region D).

To further investigate nucleosome positioning across the *PED* promoter, mononucleosomal DNA averaging 150 bp in size was obtained by nuclear MNase digestion of HeLa cells (either transfected with HNF-4α or untransfected) and HepG2 cells (transfected with HNF-4α-sh or untransfected; Fig. 2a). This DNA was subsequently amplified using the PCR primer sets for the C and D regions shown in Fig. 1b. Figure 2b shows the results obtained with primer set C; similar results were obtained with primer set D (data not shown). In agarose gel electrophoresis, the amplification products were barely detectable when using the mononucleosomal DNA from HeLa cells, but were significantly increased with the DNA from the $HeLa_{HNF\text{-}4\alpha}$ cells (C region). Consistently, only a weak band was obtained in HNF-4α-silenced ($HepG2_{HNF\text{-}4\alpha\text{-}sh}$) cells compared with the untransfected HepG2 cells (C region). The use of undigested DNA in control PCR assays led to the amplification of a 120 bp band with all of the cell lines (C region). Also, upon MNase treatment, the nucleosome-free exon 2 allowed no PCR amplification with F region primers (Fig. 2c), although clear amplification bands were obtained with the undigested DNA (F region). These data

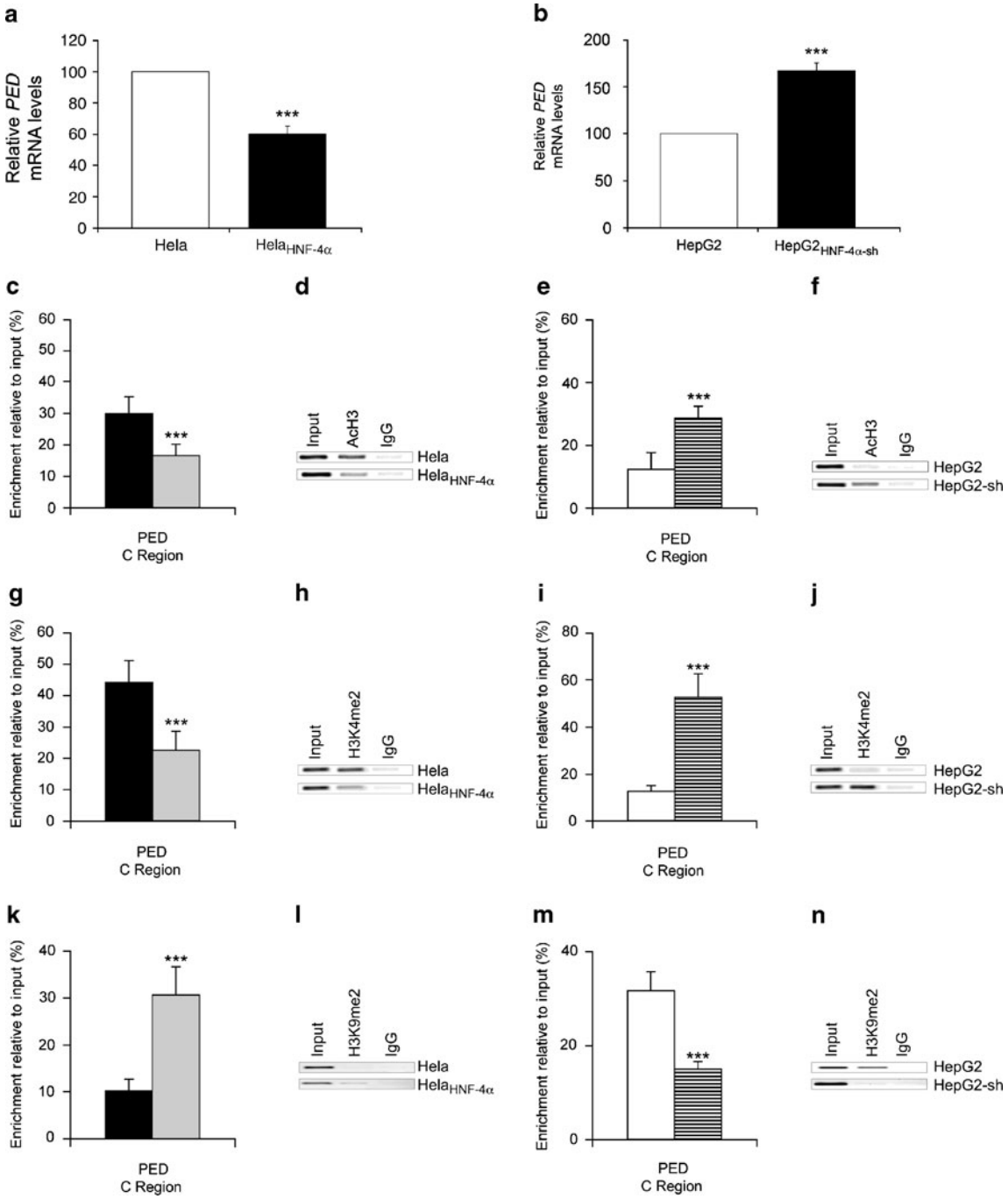

Fig. 3 HNF-4α production determines repressive histone modifications at the *PED* promoter. **a**, **b** Hela and HepG2 cells were transfected with 1 μg of the pCDNA3/HNF-4α expression vector and of the HNF-4α-specific shRNA clone, respectively. At 48 h after transfection, total RNAs were extracted from transfected and non-transfected cells. *PED* mRNA levels were then quantified by RT-PCR. Data were normalised to β-actin mRNA and are expressed as per cent decrease or increase vs control (untransfected cells). ChIP experiments were performed using antibodies against active histone marks, i.e. (**c**–**f**) acetyl-histone H3 and (**g**–**j**) H3K4me2, in the *PED* gene in HeLa (black bars) and HeLa$_{HNF-4\alpha}$ cells (grey bars), and in HepG2 (white bars) and HepG2$_{HNF-4\alpha-sh}$ (striped bars) cells. ChIP was also performed against the repressive histone mark H3K9me2 (**k**–**n**) in HeLa and HeLa$_{HNF-4\alpha}$ cells, and in HepG2 and HepG2$_{HNF-4\alpha-sh}$ cells. ChIPs were followed by quantitative PCR amplification with primer set for the C region of the *PED* promoter. Representative gels (**d**, **f**, **h**, **j**, **l**, **n**) are shown. Levels in bar graphs (**c**, **e**, **g**, **i**, **k**, **m**) are presented as per cent enrichment relative to input DNA and corrected for IgG control levels as analysed by quantitative PCR. Bars represent the mean ± SE of three independent experiments each performed in triplicate. Statistical significance was assessed by *t* test analysis. ***$p<0.001$

suggest that HNF-4α production and binding to the HRE causes nucleosome positioning at C and D regions in the proximal *PED* gene promoter.

HNF-4α induces histone deacetylation and methylation at the PED promoter We next focused on the significance of HNF-4α cellular levels for the epigenetic state of the *PED* promoter region. To this end, we looked for typical transcriptional activation and repression marks in the cells with high ($HeLa_{HNF\text{-}4\alpha}$, HepG2) and low (HeLa, $HepG2_{HNF\text{-}4\alpha\text{-}sh}$) HNF-4α levels, in which *PED* transcription is suppressed and active, respectively (Fig. 3a, b). ChIP assays were performed using antibodies recognising histone modifications, as well as normal rabbit IgG as a negative control, with the purified DNA from the immunoprecipitates being used for real-time PCR analysis with primer sets amplifying the C region nucleosome. In $HeLa_{HNF\text{-}4\alpha}$ and HepG2 cells we saw an almost twofold reduction in histone H3 acetylation at lysines 9 and 14 (a mark of active transcription) compared with HeLa and the $HepG2_{HNF\text{-}4\alpha\text{-}sh}$ cells (Fig. 3c, e). A further mark of active transcription [30], lysine 4 dimethylated histone H3, was similarly reduced in these cells (Fig. 3g, i). Also, the dimethylation of histone H3 at lysine 9 (H3K9me2), a mark typical of repressed gene promoters [31], was almost threefold higher at the C region nucleosome from $HeLa_{HNF\text{-}4\alpha}$ and HepG2 as compared with HeLa or $HepG2_{HNF\text{-}4\alpha\text{-}sh}$ cells (Fig. 3k, m). Similar results were obtained with the D region nucleosome (data not shown). Thus, HNF-4α production and response element binding is accompanied by enrichment in repressive histone modifications together with reduced rate of *PED* expression.

In addition, the $HepG2_{HNF\text{-}4\alpha\text{-}sh}$ cells, which feature high levels of *PED* mRNA, exhibited reduced hepatic glycogen content compared with control cells. Similar results were obtained in stably transfected HepG2 cells overexpressing human *PED* (Fig. 4a).

We also analysed glycogen content in livers from PED transgenic mice. These animals have been previously characterised and described [26]. As shown in Fig. 4b, the abundance of hepatic glycogen content was lower in transgenic mice than in control non-transgenic littermates (Fig. 4b).

HNF-4α recruits repressive enzymes at the PED promoter and silences expression Since HNF-4α production results in decreased histone acetylation, we investigated the presence of histone-modifying enzymes at the HRE region in the *PED* promoter in the presence and absence of HNF-4α. Using ChIP assays, we demonstrated the presence of the SMRT co-repressor complex at the HNF-4α in HepG2 cells but not in Hela cells (Fig. 5a). Importantly, HeLa and HepG2 cells feature very comparable levels of SMRT, indicating that

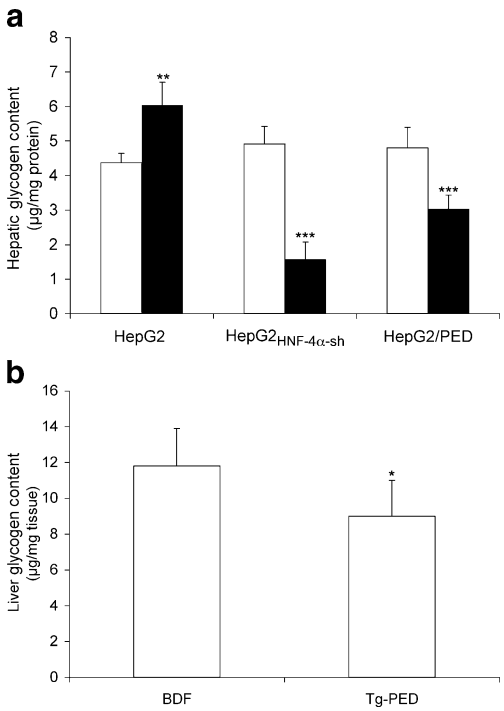

Fig. 4 Effect of PED overproduction on hepatocyte glycogen content. **a** HepG2, $HepG2_{HNF\text{-}4\alpha\text{-}sh}$ and HepG2/PED cells were assayed for glycogen content after incubation with 100 nmol/l insulin (black bars) as described above. White bars, without insulin. **b** Glycogen content was also compared in liver tissue from transgenic mice overexpressing PED (Tg-PED) and from their non-transgenic littermates (BDF) maintained under random-feeding conditions. Bars represent the means ± SE of three (**a**) and four (**b**) independent measurements each in triplicate. *$p<0.05$, **$p<0.01$ and ***$p<0.001$

the presence of SMRT at the HRE observed in the HepG2 cells is not dependent on SMRT levels (ESM Fig. 1a). The assembly of HNF-4α/SMRT complexes on the *PED* promoter region was then investigated by Re-ChIP experiments using HNF-4α antibody in the first ChIP and a SMRT antibody in the second ChIP. As shown in Fig. 5b, c, we detected HNF-4α together with SMRT at the HRE in $HeLa_{HNF\text{-}4\alpha}$ and HepG2 cells, while the complex was barely detectable in cells producing lower amounts of HNF-4α (HeLa and the $HepG2_{HNF\text{-}4\alpha\text{-}sh}$). Nuclear extracts from each cell type were immunoprecipitated with the SMRT antibody and the immunocomplexes blotted with the HNF-4α antibody. Again, we detected an HNF-4α/SMRT interaction only in the HNF-4α-producing cells, $HeLa_{HNF\text{-}4\alpha}$ and HepG2, compared with HeLa and $HepG2_{HNF\text{-}4\alpha\text{-}sh}$ cells, respectively (Fig. 5d), indicating that recruitment of the co-repressor SMRT was entirely dependent on the presence of HNF-4α.

Re-ChIP experiments using antibodies toward the repressive histone mark H3K9me2 followed by HNF-4α or SMRT antibodies revealed that levels of these complexes were reduced in the cells with low HNF-4α levels

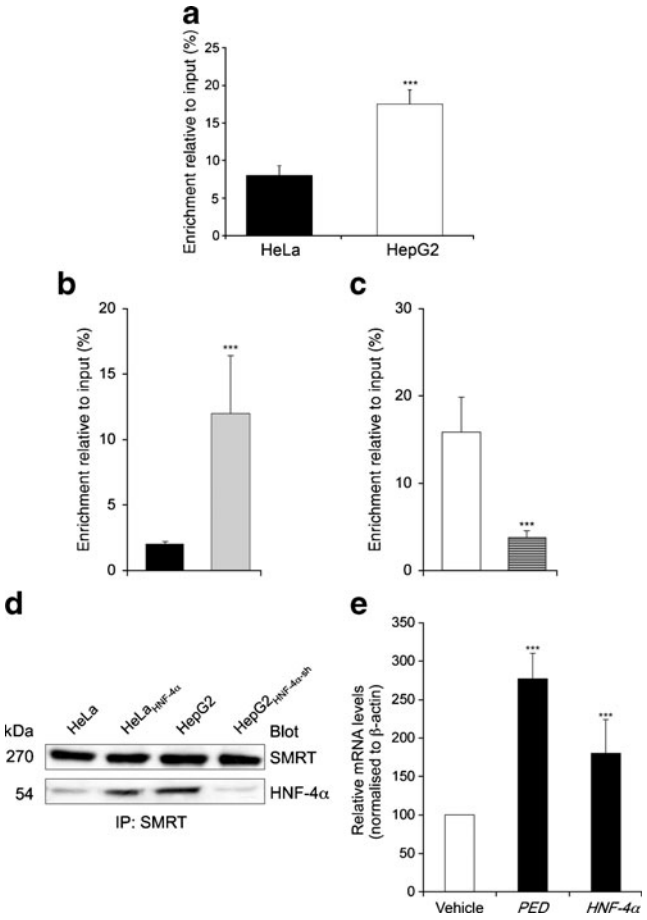

Fig. 5 Recruitment of repressive enzymes at the *PED* promoter is dependent on HNF-4α. ChIP experiments were performed using antibodies against SMRT (**a**) and HNF-4α (**b**, **c**). The binding of SMRT to the HRE of *PED* was analysed by quantitative PCR in (**a**) HeLa and HepG2 wild-type cells. HNF-4α binding was analysed by quantitative PCR in the HRE of *PED* in HeLa (black bar) and $HeLa_{HNF\text{-}4\alpha}$ (grey bar) (**b**), and (**c**) in HepG2 (white bar) and $HepG2_{HNF\text{-}4\alpha\text{-}sh}$ (striped bar) cells. Re-ChIP experiments were performed using antibodies against SMRT (**b**, **c**) to identify protein complexes at the HRE of *PED*. The amount of precipitated DNA from the first ChIP was used as input. Results are expressed as enrichment relative to input (%) and corrected for IgG control levels. **d** HeLa, $HeLa_{HNF\text{-}4\alpha}$, HepG2 and $HepG2_{HNF\text{-}4\alpha\text{-}sh}$ cells were grown as described and total lysates of the cells immunoprecipitated with antibodies against SMRT and then analysed by immunoblot with antibodies against HNF-4α and SMRT. Filters were revealed by ECL. The autoradiograph shown is representative of four independent experiments. **e** HepG2 cells were treated with 330 nmol/l trichostatin A (black bars) for 24 h. White bar, vehicle. *PED* and *HNF-4α* expression were determined by real-time PCR. Data were normalised to β-actin levels and expressed as relative to vehicle treatments. Bars (**a**–**c**, **e**) represent the mean ± SE of at least three independent experiments each performed in triplicate. Statistical significance was assessed by *t* test analysis. ***$p<0.001$

(HeLa and the $HepG2_{HNF\text{-}4\alpha\text{-}sh}$), in which *PED* transcription is active. This finding indicates that HNF-4α/SMRT assembly to the *PED* gene is accompanied by histone deacetylation and methylation at its proximal promoter (ESM Fig. 1b).

Since HNF-4α production results in changes of the epigenetic state of chromatin, we investigated the possibility of activating the *PED* gene by pharmacological inhibition of histone deacetylation. Incubation of HepG2 cells with the deacetylase inhibitor trichostatin A revealed an increase in *PED* expression in these cells (Fig. 5e). Since HNF-4α levels also significantly increased upon trichostatin A treatment, we sought to verify whether hyperacetylation induced by trichostatin A treatment impairs HNF-4α binding to its response element, as this effect may have been sufficient to enhance *PED* transcription. We found no difference in HNF-4α at its B region-amplified response element in HepG2 cells, whether preincubated with trichostatin A or not (ESM Fig. 2). This supports the role of histone deacetylation in restraining *PED* activity. We conclude that histone deacetylation is required for HNF-4α-mediated *PED* repression.

SMRT silencing rescues PED expression in HepG2 cells To further address the role of SMRT in HNF-4α-dependent repression of *PED* function, HepG2 cells were transiently transfected with siRNAs for *SMRT* (also known as *NCOR2*)-α and *SMRTβ* (panSMRT) or a control siRNA [25]. Real-time PCR assays on total RNA from panSMRT-silenced HepG2 cells showed about twofold increased *PED* RNA levels compared with control siRNA and wild-type cells (Fig. 6a). Western blot analysis of extracts from the different cell types also revealed significantly increased PED and decreased SMRT protein levels upon the panSMRT transfection (Fig. 6b). In addition, ChIP assays in panSMRT-treated HepG2 cells using acetyl-histone H3 (K9/K14) and H3K9me2 antibodies showed significantly increased acetylation and decreased methylation of the histone H3 lysine 9 compared with controls (Fig. 6c).

The role of SMRT in HNF-4α regulation of *PED* expression was further addressed in HepG2 cells transfected with a *PED* promoter luciferase construct featuring the HRE (pPED477). Co-transfection of the panSMRT siRNA in these cells increased the pPED477 reporter gene activity by twofold. Importantly, the luciferase activity of a vector containing the mutagenised HNF-4α binding sequence (pPED477mut) abolishing its transcriptional activity was increased at similar levels in control and panSMRT transfected HepG2 cells (Fig. 6d) compared with HepG2 wild-type cells transfected with the pPED477 vector alone (Fig. 6d). This indicates that the recruitment of HNF-4α and SMRT to the HRE at the *PED* promoter is necessary for *PED* transcriptional inhibition.

SMRT enables HNF-4α inhibition of GRB14 and USP21 genes To verify whether SMRT action on HNF-4α silencing is unique to the *PED* gene, we analysed expression of the two other genes repressed by HNF-4α, *GRB14* and

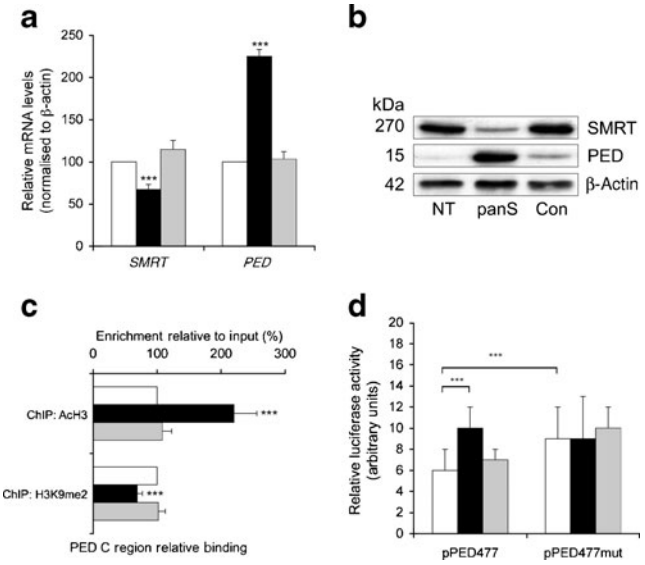

Fig. 6 Effect of SMRT depletion on *PED* expression in HepG2 cells. HepG2 cells were transfected with Silencer negative control siRNA (grey bars) or siRNAs for panSMRT (black bars). **a** *SMRT* and *PED* mRNA levels were quantified by real-time PCR. Data were normalised to β-actin mRNA and are expressed as fold over control (untransfected cells [NT], white bars). **b** Lysates prepared from HepG2 cells transfected with siRNAs were western-blotted with PED and SMRT antibodies and further analysed by ECL and autoradiography. The autoradiograph shown is representative of four independent experiments. **c** ChIP experiments were performed using antibodies against active (acetyl-histone H3 [AcH3]) or repressive (H3K9me2) histone marks. Their binding was analysed by quantitative PCR in the nucleosome C region of *PED* promoter in control or (panSMRT) HepG2 cells and expressed as fold over control (untransfected cells). **d** HepG2 cells were co-transfected with 3 μg of the indicated *PED* promoter–luciferase constructs (or 3 μg of the promotorless pGL3 basic vector) alone or in combination with SMRTα and SMRTβ siRNAs or the Silencer negative control siRNA and 1 μg of the pRSVβ-gal vector DNA. Luciferase activity was assayed as described and is presented as the increase above the activity measured with the control pGL3 basic vector. Bars represent the mean ± SE of three independent experiments each performed in triplicate. Statistical significance was assessed by *t* test analysis. ***$p<0.001$

USP21. Interestingly, *GRB14* and *USP21* were expressed at reduced levels in the $HeLa_{HNF\text{-}4\alpha}$ compared with untransfected cells (Fig. 7a). In addition, expression of these genes was rescued by HNF-4α silencing in $HepG2_{HNF\text{-}4\alpha\text{-}sh}$ cells, further supporting the repressor function of HNF-4α (Fig. 7b). The regulatory region of *GRB14* and *USP21* has not been reported yet. By in silico analysis, we therefore identified their HREs at −700 and −450 bp upstream of their transcriptional start sites, respectively (Fig. 7c). ChIP and Re-ChIP assays with specific antibodies and HRE primer sets revealed largely increased HNF-4α and HNF-4α/SMRT complex abundance at the HRE in the $HeLa_{HNF\text{-}4\alpha}$ compared with untransfected cells (Fig. 7d). Consistently, the presence of HNF-4α and HNF-4α/SMRT complex at the response element was significantly reduced in HepG2 cells transfected with the HNF-4α-sh (Fig. 7e). We then examined the acetylation state of the *GRB14* and *USP21* proximal regulatory regions and performed ChIP assays using acetyl-histone H3 (K9/K14) antibodies and

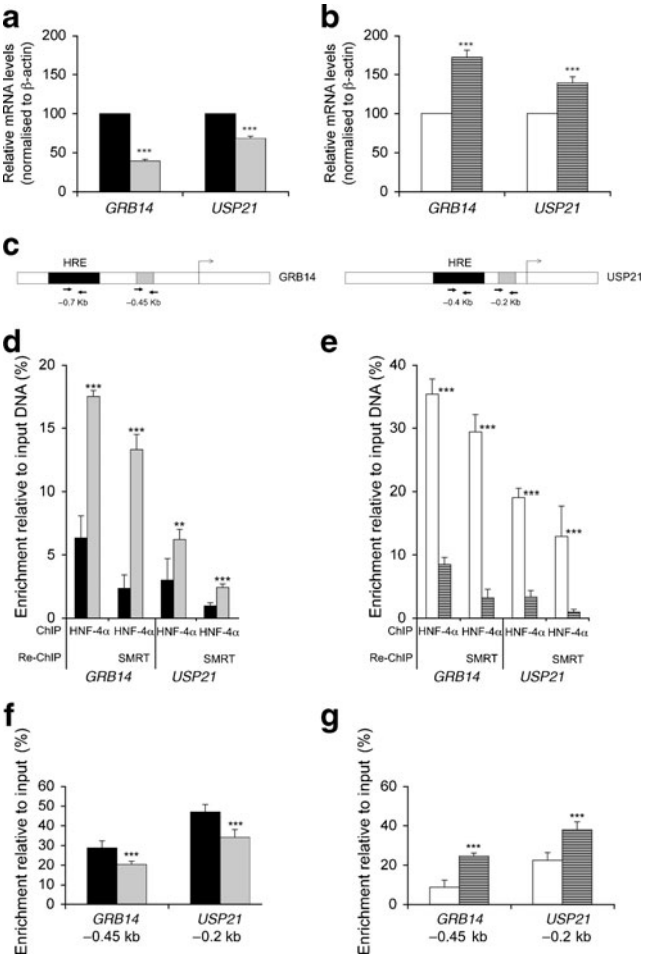

Fig. 7 HNF-4α-dependent inhibition of *GBR14* and *USP21* expression. Total RNA preparations were obtained (**a**) from HeLa (black bars) and $HeLa_{HNF\text{-}4\alpha}$ (grey bars) cells, and (**b**) from HepG2 (white bars) and $HepG2_{HNF\text{-}4\alpha\text{-}sh}$ (striped bars) cells. Levels of *GRB14 and USP21* mRNA were then determined by real-time PCR and normalised to β-actin mRNA. mRNA levels are relative to those in control (HeLa, HepG2) cells. **c** Schematic representation of the *GRB14* and *USP21* genes, with arrows indicating ChIP primers against the HNF-4α binding site (HRE) and the region downstream the HRE. ChIP experiments were performed using antibodies against HNF-4α (**d**, **e**) and (**f**, **g**) active histone marks (acetyl-histone H3). HNF-4α binding was analysed by quantitative PCR in the HRE of *GRB14* and *USP21* in HeLa and $HeLa_{HNF\text{-}4\alpha}$ (**d**) and HepG2 and $HepG2_{HNF\text{-}4\alpha\text{-}sh}$ (**e**) cells. Acetyl-histone H3 enrichment at the *GRB14* and *USP21* regulatory regions was analysed by quantitative PCR in HeLa and $HeLa_{HNF\text{-}4\alpha}$ (**f**), and HepG2 and $HepG2_{HNF\text{-}4\alpha\text{-}sh}$ (**g**) cells. Re-ChIP experiments were performed using antibodies against SMRT (**d, e**) to identify protein complexes at the HRE of *GRB14* and *USP21* genes. The amount of precipitated DNA from the first ChIP was used as input. Results are expressed as per cent enrichment relative to input DNA and corrected for IgG control levels. Bars represent the mean ± SE of three independent experiments each performed in triplicate. Statistical significance was assessed by *t* test analysis. **$p<0.01$, ***$p<0.001$

primer sets amplifying a 300 bp region downstream of the HREs. Histone H3 (K9/K14) acetylation was significantly reduced in the $HeLa_{HNF\text{-}4\alpha}$, but rescued in the $HepG2_{HNF\text{-}4\alpha\text{-}sh}$ cells (Fig. 7f, g), indicating common mechanisms in the silencing of the *PED*, *GRB14* and *USP21* genes by HNF-4α.

Discussion

Previous work has established the significance of the nuclear receptor superfamily in regulating a broad range of cellular processes by activating or repressing different sets of genes that harbour nuclear receptor-recognising DNA motifs [32]. Several mechanisms leading to transcriptional activation by the nuclear receptors have been elucidated in considerable detail [33]. Against this, the molecular bases of transcriptional repression remain more unclear [34, 35].

In the present study, we show that HNF-4α, a member of the steroid receptor class of nuclear receptors [36, 37], triggers SMRT recruitment to the *PED* proximal promoter and causes histone tail hypoacetylation at H3-K9/K14, inducing a transcriptionally non-permissive state of the gene. These changes are followed by the appearance of H3K9 hypermethylation and H3K4 hypomethylation, two marks of heterochromatin (Fig. 8). These findings indicate for the first time that, in intact cells, HNF-4α represses gene transcription by directly recruiting SMRT to the promoter region, leading to histone deacetylation-associated remodelling of chromatin.

Previous studies in HNF-4α-producing cells and in cells with no HNF-4α production have shown that SMRT represses HNF-4α-mediated transcription of reporter constructs containing heterologous, as well as native promoters [38]. In addition, using glutathione *S*-transferase pull-down assays, the same team of authors showed that HNF-4α directly binds the receptor interacting domain 2 of SMRT in vitro [38]. These observations suggest that SMRT repression might represent a physiologically relevant mechanism responsible for HNF-4α regulation and that functional cooperation requires physical interaction of SMRT and HNF-4α. The finding we now report, namely that the HNF-4α/SMRT complex induces *GRB14* and *USP21* repression in addition to *PED* gene silencing, further underlines the significance of these mechanisms to the in vivo transcriptional repressor activity of HNF-4α.

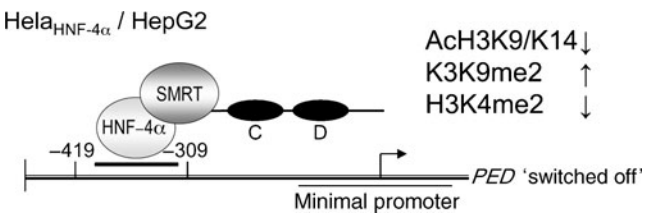

Fig. 8 Epigenetic changes induced by HNF-4α to *PED* expression. HNF-4α production and binding to its response element causes chromatin packaging at the *PED* promoter and enrichment of histone H3 methylation at lysine 9 (H3K9me2), a mark typical of repressed gene promoters. HRE binding also causes a decrease in acetylation at lysine 9 and 14 (AcH3K9/K14) and dimethylation of lysine 4 of histone H3 (H3K4me2), two marks of active transcription

HNF-4α has long been known to serve as a transcriptional activator [39]. Indeed, HNF-4α can: (1) activate transcription in the absence of exogenously added ligands [40]; and (2), in mammalian cells, in yeasts and in vitro, respond to several coactivators including glucocorticoid receptor interacting protein 1 (GRIP1), steroid receptor coactivator 1 (SRC-1) and CREB binding protein (CBP)-p300 [41, 42]. However, Ruse et al. reported that HNF-4α regulation by these coactivators can be competitively abolished by interaction of the histone deacetylase-associated co-repressor SMRT with the F domain of HNF-4α [38]. Thus, the nature of the recruited co-regulator and of its association with direct effectors of histone modifications such as histone deacetylases appears to determine the transcriptional activity of HNF-4α.

Recently, it has been shown that a knock-in mouse bearing a mutation in the receptor interacting domain of SMRT ($SMRT^{mRID}$) that disrupts its interaction with the nuclear hormone receptor [43] develops multiple metabolic defects including altered insulin sensitivity and 70% increased adiposity. These findings indicate that major districts of metabolic regulation such as insulin sensitivity and fat mass depend on the molecular balance of co-repressors and coactivators, which modulate the status of chromatin and nuclear receptor signalling and ultimately regulate gene expression in response to specific physiological situations.

PED expression is upregulated in individuals with type 2 diabetes and in the euglycaemic offspring of these patients, impairing insulin action and insulin secretion [5, 7]. However, the causes for *PED* upregulation required additional investigation. In the present study, we demonstrated that HNF-4α silencing alters the epigenetic state of the *PED* gene and determines its overexpression in liver cells. We further show that induction of *PED* gene expression in hepatocytes is paralleled by reduced hepatic glycogen content. We have also very recently demonstrated that activation of *PED* expression in HepG2 cells is paralleled by the establishment of a partially dedifferentiated phenotype, accompanied by reduced mRNA levels of genes expressed during normal liver development [11]. Thus HNF-4α-regulated *PED* gene may have a role in hepatocyte differentiation. Epigenetic changes upregulating its expression might impair development of normal liver function, thereby contributing to progression toward diabetes. Environmental factors have been reported to induce epigenetic changes, leading to the development of

abnormal phenotypes [44, 45]. For instance, diet and ageing have been reported to perturb gene expression by inducing DNA methylation and histone modifications [46]. Also, intrauterine growth retardation, a common complication of pregnancy, has been associated with later development of type 2 diabetes, in part through chromatin remodelling effects and epigenetic modulation of the expression of several genes [47]. Type 2 diabetes is a genetically heterogeneous disease resulting from complex interactions of genetic and environmental determinants. Previous studies using different approaches have uncovered a number of type 2 diabetes susceptibility genes, but it remains less clear how these genes determine type 2 diabetes. In particular, the molecular details of gene–environment interplay in diabetes onset have received less attention. Exposure to certain environmental determinants, including maternal obesity [48], intrauterine environment [49, 50] and nutritional factors [51], affects key developmental sequences programming metabolic responsiveness to environmental stimuli during later life. Such concepts are now supported by studies of monozygotic twins, where diabetes risk is discordant and linked to birthweight [52]. Laboratory studies are in progress to assess whether *PED* may serve as an environment gene target contributing to type 2 diabetes progression.

In conclusion, in the present work, we demonstrate that HNF-4α inhibits *PED* expression by inducing chromatin remodelling and histone modifications at nucleosomes located in the regulatory region of the gene. Dysregulation of these mechanisms might promote pathogenetic sequences leading to type 2 diabetes.

Acknowledgements This work was supported by the European Foundation for the Study of Diabetes (EFSD), the European Community's FP6 EUGENE2 (LSHM-CT-2004-512013) and PREPOBEDIA (201681) programes, and grants from the Associazione Italiana per la Ricerca sul Cancro (AIRC) and from the Ministero dell'Università e della Ricerca Scientifica (PRIN and FIRB). The financial support of Telethon - Italy is also gratefully acknowledged. We thank F. Blasi (Fondazione Istituto FIRC di Oncologia Molecolare, Milano, Italy) and L. Chiariotti (Dipartimento di Biologia e Patologia Cellulare e Molecolare "L. Califano", Università di Napoli Federico II, Napoli, Italy) for their critical reading this manuscript.

Duality of interest The authors declare that there is no duality of interest associated with this manuscript.

References

1. Sladek R, Rocheleau G, Rung J et al (2007) A genome-wide association study identifies novel risk loci for type 2 diabetes. Nature 445:881–885
2. Saxena R, Voight B, Lyssenko V et al (2007) Genome-wide association analysis identifies loci for type 2 diabetes and triglyceride levels. Science 316:1331–1336
3. Prokopenko I, McCarthy M, Lindgren C (2008) Type 2 diabetes: new genes, new understanding. Trends Genet 24:613–621
4. Danziger N, Yokoyama M, Jay T, Cordier J, Glowinski J, Chneiweiss H (1995) Cellular expression, developmental regulation, and phylogenic conservation of PEA-15, the astrocytic major phosphoprotein and protein kinase C substrate. J Neurochem 64:1016–1025
5. Condorelli G, Vigliotta G, Iavarone C et al (1998) PED/PEA-15 gene controls glucose transport and is overexpressed in type 2 diabetes mellitus. EMBO J 17:3858–3866
6. Condorelli G, Vigliotta G, Trencia A et al (2001) Protein kinase C (PKC)-alpha activation inhibits PKC-zeta and mediates the action of PED/PEA-15 on glucose transport in the L6 skeletal muscle cells. Diabetes 50:1244–1252
7. Valentino R, Lupoli GA, Raciti GA et al (2006) In healthy first-degree relatives of type 2 diabetics, ped/pea-15 gene is overexpressed and related to insulin resistance. Diabetologia 49:3058–3066
8. Perfetti A, Oriente F, Iovino S et al (2007) Phorbol esters induce intracellular accumulation of the anti-apoptotic protein ped/pea-15 by preventing ubiquitinylation and proteasomal degradation. J Biol Chem 282:8648–8657
9. Hayhurst G, Lee Y, Lambert G, Ward J, Gonzalez F (2001) Hepatocyte nuclear factor 4 alpha (nuclear receptor 2A1) is essential for maintenance of hepatic gene expression and lipid homeostasis. Mol Cell Biol 21:1393–1403
10. Pereira F, Tsai M, Tsai S (2000) COUP-TF orphan nuclear receptors in development and differentiation. Cell Mol Life Sci 57:1388–1398
11. Ungaro P, Teperino R, Mirra P et al (2008) Molecular cloning and characterization of the human PED/PEA-15 gene promoter reveal antagonistic regulation by hepatocyte nuclear factor 4 alpha and chicken ovalbumin upstream promoter transcription factor II. J Biol Chem 283:30970–30979
12. Li J, Ning G, Duncan SA (2000) Mammalian hepatocyte differentiation requires the transcription factor HNF-4a. Genes Dev 14:464–474
13. Parviz F, Matullo C, Garrison W et al (2003) Hepatocyte nuclear factor 4 alpha controls the development of a hepatic epithelium and liver morphogenesis. Nat Genet 34:292–296
14. Black MH, Fingerlin TE, Allayee H et al (2008) Evidence of interaction between PPARG2 and HNF4A contributing to variation in insulin sensitivity in Mexican Americans. Diabetes 57:1048–1056
15. Menjivar M, Granados-Silvestre MA, Montùfar-Robles I et al (2008) High frequency of T130I mutation of HNF4A gene in Mexican patients with early-onset type 2 diabetes. Clin Genet 73:185–187
16. Johansson S, Raeder H, Eide SA et al (2007) Studies in 3,523 Norwegians and meta-analysis in 11,571 subjects indicate that variants in the hepatocyte nuclear factor 4 alpha (HNF4A) P2 region are associated with type 2 diabetes in Scandinavians. Diabetes 56:3112–3117
17. Rosenfeld MG, Lunyak VV, Glass CK (2006) Sensors and signals: a coactivator/corepressor/epigenetic code for integrating signal-dependent programs of transcriptional response. Genes Dev 20:1405–1428
18. Strahl BD, Allis CD (2000) The language of covalent histone modifications. Nat Genet 403:41–45
19. Kouzarides T (2007) Chromatin modifications and their function. Cell Mol Life Sci 128:693–705
20. Saha A, Wittmeyer J, Cairns BR (2006) Chromatin remodelling: the industrial revolution of DNA around histones. Nat Rev Mol Cell Biol 7:437–447
21. Roth TY, Cuddapah S, Cui K, Zhao K (2006) The genomic landscape of histone modifications in human T cells. Proc Natl Acad Sci USA 103:15782–15787
22. Kurdistani SK, Tavazoie S, Grunstein M (2004) Mapping global histone acetylation patterns to gene expression. Cell 117:721–733

23. Schubeler D, MacAlpine DM, Scalzo D et al (2004) The histone modification pattern of active genes revealed through genome-wide chromatin analysis of a higher eukaryote. Genes Dev 18:1263–1271
24. Fischle W, Wang Y, Allis CD (2003) Histone and chromatin cross-talk. Curr Opin Cell Biol 15:172–183
25. Peterson TJ, Karmakar S, Pace MC, Gao T, Smith CL (2007) The silencing mediator of retinoic acid and thyroid hormone receptor (SMRT) corepressor is required for full estrogen receptor alpha transcriptional activity. Mol Cell Biol 27:5933–5948
26. Vigliotta G, Miele C, Santopietro S et al (2004) Overexpression of the ped/pea-15 gene causes diabetes by impairing glucose-stimulated insulin secretion in addition to insulin action. Mol Cell Biol 24:5005–5015
27. Rao S, Procko E, Shannon MF (2001) Chromatin remodeling, measured by a novel real-time polymerase chain reaction assay, across the proximal promoter region of the IL-2 gene. J Immunol 167:4494–4503
28. Hogan GJ, Lee C, Lieb JD (2006) Cell cycle-specified fluctuation of nucleosome occupancy at gene promoters. PLoS Genetics 2:1433–1450
29. Overbergh L, Valckx D, Waer M, Mathieu C (1999) Quantification of murine cytokine mRNAs using real time quantitative reverse transcriptase PCR. Cytokine 11:305–312
30. Santos-Rosa H, Schneider R, Bannister AJ et al (2002) Active genes are tri-methylated at K4 of histone H3. Nature 419:407–411
31. Lachner M, O'Sullivan RJ, Jenuwein T (2003) An epigenetic road map for histone lysine methylation. J Cell Sci 116:2117–2124
32. Chen J, Kinyamu HK, Archer TK (2009) Changes in attitude, changes in latitude: nuclear receptors remodeling chromatin to regulate transcription. Mol Endocrinol 20:1–13
33. McKenna NJ, O'Malley BW (2002) Combinatorial control of gene expression by nuclear receptors and coregulators. Cell 108:465–474
34. Grignani F, de Matteis S, Nervi C et al (1998) Fusion proteins of the retinoic acid receptor-alpha recruit histone deacetylase in promyelocytic leukaemia. Nature 391:815–818
35. Guenther MG, Lane WS, Fischle W, Verdin E, Lazar MA, Shiekhattar R (2000) A core SMRT corepressor complex containing HDAC3 and TBL1, a WD40-repeat protein linked to deafness. Genes Dev 14:1048–1057
36. Gupta R, Vatamaniuk M, Lee C et al (2005) The MODY gene HNF4alpha regulates selected genes involved in insulin secretion. J Clin Invest 115:1006–1015
37. Hohmeier H, Mulder H, Chen G, Henkel-Rieger R, Prentki M, Newgard C (2000) Isolation of INS-1 derived cell lines with robust ATP-sensitive K^+ channel-dependent and -independent glucose-stimulated insulin secretion. Diabetes 49:424–430
38. Ruse MDJ, Privalsky ML, Sladek FM (2002) Competitive cofactor recruitment by orphan receptor hepatocyte nuclear factor 4 alpha 1: modulation by the F domain. Mol Cell Biol 22:1626–1638
39. Odom DT, Zizlsperger N, Gordon DB et al (2004) Control of pancreas and liver gene expression by HNF transcription factors. Science 303:1378–1381
40. Sladek F, Zhong WM, Lai E, Darnell JE (1990) Liver-enriched transcription factor HNF-4 is a novel member of the steroid hormone receptor superfamily. Genes Dev 4:2353–2365
41. Wang JC, Stafford JM, Granner DK (1998) SRC-1 and GRIP1 coactivate transcription with hepatocyte nuclear factor 4. J Biol Chem 273:30847–30850
42. Yoshida E, Aratani S, Itou H et al (1997) Functional association between CBP and HNF-4 in trans-activation. Biochem Biophys Res Commun 241:664–669
43. Nofsinger RR, Li P, Hong SH et al (2008) SMRT repression of nuclear receptors controls the adipogenic set point and metabolic homeostasis. Proc Natl Acad Sci USA 105:20021–20026
44. Jaenisch R, Bird A (2003) Epigenetic regulation of gene expression: how the genome integrates intrinsic and environmental signals. Nat Genet Supplement 33:245–254
45. Tremblay J, Hamet P (2008) Impact of genetic and epigenetic factors from early life to later disease. Metabolism 57:S27–S31
46. Jirtle RL, Skinner MK (2007) Environmental epigenomics and disease susceptibility. Nat Rev Genet 8:253–262
47. Park JH, Stoffers DA, Nicholls RD, Simmons RA (2008) Development of type 2 diabetes following intrauterine growth retardation in rats is associated with progressive epigenetic silencing of Pdx1. J Clin Invest 118:2316–2324
48. Dabelea D, Mayer-Davis E, Lamichhane A et al (2008) Association of intrauterine exposure to maternal diabetes and obesity with type 2 diabetes in youth: the SEARCH Case–Control Study. Diabetes Care 31:1422–1426
49. Gill-Randall R, Adams D, Ollerton R, Lewis M, Alcolado J (2004) Type 2 diabetes mellitus—genes or intrauterine environment? An embryo transfer paradigm in rats. Diabetologia 47:1354–1359
50. Dabelea D, Pettitt D (2001) Intrauterine diabetic environment confers risks for type 2 diabetes mellitus and obesity in the offspring, in addition to genetic susceptibility. J Pediatr Endocrinol Metab 14:1085–1091
51. Diakoumopoulou E, Tentolouris N, Kirlaki E et al (2005) Plasma homocysteine levels in patients with type 2 diabetes in a Mediterranean population: relation with nutritional and other factors. Nutr Metab Cardiovasc Dis 15:109–117
52. Poulsen P, Kyvik KO, Vaag A, Beck-Nielsen H (1999) Heritability of type II (non insulin-dependent) diabetes mellitus and abnormal glucose tolerance—a population-based twin study. Diabetologia 42:139–145